ROLE OF THE CYTOSKELETON IN CHOLERA TOXIN DIFFUSION AND ENDOCYTOSIS

By

Charles A. Day

Dissertation

Submitted to the Faculty of the

Graduate School of Vanderbilt University

in partial fulfillment of the requirements

for the degree of

DOCTOR OF PHILOSOPHY

in

Molecular Physiology and Biophysics

May, 2013

Nashville, Tennessee

Approved:

Professor Alyssa Hasty

Professor Dave Piston

Professor Jay Jerome

Professor Aurelio Galli

To Ellie and Benton,

ACKNOWLEDGEMENTS

I am extremely thankful to have had the opportunity to study at Vanderbilt University under the mentorship of Dr. Anne K. Kenworthy. Anne has been a fantastic mentor and has pushed me to become a better scientist. I must also thank the current and recent Kenworthy lab members; Dr. Minchul Kang, Dr. Caroline Hanson, Kimberly Drake, Lewis Kraft, Bing Han and Courtney Copeland. You have aided in physically doing research, but have also inspired, challenged and taught me a great deal.

I must thank a number of people at Vanderbilt outside the Kenworthy lab. First on this list are my committee members; Dr. Aurelio Galli, Dr. Jay Jerome, Dr. Dave Piston and my committee chair, Dr. Alyssa Hasty. Many of the facility, staff and students at Vanderbilt University have helped in my training and I could never thank all of them. I do however need to thank the lab of Dr. Al Beth for the continuous use of their equipment and reagents. Additionally, I need to thank David Shifrin, Dr. Joseph Roland, Dr. Lynne LaPierre, Dr. Nicholas Baetz, Amicia Elliott and Tessy Sebastian, for always being there when I needed a construct, a protocol, or a valuable second opinion. Also, a number of collaborators aided us in the endocytosis research (Chapters IV and V) and I am thankful for it. They are Dr. Wayne Lencer (Harvard Medical School), Dr. Michael Davidson (The Florida State University), Michelle Baird (The Florida State University), Randall Holmes (University of Colorado), Michael Jobling (University of Colorado), and Trina Schroer (The Johns Hopkins University).

I need to thank the many teachers I have had throughout my education who have nurtured my curiosity and guided me to this place. In particular, Dr. Russell Camp of Gordon College for encouraging me to pursue a carrier in research. And my former coworkers at Elucida Research. I would never be here today if wasn't the

TABLE OF CONTENTS

LIST OF TABLES

LIST OF FIGURES

LIST OF ABBREVIATIONS

A488 ....Alexa Fluor® 488

A546 ....Alexa Fluor® 546

A555 ....Alexa Fluor® 555

AP2 .... adaptor protein 2

Arf6 .... ADP-ribosylation factor 6

BAR domain .... Bin–Amphiphysin–Rvs domain

Cav-1 .... Caveolin 1

Cav-2 .... Caveolin 2

Cav-3 .... Caveolin 3

CC1 .... coiled-coiled domain 1 of p150^{glued}

CIE .... clathrin independent

CME.. clathrin mediated endocytosis

CTx ....cholera holotoxin

CTxB ....cholera toxin B subunit

D..diffusion coefficient

DiIC$_{16}$ .... 1,1'-Dihexadecyl-3,3,3',3'-Tetramethylindocarbocyanine Perchlorate

L_o .... liquid ordered

MβCD .... methyl-β-cyclodextran

MEF ....mouse embryonic fibroblast

M_f .... mobile fraction

MTOC ....microtubules organizing center

NZ .... nocodazole

Rho .... rhodamine

SPT ....single particle tracking

STxB .... Shiga toxin B subunit

SV40 ....simian virus 40

UtrCH ....calponin homology domain of utrophin

YFP .... yellow fluorescent protein

CHAPTER I

INTRODUCTION

Overview

Cholera toxin is a member of a family of bacterial toxins, known as AB5 toxins (Figure 1). These toxins share a basic structural motif, consisting of an enzymatically active A subunit and a pentameric lipid binding B subunit. In addition to cholera toxin, this family includes such toxins as pertussis toxin, Shiga toxin, and heat labile enterotoxin [1]. Together the diseases induced by these toxins account for a huge human health burden. Cholera alone is estimated to cause approximately 100,000 to 120,000 fatalities annually [2]. Of the fatalities many are children, making cholera the second leading killer of children under 5 years of age [3].

Cholera toxin is produced by the gram-negative bacteria, *Vibrio cholera*. Specifically it is the 01 and 0139 serogroups which produce the toxin [4]. *Vibrio cholera* is passed from host to host through contaminated drinking water. Once ingested the bacteria gains access to the large intestine. There cholera toxin is endocytosed into the gut epithelial cells where it triggers a signaling cascade leading to dysentery. This dysentery can persist for up to two weeks and causes death by dehydration.

Current efforts to combat cholera are focused primarily on preventative measures and alleviating the symptoms, rather than combating the disease itself. Vaccines are available for cholera. However, these vaccines are not readily available in impoverished nations [4]. Additionally public works measures such as sewage and water treatment have dramatically reduced the prevalence of the disease. For this reason, cholera has been almost eradicated in the United States and other developed countries. However, in parts of the undeveloped world cholera remains a major health concern with cholera is still endemic in more than 50 countries [4].

Once cholera has been diagnosed the infection may be treated with antibiotics. However, as with the vaccine for cholera, antibiotics are often unavailable in the hardest hit regions. Furthermore, the change in cell signaling triggered by the toxin persists for many days after clearance of the bacteria. Therefore, treatment with antibiotics can only have limited benefits. A much more effective treatment method has been to counteract the dehydration caused by cholera through intravenous rehydration or oral salts. If diagnosed early and treated for dehydration, the survival rate for a cholera patient improves from less than 50% to 99.8% [4].

Even though public works measures and rehydration therapy have proven tremendously beneficial in the control and treatment of cholera, this does not mean that research into this disease is not worthwhile. The retrograde trafficking regime utilized by cholera toxin is conserved across the AB5 family of toxins. Furthermore, the medical approaches of public sanitation projects and control of symptoms has been less effect in controlling diseases associated with other AB5 toxins (primary pertussis, *E. coli* borne dysentery and Shiga toxin induced haemolytic uremic syndrome). Through better understanding of the workings of cholera toxin, we may build models which will serve to aid research into these diseases.

Toxicity of AB5 toxins is dependent on cellular uptake and specific trafficking within the cells. Once the bacterium has infected the host organism, the toxins they produce are targeted to the host's cell. This occurs through the toxin's multimeric binding to gangliosides of the host cells plasma membrane (Figure 2). Following binding, the toxins are endocytosed and trafficked retrograde to the trans-Golgi and endoplasmic reticulum (ER) [1, 5] (Figure 3). It is only those toxins which have made it the ER that can stimulate pathogenicity leading to disease. In this way, sorting of the toxin at the plasma membrane into specific class(es) of nascent endocytic vesicles and/or within the endosomal system is a primary factor in determining if the bacterial infection will lead to disease.

This raises a major question: what is it about AB5 toxin that causes them to be trafficked to the trans-Golgi, as opposed to being recycled back to the plasma membrane or taken to the lysosome for degradation? In addressing this question, a large amount of attention has been focused on the idea that the toxins may be sorted through interactions of the toxin's lipid receptors with lipid rafts, i.e. putative domains with cellular membranes
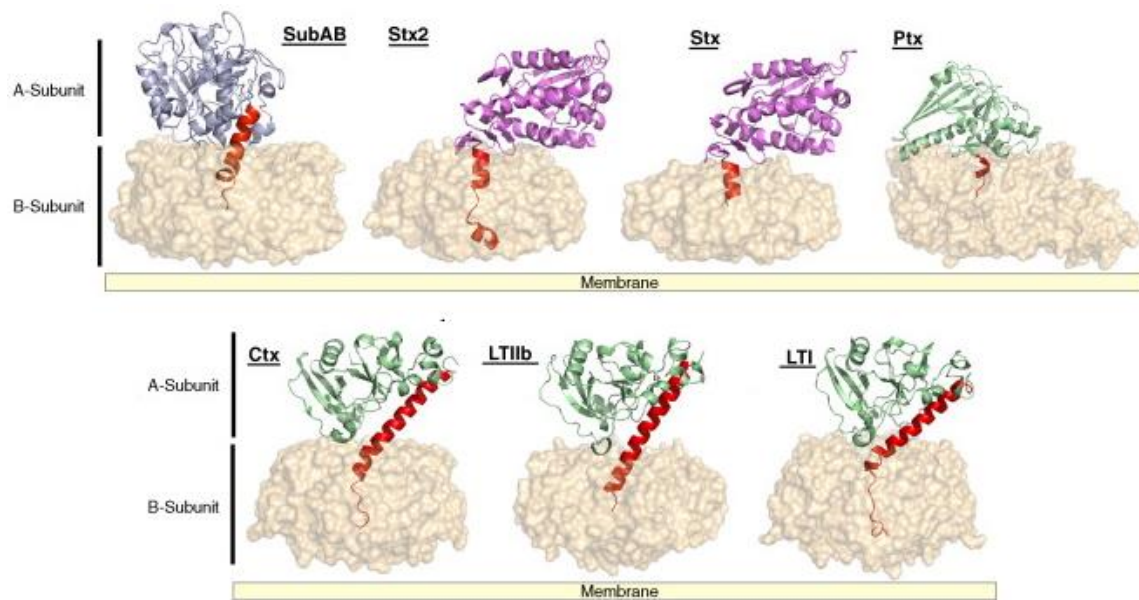
Figure 1. Molecular structures of AB5 toxins. The B-subunit is represented as a molecular surface. The A-subunits of subtilase cytotoxin (SubAB), Ctx, heat labile enterotoxin (LT), Stx and pertussis toxin (Ptx) are shown in cartoon representation and colored according to the respective catalytic activity (light blue for subtilase activity, light green for ADP-ribosylase activity and purple for RNA N-glycosidase activity). The common structural element (helix A2) is colored red, and the level of sequence identity of the A-subunit inside a family is indicated (modified from [1]).
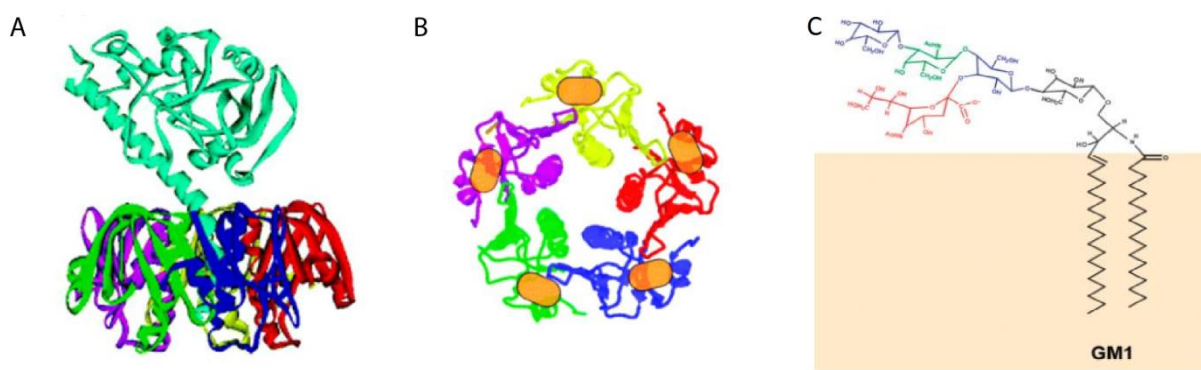
Figure 2. Ribbon diagram of the structure of cholera toxin and its receptor, GM$_1$. (A) Three-dimensional structure of cholera toxin. The A chain noncovalently associates with the central pore of the pentameric B-subunit via the rod-like A2-chain. (B) Top view of the homopentameric ring-like structure formed by CT B-subunit. Five binding sites (orange) for the GM1 receptor are formed by mutual contribution at the interface of neighboring subunits. (C) Molecular structure of the ganglioside receptor for CTxB, GM$_1$. (modified from [5])
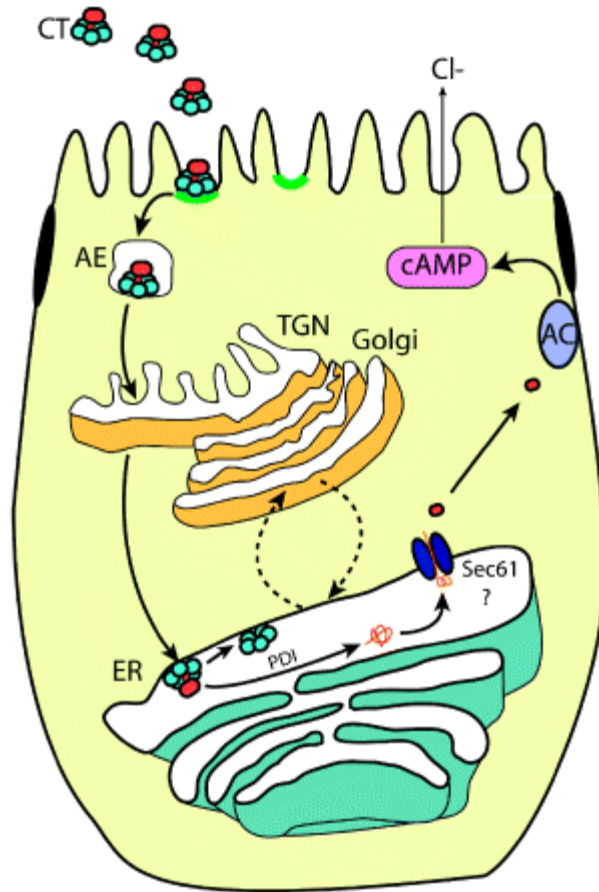
Figure 3. General pathway for CT entry into intestinal cells via lipid rafts. Cholera toxin binds to GM_1 localized in lipid raft domains (green) on the apical membrane via the B-subunit and is internalized into apical early endosomes. CT is then trafficked to the trans-Golgi network (TGN) and bypasses the Golgi apparatus on its way to the ER. Once inside the ER, protein disulfide isomerase (PDI) recognizes the cleaved form of the A1 chain (shown in red), where it is unfolded and dissociated from the B-subunit (in blue). The A1-chain is then retro-translocated to the cytosol, presumably by the Sec61 channel. CT can also recycle between the Golgi and ER via anterograde and KDEL-dependent COPI-mediated pathways (dotted arrows). Once in the cytosol, CT A-chain then induces chloride secretion by increasing cyclic AMP (cAMP) levels via adenylate cyclase (AC) by ADP ribosylating $G_s-\alpha$ (from [5]).

generated by weak lipid-lipid interactions. The lipid raft model proposes that rafts contain specific lipid compositions and that proteins partition preferentially into membrane domains of specific lipid compositions. By sorting components important for performing a specific task, such as signal transduction across the membrane or endocytosis, it is thought that rafts exercise a functional control over these processes [6].

In the case of cholera toxin, its association with plasma membrane rafts may function as a means to target the toxin to specific classes of nascent endocytic vesicles and thus regulating CTxB uptake [7-9]. Similarly, raft mediated sorting may have a role in sorting the toxin inside the early endosomes [7, 10, 11]. The concept that the toxin associates with lipid rafts originates from early work on rafts in which biochemical extraction of rafts, from non-raft membrane, was attempted. This work quickly identified cholera toxin as a putative raft associated protein [12]. Later, work in model membranes discovered cholera toxin to be highly enriched in putative raft-like regions within model membranes [13]. However, attempts to directly visualize rafts in live cell membranes have been largely unsuccessful, suggesting that rafts are too small and/or too dynamic to be imaged with current techniques. To overcome this obstacle the field has turned to microscopy based biophysics techniques (such as fluorescence recovery after photobleaching (FRAP), Förster resonance energy transfer (FRET) and fluorescence correlation spectroscopy (FCS)) to indirectly detect rafts. However, such biophysical approaches have yielded mixed results when it comes to detecting and characterizing lipid rafts.

An alternative approach to studying rafts has been to look at the functional consequences of cellular treatments predicted to perturb lipid rafts. Biochemical extraction and model membrane work has long indicated that cholesterol is necessary for raft formation [14], and so the consequences of cholesterol depletion on cellular processes has become the primary technique used to examine possible roles of lipid rafts in cells. For example, clathrin independent endocytosis is especially sensitive to cellular cholesterol and can be inhibited with acute cholesterol depletion, leading to the assumption that these are raft based mechanisms [15]. In fact, cholera toxin was one of the first cargo molecules observed to be using clathrin independent endocytosis [16, 17]. Additionally,

it has been shown that cholesterol depletion impairs the endocytosis of cholera toxin [18].   While these studies make a correlative argument for the involvement of rafts in toxin endocytosis, they leave much unanswered.

While evidence supports the idea that CTxB labels, and even aggregates, lipid rafts, how these rafts modulate CTxB dynamics and endocytosis remains unclear.   My work has addressed these issues in two ways: by focusing on the membrane organization of CTxB and by examining the uptake of CTxB by cells. First, by examining the diffusional properties of cholera toxin at the cell surface, I tested specific models of membrane organization in an attempt to detect diffusional properties consistent with (or contradictory to) previously published models of membrane organization, including lipid rafts. An abundance of literature exists to point to cholera toxin as a raft marker, and some studies indicate that CTxB cross-links rafts. Based on my research into CTxB, I cannot comment on the validity of CTxB as a raft marker, although I found no clear evidence that CTxB is cross-linking rafts. I did, however, find that the diffusion of CTxB is governed by actin.

Second, through live cell studies of the uptake of cholera toxin, I tested a very specific mechanism for the endocytosis in which toxin-stabilized rafts are absolutely necessary for uptake, a model henceforth referred to as "toxin-induced endocytosis". As with the FRAP work, my research into toxin-induced endocytosis demonstrates that this process is not-dependent on raft cross-linking by toxin; as previously proposed [19, 20]. Rather, this is an endogenous process which does not require the toxin at all.   Most importantly, we have established a novel role for cytoplasmic dynein and microtubules in bending the plasma membrane. Once published, our work will be only the second report indicating a role for dynein in endocytosis, and the first to show a role for this protein in microendocytosis (as the first involved a role in macropinosomes formation [21]). Furthermore, the toxin induced model has previously been implicated in the uptake of other lipid binding toxins and viruses. Therefore, our work on CTxB may prove important for a wide variety of diseases in addition to cholera.

Cholera toxin

Cholera toxin is secreted by the bacteria *Vibrio cholerae.* The toxin itself is a member of the AB5 class of bacterial toxins, and as such is comprised of a homopentameric B subunit and an enzymatically actively A subunit. The B subunit of the toxin is responsible for binding of the toxin to the host cells. It does this through 5 lipid binding sites located at the cleft between each subunit (Figure 2) [22, 23]. The toxin is generally considered to bind the ganglioside lipid GM_1, although other possible binding partners do exist [24-26].

The A subunit of cholera toxin is a single peptide comprised of two domains, A1 and A2. The A1 domain contains the catalytic domain while the A2 domain tethers the A subunit to the B subunit [1]. The A subunit functions as an ADP-ribosyltransferase that constitutively activates the G_s-α protein [27]. This activation of G_s-α results in activation of adenyl cyclase and elevation of cAMP levels, which results in mass chloride and water excretion [5]. When this processes occurs in the gut of the host organism the elevated chloride and water excretion results in dysentery.

Lateral membrane organization

Membrane organization of cholera toxin

Cholera toxin has become a popular tool for the study of the plasma membrane organization because of its common association with lipid rafts. The lipid raft model defines rafts as regions of cellular membranes containing a unique composition brought about through lipid-lipid interactions [6]. These lipid-microenvironments are thought to be preferential for specific proteins and not for others, leading to the lateral organization of lipids and protein in the membrane.

It was the observation that CTxB associates with DRM's that provided the initial evidence supporting an association between CTxB and lipid rafts [12, 28, 29]. Later *in vitro* studies collaborated this designation as fluorescently tagged toxin associates with raft-like, liquid ordered (L_o) membrane regions in GUV's and GPMV's [13, 30, 31].

While biochemical analysis and studies in model membranes indicate CTxB associates with lipid rafts, its interaction with rafts in live cell studies have been more difficult to demonstrate. In live cell microscopy studies, cholera toxin appears to be uniformly distributed at the cell surface [32, 33]. Lipids generally diffuse much faster than transmembrane proteins within the membrane [33], and so one would expect that a lipid bound protein would diffuse quickly like a lipid. However, biophysical studies of cholera toxin diffusion in live cells have revealed that its diffusion is slower than many other lipid anchored proteins [33, 34]. One plausible explanation for this slow diffusion is that CTxB may be associated with large immobile rafts.

One example of a class of large, immobile rafts is caveolae. These are flask shaped invaginations found on the plasma membrane (for more on caveolae see the "Nascent endocytic vesicles" and "Caveolae-mediated endocytosis" sections below). Since caveolae are known to be immobile in the plane of the membrane [35], the association of CTxB with caveolae seems like a likely explanation for the slow diffusion of CTxB. In fact, at least two studies have found that knocking down caveolin-1 resulted in increased mobility of CTxB at the cell surface [36, 37]. Further evidence for caveolae slowing CTxB comes from work investigating the intra-endosomal mobility of CTxB [7]. In this study, cholera toxin diffusion was examined enlarged endosomes were generated by expressing the constitutively active Rab5 Q79L mutant. This mutant form of Rab5 generates enlarged early endosomes, such that membrane domains can be visualized in the early endosomes. In Rab5 Q79L expressing cells, Caveolin-1-GFP was immobilized within enlarged endosomes, whereas CTXB was not. However, when cells were incubated in the presence of NH_4Cl to neutralize endosomal pH, CTXB became diffusionally restricted at sites enriched in caveolin-1-GFP [7]. These findings suggest that CTxB diffuses slowly at the cell surface as the result of its interaction with caveolar domains at neutral pH [7].

CTxB may not only report on membrane organization but also has the capacity to remodel membranes. CTXB binding has been shown to modulate the phase behavior of L_o/L_d mixtures in model membranes [13]. Giant unilamellar vesicles consisting of phosphatidylcholine, phosphatidylglycerol, sphingomyelin, cholesterol, and GM_1 that are doped with fluorescent probes that preferentially segregate into the L_o or L_d fractions showed one homogenous bilayer at the resolution of fluorescence microscopy. However, following CTXB treatment clear segregation of the membrane into two phases was seen [13]. A similar result was recently reported where CTxB induced large scale separation of raft and non-raft associating fluorescent probes in cytoskeleton-free plasma membrane vesicles, which were still attached to live cells [30]. To more directly test the role of crosslinking of CTxB, a recent study evaluated the toxicity and diffusion at the plasma membrane of a chimeric mutant cholera toxin containing 0, 1 or 2 functional binding sites for GM_1, as compared to wild type holotoxin's 5 GM_1 binding sites [28]. Since only those toxins having functional binding sites adhere to the cells, it is the 1 and 2 binding chimeras that were actually studied. The chimeric toxin exhibited some toxicity, although with reduced potency compared to wild type. Endocytosis was also reduced. However, the mutant toxin had M_f and D values similar to wild type CTxB, as assessed by confocal FRAP [28]. This suggests that pentavalent binding of GM_1 by CT_XB is important for efficient toxin uptake, but that it cannot explain the slow diffusion of the toxin while at the cell surface.

In addition to modulating the lateral organization of the cell surface, CTxB may also deform membranes. X-ray scattering studies have reported that CTxB binding increases the tilt angle of GM_1 within lipid monolayers and bilayers [38, 39], which could create a depression in the membrane under the toxin. In one extreme case CTxB binding to planar lipid monolayers caused the monolayers as a whole to transform into a series of tubules defined by negative membrane curvature, a state known as hexagonal membrane phase [38]. This repositioning of lipids and apparent bending of the membrane, can be seen in studies on GUV's where vesicles developed invaginations following labeling with fluorescent-conjugated CTxB [40].

Cortical actin corrals

One prominent model for membrane organization is known as the "picket and fence" model. In this model, the actin cytoskeleton forms fences along the inner leaflet of the plasma membrane [41-44]. These fences form corrals that can separate membrane regions, restricting the movement of transmembrane proteins as well as proteins anchored on the inner leaflet. In addition to physically impeding the movement of some membrane components, other proteins are bound directly to the actin cytoskeleton. Transmembrane proteins that are anchored directly to the actin cytoskeleton form pickets along the fences and impede the movement of molecules in both leaflets of the bilayer [45]. While the corrals separated by pickets and fences segregate the plasma membrane, molecules are not completely confined to these corrals. For instance, hop diffusion, where a molecule jumps out of one corral into another has been recorded with single particle tracking [45].

Lipid rafts

Lipid rafts are putative structures within the plasma membrane brought about by lipid–lipid interactions [6]. The discovery of lipid rafts was motivated by the question of how GPI-anchored proteins and glycosphingolipids are sorted to the apical surface of polarized epithelial cells [46, 47]. Brown and Rose showed that fractionating membranes with detergent results in the solubilization of much of the membrane and the isolation of GPI and sphingomyelin enriched membrane sections [48]. These fractions became known as detergent resistant membranes (DRM's), and are proposed to be held together primarily by lipid-lipid interactions. The idea that lipids could interact with one another is supported by work in model membranes.

In protein free model membranes containing unsaturated phospholipid, sphingomyelin and cholesterol, the lipids can spontaneously segregate into two distinct phases. In one phase, the lipids assume a liquid disordered state (L_d) characterized by both highly flexible acyl chains and highly mobile lipid molecules. In the other phase, sphingomyelin and cholesterol molecules are tightly packed and exhibit more restricted motion. This phase has been called the liquid ordered or L_o phase [49]. These L_o phases produced in model membranes, as with DRMs, have been equated with lipid rafts [50]. Membrane proteins are, in turn, hypothesized to

11

preferentially associate with either L_o or L_d regions of the membrane. While these model membrane systems may be convenient tools, they are extremely simple and may not accurately reflect rafts in native membranes.

Biochemical detergent extraction and biophysical studies in model membranes have generated an enormous body of literature detailing the function of lipid rafts and physical mechanisms underlying their formation. Yet, with few notable exceptions [31, 51, 52], most attempts to visualize large-scale phase separation *in vivo* have been unsuccessful. Even some biophysical measurements with a spatial resolution of better than 100 Å have shown that the majority of raft proteins appear to exist as monomers and only a few in clusters [33, 53-55]. This has led to the conclusion that if rafts exist *in vivo* they are generally small and also likely highly dynamic.

In a hallmark paper, Saffman and Delbruck described diffusion within a lipid bilayer as inversely proportional to the hydrodynamic radius (analogous to the area at the surface of the membrane) of the diffusing particle, the viscosity of the membrane and the thickness of the membrane [56]. With the advent of the lipid raft model many years later, it was evident from Saffman and Delbruck's equation that raft markers have slowed diffusion through two mechanisms. First, since rafts lipid are thought to more highly ordered and more densely pack than non-raft lipids, the viscosity inside the rafts should be greater than the viscosity outside the raft. Therefore, raft particle will display slower diffusion as they move through rafts as compared to non-raft particles diffusing in the less viscous non-raft regions of the membrane. The second means by which rafts may alter diffusion is based on the principle that rafts are complexes of lipids and proteins. As complexes they should have effective hydrodynamic radii much larger than the hydrodynamic radius of a single lipid or protein. This enlarged effective hydrodynamic radius will in turn slow the diffusion of the raft as compared to non-raft particles, which diffuse as single entities. Based on these two lines of thinking, a wide range of models has been proposed to link diffusion to rafts [33, 57, 58]. While the idea that rafts should impact diffusion has been a promising one, experimental data has been less than decisive and even at times contradictory. A number of models have been put forth in an effort to reconcile the sometimes conflicting data on raft structure and dynamics [59-63]. Interestingly, the diffusion of CTxB is abnormally slow [33, 34], and while many factors could account for this slow diffusion, the putative association of CTxB with rafts makes raft modulated diffusion an interesting possibility.

Actively maintained domains

The classical model of lipid rafts is that their components dynamically partition into the rafts from the bulk membrane. This model implies that as the number of raft components in the membrane increases the number of raft molecules inside each raft should also increase [64]. However, cases have been reported where increasing the concentration of putative raft proteins resulted in the formation of more microdomains, while the number of proteins within each microdomain remained constant [53, 64, 65]. As this phenomenon is contradictory to the laws of mass action, it has been proposed that the cells must be actively regulating microdomain size and composition. Thus, I will refer to these domains as "actively maintained domains". It is important to note that while this model implies that energy expenditure by the cell is required to maintain these domains, this has never been directly tested.

Similar to lipid rafts, the formation and maintenance of actively maintained domains is thought to be dependent on cholesterol and sphingolipids [53, 64]. However, it appears that actin plays a major role in the maintenance of these domains. Initial evidence for this comes from the observation that these domains dissipate under actin disruption [64]. This is supported by the observation that plasma membrane blebs devoid of F-actin do not contain actively maintained domains [66]. Interestingly, conventional rafts do not dissipate but rather coalesce in the absence of cortical F-actin [31], highlighting the opposing effects of actin on these two classes of microdomains. Furthermore, actively maintained domains are dependent on myosins as treatment with blebbistatin causes them to dissipate [66]. Together, this characterization has led to a model for the formation of actively maintained domains which recently appeared in *Cell* [67]. This model proposes that small asters of cortical actin contain myosins which link the actin asters to the plasma membrane. The power stroke of the myosins leads to convection of the plasma membrane. During convection specific lipid species become trapped in small regions devoid of these short actin filaments [67].

Microtubules

There is very little known about the impact that microtubules may have on diffusion within the plasma membrane. However, a recent Cell paper by Jaqaman et al., used particle tracking to following the diffusion of receptors at the cell surface revealed such an interaction [68]. The authors found that the diffusion at the plasma membrane of one receptor in particular, CD36, was confined by cortical actin. However, unlike the corrals identified previously [69, 70], which have a semi-symmetrical shape, CD36 was confined in long rectangular actin-defined regions [68]. Furthermore, while delineated by cortical actin, these rectangular regions appeared to align with microtubules near the cell surface. Based on this finding, Jaqaman et al. proposes that the microtubules may indirectly influence the plasma membrane architecture by patterning cortical actin. Furthermore, they suggest that CTxB, like CD36, may also become trapped in these microtubule-induced corrals [68]. While an exciting observation, much more work needs to be done to understand the possible roles of microtubules in determining plasma membrane structure and function.

Caveolae

The plasma membrane serves as a physical barrier between the cell and the outside environment. Therefore, in order for many proteins to gain access to the cell they must be actively endocytosed by the cell. It is thought that nascent endocytic vesicles docked at the plasma membrane can arrange the plasma membrane by concentrating or depleting specific membrane components. While this is potentially true for all forms of endocytosis, the role of caveolae in membrane organization is the most studied.

Caveolae are large (60-80 nm), flask like invaginations on the plasma membrane composed of caveolin proteins, cavin proteins, and EHD2 [71-78]. Furthermore, they have specific lipid composition and require cholesterol for their formation [71, 79-83], potentially making them one form of lipid raft [6]. These invaginations spend large amounts of time stably docked at the cell surface with their lumens open to the fluid phase outside of the cell [84]. Eventually they separate from the membrane as caveolar vesicles to facilitate trafficking (see the "Caveolin Mediated Endocytosis" section for more on caveolin mediated endocytosis). While docked at the cell

surface caveolae are laterally immobile [35, 84]. A large body of work has examined the potential role of these

docked caveolae on the lateral organization of membrane molecules [85].   At least two studies have linked CTxB

diffusion with the presence of caveolae [36, 37].

Mechanisms of endocytosis

General process of endocytic uptake

Endocytosis is a general term that describes the vesicular mechanisms that cells use to take up cargo from

the plasma membrane or fluid phase outside of the cell. Endocytosis serves a number of important functions for

the cell, such as the facilitating the uptake of nutrients, regulation of receptor availability at the cell surface, and

regulation of plasma membrane volume. Endocytic mechanisms are generally divided into two classes; macro- and

micro-endocytosis. Macroendocytosis involves the uptake of large particles and/or large volumes of fluid phase,

such as occurs during pinocytosis and phagocytosis (figure 4) [86]. Microendocytosis, on the other hand, refers to

the wide variety of endocytic mechanisms that internalize smaller volumes of cargo (Figure 4). Formation of

vesicles in macroendocytosis is mediated primarily by actin and is a stimulated event [86]. Vesicles formed through

microendocytosis are widely thought to form by proteins binding to and bending the plasma membrane, and not

directly through cytoskeleton mediated processes.   Furthermore, microendocytosis can occur via stimulated (via

receptor mediated cell signaling) or constitutive mechanisms. Pathways which fall under this form of endocytosis

include clathrin-mediated endocytosis, as well as caveolar endocytosis, CLIC/GEEC, Arf6, and toxin induced [86,

87]. Although the word "endocytosis" specifically refers to both macro- and micro-endocytosis, it is often used in

the field interchangeably with "microendocytosis". I will follow this implied meaning of the word "endocytosis" for

the remainder of the document.

While the specifics of how endocytosis is performed in each pathway vary, the process can be broken

down into five general steps. First, endocytosis must be initiated. Often this means that receptor-mediated

signaling initiates endocytosis although some endocytosis is constitutive. Second, the cargo must be sorted into the forming vesicle. This is necessary such that the proper membrane lipids and receptors must be organized laterally such that the newly formed vesicle endocytose the proper material. Third, the plasma membrane must be deformed into an invagination. The order of these first three steps is not conserved and can be performed in different orders or simultaneously. Once a nascent vesicle has formed it must be scissioned from the plasma membrane. And lastly, the new vesicle must be trafficked to the appropriate site inside the cell.

Endocytic trafficking of cholera toxin

The endocytosis and retrograde transport of cholera toxin is vital for the protein to induce a toxic host response. However, the exact mechanism of endocytosis and sorting in the endosomal network which results in the toxin reaching the Golgi and ER remains unclear. Part of this uncertainty probably arises from the fact that the toxin is very pervasive in its utilization of endogenous endocytic pathways. Cholera toxin has been reported in the literature to utilize clathrin coated vesicles, caveolae, Arf6-positive vesicles, and the GEEC/CLIC pathway; including flotillin and GRAF-1 positive vesicles [88-93]. Additionally, in the last few years a model has been put forward that CTxB, along with other AB5 bacterial toxins, may assemble their own endocytic vesicles by remodeling the plasma membrane [20, 40].

Clathrin-mediated endocytosis

Many of the endocytic mechanisms are not well understood. However, one mechanism, clathrin-mediated endocytosis, has been extensively studied and therefore is well characterized. Clathrin mediated endocytosis occurs constitutively or can be induced through receptor activation and cell signaling [94]. Following receptor activation, a signaling cascade is initiated which leads to the recruitment of a series of lipid binding proteins to the plasma membrane [95-97]. These proteins contain special membrane binding domains (such as
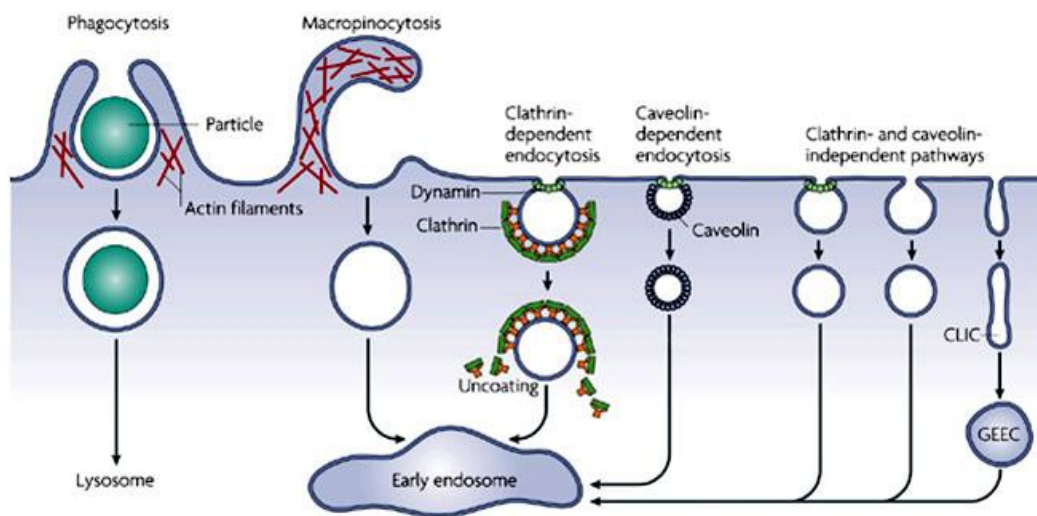
Figure 4. **Multiple mechanisms exist to facilitate endocytosis**. Large particles can be taken up by phagocytosis, whereas fluid uptake occurs by macropinocytosis. Both processes appear to be triggered by and are dependent on actin-mediated remodeling of the plasma membrane at a large scale. Compared with the other endocytic pathways, the size of the vesicles formed by phagocytosis and macropinocytosis is much larger. Most internalized cargoes are delivered to the early endosome via vesicular (clathrin- or caveolin-coated vesicles) or tubular intermediates (known as clathrin independent carriers (CLICs)) that are derived from the plasma membrane. Some pathways may first traffic to intermediate compartments, such as the glycosyl phosphatidylinositol-anchored protein enriched early endosomal compartments (GEEC), en route to the early endosome (modified from [86]).

Bin–Amphiphysin–Rvs (BAR) domains) which bend and/or stabilize curved membranes. These proteins arrive at the site in a dedicated order with those mediating the shallowest bend arriving first, followed by those having increasingly sharper angles [87, 98]. In this way these proteins are capable of mechanically deforming the planar membrane into the nascent endocytic vesicle. One protein recruited during formation is adaptor protein 2 (AP2) which recruits clathrin to the membrane. Clathrin is actually a complex of two proteins, clathrin light chain and clathrin heavy chain. Clathrin is organizes in the cytoplasm structures known as clathrin triskelion, containing three clathrin light chains and three clathrin heavy chains. It is clathrin in this triskelion conformation that binds to AP2 on the inner leaflet of the plasma membrane. As clathrin is the primary scaffolding protein for the stabilization of the endocytic vesicles, it is considered the "coat" protein for this pathway. As new clathrin triskelions arrive they interlock with one another to produce an invagination covered in clathrin.

After the clathrin coat has stabilized as a spherical, nascent vesicle the invagination must be scissioned. Scission of clathrin coated pits is facilitated by the GTPase dynamin [99]. Three distinct dynamin proteins exist. Dynamin 1 and 3 are found in a very limited number of tissues, while Dynamin 2 appears to be ubiquitously expressed [100]. Dynamin homooligomerizes around the neck of the invaginations and uses GTP hydrolysis to power a conformational change that scissions the nascent vesicle from the plasma membrane [101]. This scission event coincides with a buildup of F-actin between the nascent vesicle and the plasma membrane [102]. This actin has been proposed to aide both in the scission of the vesicle and in the early trafficking of the vesicle [103]. However, it is important to note that in most mammalian cells types, F-actin alone cannot scission clathrin vesicles from the plasma membrane [104, 105].

Caveolin-mediated endocytosis

After clathrin-mediated endocytosis the next best characterized form of endocytosis is caveolin-mediated endocytosis. This pathway is mediated by flask like invaginations of the plasma membrane known as caveolae. Three classes of proteins have thus far been identified as stable components of caveolae; the caveolin proteins, the cavin proteins and EHD2 [75, 106, 107]. The caveolin family has three members; Cav-1, Cav-2 and Cav-3.

Caveolin-1 and Caveolin-2 are ubiquitously expressed throughout the body while Cav-3 is found primarily in muscle. Cav-1 or Cav-3 must be present for caveolae to form [72, 108]. Caveolin-2 incorporates into caveolae but appears to not be necessary for caveolae formation [109].

Additionally, caveolae have specific lipid compositions, as they are enriched in sphingolipids, cholesterol and GPI-anchored proteins [110]. Caveolae require cholesterol for their formation [84, 106, 111, 112]. This specific lipid composition and dependence on cholesterol has led to caveolae being considered a specific type of lipid raft [6].

Unlike clathrin coated vesicles which acquire their coat after membrane deformation and lose it following scission from the plasma membrane, caveolae are stable complexes which retain their coat proteins. They assemble as complexes in the Golgi apparatus [84] and then bud and fuse with various membranes in the cells to facilitate intracellular trafficking. When they traffic to the plasma membrane the caveolin-containing vesicles dock at the cell surface with their lumens open to the fluid phase. Caveolae spend considerable amounts of time docked like this before scissioning and again trafficking cargo [35, 84, 113]. The scission of caveolae is mediated by dynamin [114]. Furthermore, EHD2 has recent been reported to play a role in scission of caveolae as well [75]. Although for many years it was though that caveolae traffic to a dedicated early endosome, dubbed the "caveosome", it now appears that the caveosome does not exist [112]. Rather, most cargo entering cells via caveolin vesicles is transported direct to classical early endosomes [112].

Arf6 endocytosis

One example of a less well characterized clathrin independent endocytic mechanism is the Arf6 endocytic pathway. This endocytic pathway was first discovered by Julie Donaldson's group at the NIH, when they identified the Arf6 G protein trafficking from the plasma membrane in vesicles that were neither clathrin nor caveolae [115]. In addition to Arf6 a large number of cargo proteins have been associated with Arf6 endocytosis including CTxB, MHC-Class I, and H-Ras [93, 116, 117], among others [118, 119].

As of yet, no coat proteins have been associated with this endocytic mechanism. Furthermore this pathway is dynamin independent [120], although a scission mechanism has not been clearly established. Furthermore, very little research has been done into the mechanism responsible for early movements of Arf6 vesicles. One paper does however indicate that intact microtubules are necessary for Arf6 endocytosis [93].

CLIC/GEEC pathway

An alternative clathrin independent pathway has been described which specifically internalizes GPI-anchored proteins, a pathway commonly referred to as the CLIC/GEEC pathway (clathrin independent carriers and GPI enriched endocytic compartments) [121]. Endocytic vesicles in this pathway, known as CLIC's, are tubular and are thought to fuse together to generate a unique early endosomes, the GEEC [108]. GEEC's go on to acquire the endosomal markers Rab5 and EEA-1, and merge with the conventional Rab5/EEA-1 early endosomes [122].

It was initially reported that CLICs are uncoated [108], but more recent studies indicate the presence of two coat proteins, GRAF-1 and flotillin, on CLICs [90, 92]. GRAF-1 is a Rho GEF which contains both a dynamin binding site and a BAR domain [92]. As a BAR domain protein GRAF-1 labels tubular CLICs inside the cell [92]. Work with this protein suggests that it homooligomerizes around tubular vesicles, which under EM appear morphologically similar to CLICs [90]. Furthermore, GRAF-1 positive tubules colocalize with a model GPI-AP, GFP-GPI [92]. The second coat protein which may associate with CLIC's is flotillin [90, 91]. This protein was originally identified in the low buoyancy fractions of DRM and thought to be a component of caveolae [123]. However, it was later shown that flotillin can act as a coat separate from caveolae, to facilitate endocytosis of GPI-anchored proteins [91]. While flotillin is most commonly observed as puncta at the fluorescence microscopy level [91], flotillin has also been found on tubular vesicles thought to be CLICs [90]. While recent data indicates that GRAF-1 and flotillin coated vesicles are the same class of structure, the data come primarily from one recent paper [90] and to what extent CLIC's, GRAF-1 positive, and flotillin positive vesicles overlap remains unclear.

The exact mechanical process which leads to the formation of CLIC's is not well understood. However, a number of cellular factor have been identified as being important to the process. First, endocytosis of GPI-AP's is sensitive to both cholesterol and sphingolipid depletion [124, 125], suggesting that lipid rafts play an important role in CLIC formation. Furthermore, actin is extremely important to GPI-AP uptake as uptake is impaired by actin disruption (with Lat A or Cytochalasin D) or actin stabilization with Jasplakinolide [124]. It has been shown that the role of actin in CLIC endocytosis is regulated through Arf1 signaling [126]. This G protein regulates the GTP/GDP cycle of the Rho family GTPase, Cdc42 [126]. Cdc42 is a major signaling regulator of the F-actin nucleating protein, N-WASP, and thus it is thought that interfering with Cdc42 impairs N-WASP and alters actin dynamics [124]. Additionally, expression of dominant negative Cdc42 (myc-Cdc42(N17)) reduced the number of GEEC's [121]. While actin is clearly important to the formation of CLIC's it is currently unclear if actin's role in the process is in membrane organization, membrane deformation or scission.

Along these same lines there is uncertainty about the role of dynamin in the scission of CLIC's from the plasma membrane. Endocytosis of GPI-AP's is insensitive to dynamin inhibition [121]. However, GRAF-1 specifically binds to dynamin and dynamin is responsible for the scission of GRAF-1 positive tubules from the plasma membrane [92].

Toxin-induced endocytosis

While the evidence suggests that cholera toxin will utilize almost any available constitutive endocytic mechanism [88-93], a model has emerged in recent years proposing that the toxins may also induce the formation of endocytic vesicles [19, 20]. Evidence for toxin-induced endocytosis comes primarily from work with another AB5 bacterial toxin, Shiga toxin B subunit (STxB) [20]. More recently data has emerged supporting the concept that this form of endocytosis is also utilized by the CTxB and the SV40 virus, which also binds multiple GM_1's [40].

This form of endocytosis is based on the initial observation that STxB is found in plasma membrane invaginations under ATP depletion, actin disruption, dynamin inhibition and cholesterol depletion [20] (Figure 5).

These data have been interpreted as showing that these treatments inhibit the scission of endocytic vesicles from the cell surface and the invaginations therefore represent nascent endocytic structures. An intercalating membrane dye, FM4-64, was not seen in invaginations under ATP depletion in the absence of STxB, suggesting that the toxin is required for the formation of these invaginations [20]. Furthermore, the fact that these invaginations appear in ATP depleted cells, indicated to the authors that the mechanical force deforming the membrane must be coming from the toxins, and not from an endogenous, energy dependent processes [20]. Confirming this interpretation was the observation that GUV's labeled with STxB contain invaginations, showing that toxins are intrinsically capable of deforming membranes [20]. This ability to deform the membrane is dependent on multivalent binding of the Gb_3 by STxB, as a mutant form of STxB with a reduced number of functional lipid binding sites could not generate tubules in GUVs [20]. Interestingly, the multivalent binding of Gb_3 by STxB can induce formation of large, toxin-enriched membrane domains [127]. It is thought that these patches may form through the cross-linking and stabilization of subresolution Gb_3 positive lipid rafts [128]. The model in the literature for invagination assembly proposes that the toxin reorients Gb_3 in the membrane to generate negative curvature under the protein. Cross-linking of membrane microdomains allows the depression under each individual toxin to become exaggerated over the entire domain until a membrane invagination is created [19, 20, 128]. The fact that these invaginations grow under cholesterol depletion, actin disruption, ATP depletion, and dynamin inhibition has been interpreted as evidence that each of these factors is important for scission from the plasma membrane. If scission is inhibited, additional toxins cluster at the invaginations and "push" the invagination deeper into the cell [20].

Although it has been proposed that toxin-induced tubules represent a novel class of endocytic structures, there is conflicting evidence about their relationship to known endocytic pathways. Stalled STxB invaginations formed in ATP depleted cells lack clathrin [20]. However, tubules formed in the absence of STxB under actin disruption appear to be derived in part from clathrin-coated pits as the invaginations contain the canonical CME marker, transferrin receptor [129]. STxB positive tubules formed under ATP depletion were initially shown to lack caveolin-1 and form in caveolin-1 KO MEF's, indicating that they are not caveolar in origin [20]. A separate group has found caveolin on STxB positive invaginations under ATP depletion [76]. Additionally, in an extensive study of

CTxB positive invaginations under actin disruption, the invaginations were positive for Caveolin-1 [130]. A variety of endocytic mechanism beside clathrin and caveolin based uptake are known to exist including Arf6 and CLIC/GEEC pathways. There is currently no data in the literature to establish whether or not toxin-induced endocytosis is related to these pathways.

Additionally, nothing is known about the potential role of other cellular machinery in generating these tubules. In fact the current model proposes that AB5 toxins are sufficient to generate membrane invaginations, without involvement from endogenous proteins. This said, a rigorous search for endogenous proteins which may be involved in the formation of toxin-induced invaginations has not been carried out.

Cytoskeleton and endocytic trafficking

Actin and myosins

Once an endocytic vesicle has been formed it must be trafficked to its target organelle. Regardless of where the vesicle is going, microfilaments are required to move the vesicle to its destination. The literature indicates that the movement of endocytic vesicles from the plasma membrane is largely an actin-based process. In yeast, clathrin coated and uncoated vesicles can clearly be seen moving along actin cables to the early endosomes [131, 132]. This movement along actin filaments would imply that actin motors, myosins, are providing the physical force for movement. In fact, in mammalian cell one specific myosin species, myosin VI, has been closely tied to endocytosis. This myosin has been shown to colocalize with endocytic vesicles in the cell periphery. Also, impairing myosin VI through the overexpression of its tail domain leads to the accumulation of uncoated, transferrin positive vesicles near the cell surface. And, overexpression of the tail domain slows the accumulation of transferrin in early endosomes [133]. In summation, this data provides evidence for a dependence on myosin VI in clathrin mediated endocytosis, and supports a model of endocytic trafficking along actin cables in mammalian cells.
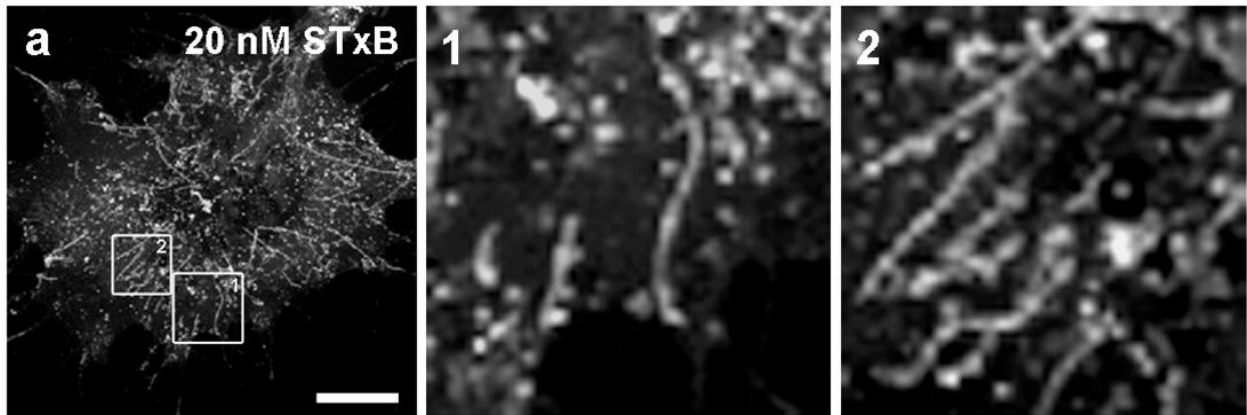
Figure 5. STxB accumulates in plasma membrane invaginations under ATP depletion. HeLa cells were ATP depleted with 2-deoxy-glucose and sodium azide for 30 minutes prior to labeling with Cy3-STxB. Under continued ATP depletion conditions at 37°C, the toxin can be seen in plasma membrane invaginations (modified from [20]).
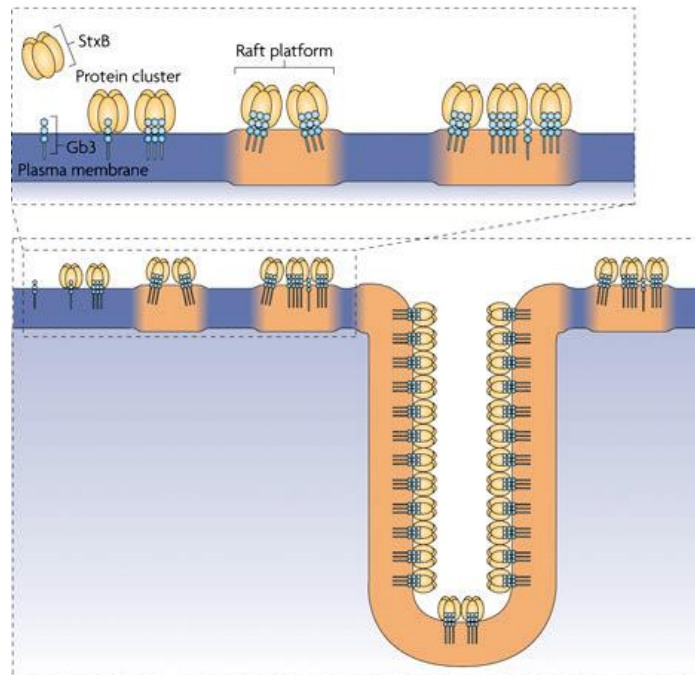
Figure 6. **Model for the induction of plasma membrane invaginations by the B subunit of Shiga toxin.** The pentavalent Shiga toxin B binds to up to 15 G_{b3} globosides. This binding in predicted to cluster and stabilize lipid rafts, enriched in the toxin. Repositioning of Gb_3 within the membrane of the membrane leads to localize membrane deformation, which becomes exaggerated when the toxins are clustered in a raft. Under cellular perturbations that inhibit scission these invaginations elongate from the cell surface, but it has been proposed [20] that in the absence of these perturbations the cells would recognize the invaginations, scission them and thus form endocytic vesicles (modified from [128]).

Alternatively, actin may nucleate behind the vesicle to "push" the vesicle into the cell. It is well documented that the listeria bacteria, once endocytosed, utilizes actin polymerization to force the bacteria containing vesicle through the cytoplasm [134]. These actin comets have recently been shown to originate at partially formed clathrin coated pits on the vesicles [135], suggesting that actin polymerization is being driven through a clathrin associated process. Similarly, there is a growing body of evidence to indicate that new F-actin polymerization is important for conventional clathrin mediated endocytosis. It has been observed that there is a build-up of actin at clathrin coated vesicle which temporally coincides with the movement of vesicles from the plasma membrane. This same study reported that this movement could be blocked with actin disrupting drugs [136]. A similar process may be involved in early movement of caveolae [137].

Microtubules and microtubule motors

Microtubules are intracellular filaments composed of polymerized α- and β-tubulins. In non-dividing cells, microtubule originate primarily from γ-tubulin containing complexes at the microtubule organizing center (MTOC) and Golgi complex, with a very small number also originating at the primary cilia [138-141]. The growth of microtubules is polarized, with the minus end at the nucleating site and the plus tip at the distal end.

Microtubules serve as tracks along which intracellular trafficking occurs. This occurs through microtubule motor proteins which bind membrane associated protein complexes and use ATP to walk along microtubule tracks. The motors fall into two basic classes, kinesins and dynein. Kinesins comprise a family of over 40 motor proteins [142]. The movement of kinesin is restricted in that they typically walk from the minus to plus tip of the microtubule (i.e. away from the Golgi or MTOC). Cytoplasmic dynein is only a single protein, and is the primary microtubule motor to facilitate minus-end directed vesicle movement towards the Golgi or MTOC.

There is very little evidence that microtubule motors are directly involved in the early stages for endocytosis. It is thought that kinesin-1 may facilitate endocytosis of focal adhesions [143], the site where plasma

membrane proteins bind the cell to its substrate. Since dynein's function is to move cargo from the cell periphery inward, it seems like a likely candidate for facilitating movement of endocytic vesicles. However, the major consensus in the field is that dynein plays no direct role in endocytosis, as one recent review of endocytosis stated that no evidence exists for dynein mediated movement of endocytic vesicles [144]. However, there is in fact one paper, supporting a primary role for dynein in pinosome trafficking and even formation [21]. This paper found that disruption of dynamin has no effect on transferrin uptake but significant decreased the uptake of the fluid phase marker, dextran. Furthermore, there is limited evidence some kind of microtubule involvement in caveolae, clathrin, and Arf-6 endocytosis [93, 129, 130]. However, these studies did not examine the mechanism through which microtubules were involved, so whether cytoplasmic dynein is important for the processes remains unclear.

CHAPTER II

METHODS

Cells and reagents

COS-7 cells, HeLa, caveolin-1$^{+/+}$ mouse embryonic fibroblasts (MEF), and caveolin-1$^{-/-}$ MEFs were acquired from ATCC (Manassas, VA). BSC-1 cells were a kind gift from Ramiro Massol (Harvard University). RFP-α-tubulin stably expressing HeLa lines were a kind gift from Paul Chang (M.I.T). COS-7, MEF, and BSC-1 cell lines were maintained in Dulbecco's modified Eagle medium (DMEM) containing 10% fetal bovine serum at 37ºC and 5% CO_2. HeLa cells were maintained in Roswell Park Memorial Institute medium (RPMI) containing 10% fetal bovine serum at 37°C and 5% CO2. RFP-tubulin HeLa were grown at 37°C and 5% CO2 in RPMI containing 10% fetal bovine serum and G418. Cells were plated on coverslips or MatTek dishes two days prior to experiments. Hela and COS-7 cells were transfected using Fugene6 (Roche). BSC-1 cells were transfected with Xfect (Clontech). All transfections were performed 24 hours prior to imaging or fixation.

Cholera toxin B subunit from *Vibrio cholerae* (Sigma-Aldrich, St. Louis, MO) was labeled with Alexa546 using an Alexa546 fluorophore protein labeling kit (Invitrogen, Carlsbad, CA). Cy5-CTxB was produced using Cy5 monoreactive dye packs (Amersham Bioscience, Piscataway, NJ). Alexa488-CTxB, Alexa555-CTxB and DiIC$_{16}$ (1,1'-dihexadecyl-3,3,3',3'-tetramethylindocarbocyanine perchlorate) were obtained from Invitrogen (Carlsbad, CA). Rhodamine phalloidin was from Invitrogen-Molecular Probes (Carlsbad, CA). Yellow fluorescent protein (YFP) tagged versions of a model GPI-anchored protein (YFP-GL-GPI) and a model transmembrane protein (YFP-GT46) have been previously described [145-147]. Alexa488-STxB and a plasmid encoding Gb$_3$ synthase [148, 149] were gifts from Dr. Ludger Johannes (Institut Curie, Paris, France). Plasmids containing EGFP-HRas and EGFP-381 (consisting of GFP fused to the C-terminal 10 amino acid residues of HRas) were provided by Mark Philips (NYU

School of Medicine) [150]. GFP-UtrCH [151] was a gift from Matt Tyska (Vanderbilt University). GFP-F-tractin [152] was provided by John Hammer (NIH). The mCherry-α-tubulin plasmid was provided by Irina Kaverina (Vanderbilt University). GFP-EB3 [153] was a gift from Anna Akhmanova (Utrecht University). CC1-dsRed and GFP-p50 [154, 155] were gifts from Trina Schroer (Johns Hopkins). mCherry-Rab11a and mVenus-Rab11a generated from previously reported Rab11a fusion proteins [156] were provided by Jim Goldenring (Vanderbilt University). Mouse anti-GFP antibody was acquired through Invitrogen-Molecular Probes (Carlsbad, CA).

mCherry-LAMP-1 provided by Mike Davidson was constructed by fusing the mammalian expression plasmid for mCherry to rat lysosomal membrane glycoprotein 1 (LAMP1; NM_012857; gift from George Patterson, NIH). The following primers were used to PCR amplify LAMP1: forward (with XhoI restriction enzyme site): GGA CTC AGA TCT CGA GCG CCA CCA TGG CGG CCC CGG GCG CCC GG; reverse (with BamHI restriction enzyme site): GTC ACG CGG GCT ATC AGA CCA TCT CGG AAT TCG GCT CCA CCG GCT CCA CCG GCT CCA CCG GCG CGG ATC CAC CGG TCG. The PCR product was gel-purified and sequentially digested with XhoI and BamHI and ligated into a similarly digested mCherry-N1 cloning vector to produce mCherry-LAMP1 with a 20-amino acid linker separating mCherry from LAMP1.

D(+)glucose, sodium azide, 2-deoxyglucose, bovine serum albumin (BSA), trichloroacetic acid, Latrunculin A, nocodazole, dynasore and HPI-4 (ciliobrevin A) were purchased from Sigma Aldrich. Jasplakinolide was purchased through Invitrogen (Carlsbad, CA). Taxol was from Alexis Biochemical (San Diego, CA). HEPES and TAE buffers were purchased from Mediatech, Inc (Manassas, VA).

Treatments

Exogenous cell labeling

Cells were rinsed twice with imaging buffer (composed of phenol red-free DMEM supplemented with 25 mM HEPES (Sigma-Aldrich), and 1 mg/ml albumin bovine serum (Sigma-Aldrich)), and then incubated for 5 minutes

at room temperature with the indicated concentration of CTxB (1 nM - 1 μM), 5 μg/ml DiIC$_{16}$ or 75 nM STxB. Cells were then rinsed twice with imaging buffer and imaged.

Phalloidin staining of F-actin

For phalloidin staining, cells were fixed in 3.7% PFA for 15 min at RT. They were then washed, permeabilized with 0.1% saponin in PBS containing 1 mg/ml bovine serum albumin for 15 min at room temperature (RT), and labeled with rhodamine-phalloidin (1:40) for 30 min at RT. Next cells were washed with 1x PBS and mounted in Fluoromount G (Southern Biotech, Birmingham, AL) supplemented with 25 mg/ml DABCO (1,4 diazabicyclo[2.2.2]octane) (Sigma-Aldrich) and allowed to solidify overnight prior to imaging.

ATP depletion

ATP depletion was performed by pre-incubating cells at 37°C and 5% CO$_2$ for 15 min in ATP depletion medium, composed of phenol-red free DMEM containing 50 mM 2-deoxy-D-glucose (Sigma-Aldrich), 0.02% sodium azide (Amersham Pharmacia Biotech), 25 mM HEPES (Sigma-Aldrich), and 1 mg/ml bovine serum albumin (Sigma-Aldrich)), as described in [157]. Control cells were incubated in ATP control medium (composed of phenol-red free DMEM with 50 mM D-(+)-glucose (Sigma-Aldrich), 25 mM HEPES, and 1 mg/ml BSA). Cells were then washed with their respective medium, incubated for 5 minutes in 1 μM Alexa546-CTxB, 5 μg/ml DiIC$_{16}$ or 75 nM Alexa488-STxB (in either ATP depletion or control medium), washed again, and imaged in the continued presence of ATP depletion or control medium.

Actin disruption

For actin disruption by Latrunculin A, cells were first washed with imaging buffer, incubated for 5 minutes in either 1 μM Alexa546-CTxB or 5 μg/ml DiIC$_{16}$ in imaging buffer, and washed again. Actin depolymerization was

then performed by incubating the cells at 37°C for 5 min in imaging buffer containing 1 μM Latrunculin A (LatA) (Sigma-Aldrich). Control cells were incubated in imaging buffer containing 0.1% DMSO. Cells were maintained in their respective buffer during imaging and all imaging was performed within 30 minutes of treatment. Alternatively, they were fixed and labeled with rhodamine phalloidin as indicated above.

Actin stabilization

Cells culture media was replaced with complete imaging buffer containing 250 nM Jasplakinolide or DMSO and incubated at 37°C and 5% CO_2 for 30 minutes. Cells were then labeled with 100 nM Alexa-FL CTxB for 5 minutes at RT in complete imaging buffer containing 250 nM Jasplakinolide or DMSO. Cells were rinsed and imaged in complete imaging buffer containing 250 nM Jasplakinolide or DMSO.

Dynamin inhibition

Dynamin 2 was inhibited using the small molecule inhibitor, dynasore [158]. Cells culture media was replace with freshly made serum free DMEM + 25 μM HEPES supplemented with 80 μM dynasore or DMSO. Cells were incubated in dynasore or DMSO at 37°C and 5% CO_2 for 30 minutes. Cells were then labeled with 100 nM Alexa-FL CTxB for 5 minutes at RT, rinsed and imaged in DMEM + 25 μM HEPES supplemented with 80 μM dynasore or DMSO.

Cholesterol depletion

Cells culture media was replaced with serum free imaging buffer alone or supplemented with 10 mM MβCD. Cells were incubated with or without MβCD at 37°C and 5% CO_2 for 30 minutes. Cells were then labeled with 100 nM Alexa-FL CTxB for 5 minutes at RT, rinsed and imaged in serum free imaging buffer alone or supplemented with 10 mM MβCD.

Microtubule disruption

Cell culture media was replaced with imaging buffer (phenol red-free DMEM, 10% BSA, 25 mM HEPES, and 1 mg/ml BSA) containing 16.7 μM nocodazole or DMSO and incubated at on ice for 15 minutes. Cells were then shifted to 37°C and 5% CO_2 for 1 hour. The media was then replaced with ATP depletion media or Jasplak (250 nM) containing imaging buffer, supplemented with 16.7 μM nocodazole or DMSO and incubated at 37°C and 5% CO_2 for 15 (ATP depletion) or 30 minutes (Jasplak). Cells were then labeled with 100 nM Alexa-FL CTxB for 5 minutes at RT, rinsed and imaged in the continued presence of both agents. Alternatively, following the 5 minute incubation with nocodazole or DMSO, cells were labeled with 100 nM Alexa-FL CTxB for 5 minutes at RT for 5 minutes in imaging buffer with 16.7 μM nocodazole or DMSO. The cells were then rinsed twice and imaged in imaging buffer containing 16.7 μM nocodazole or DMSO along with 1 mM Latrunculin A.

Microtubule stabilization with taxol

Cell culture media was replaced with imaging buffer containing 1 μM taxol or DMSO and incubated at 37°C and 5% CO_2 for 4 hours. Cells were then rinsed twice with ATP depletion media or ATP control medium containing 1 μM taxol or DMSO and incubated at 37°C and 5% CO_2 for 15 minutes. Cells were then labeled with 100 nM Alexa-FL CTxB for 5 minutes at RT, rinsed and imaged in ATP depletion media or ATP control medium containing 1 μM taxol or DMSO.

Microtubule stabilization with nocodazole

Short incubations with low doses of nocodazole is an alternative method to taxol for the stabilization of microtubules. Cell culture media was replaced with imaging buffer containing 150 nM nocodazole or DMSO and incubated at 37°C and 5% CO_2 for 5 minutes. The media was then replaced with ATP depletion media or Jasplak

(250 nM) containing imaging buffer, supplemented with 150 nM nocodazole or DMSO and incubated at 37°C and 5% CO_2 for 15 (ATP depletion) or 30 minutes (Jasplak). Cells were then labeled with 100 nM Alexa-FL CTxB for 5 minutes at RT, rinsed and imaged in the continued presence of both agents. Alternatively, following the 5 minute incubation with nocodazole or DMSO, cells were labeled with 100 nM Alexa-FL CTxB for 5 minutes at RT for 5 minutes in imaging buffer with 150 nM nocodazole or DMSO. The cells were then rinsed twice and imaged in imaging buffer containing 150 nM nocodazole or DMSO along with 1 mM Latrunculin A.

Inhibition of dynein motor activity

For HPI-4 dose dependence curve, HPI-4 was diluted in DMSO and stocks were produced by serial dilution in DMEM + 10% fetal bovine serum. Then cell culture media was replaced with medium containing HPI-4 or DMSO (matched to highest of volume used in the serial dilution) and incubated at 37°C and 5% CO_2 for 1 hour. Cells were labeled with 100 nM Alexa-FL CTxB in HPI-4 or DMSO containing media for 5 minutes at RT. Cells were rinsed and either fixed immediately or shifted to 37°C and 5% CO_2 for 30 minutes prior to fixation. Fixation was performed with 3.4 % PFA at RT for 15 minutes and samples were mounted in ProLong Gold (Invitrogen).

To determine the effect of HIP-4 on tubule formation, cell culture media was replaced with imaging buffer containing HPI-4 or DMSO and incubated at 37°C and 5% CO_2 for 1 hour. Cells were then rinsed twice with ATP depletion media or ATP control medium containing HPI-4 or DMSO and incubated at 37°C and 5% CO_2 for 15 minutes. Cells were then labeled with 100 nM Alexa-FL CTxB for 5 minutes at RT, rinsed and imaged in ATP depletion media or ATP control medium containing HPI-4 or DMSO. Care was taken to protect HPI-4 from light throughout the experiment.

Surface accessibility assay

To evaluate the surface accessibility of invaginations under ATP depletion, cells were ATP depleted for 15 minutes as described above. Cells were then labeled at room temperature for 5 minutes with 25 nM A555-CTxB in

ATP depletion media. Cells were rinsed and shifted in ATP depletion media to the microscope at 37°C and given approximately 30 minutes to generate tubules. While collecting time-lapse movies a highly concentrated solution of warmed A488-CTxB in ATP depletion media was injected into the chamber to bring the final concentration of A488-CTxB in ATP depletion media to 50 nM.

Acid stripping

COS-7 cells plated on cover slips were transfected with EGFP or GFP-p50. In order to quantify the cellular uptake of CTxB, cells were rinsed with cold imaging buffer and labeled with 100 nM A555-CTxB for 5 minutes on ice. For quantification of transferrin uptake, cells were serum starved using DMEM + 25 mM HEPES for 1 hour at 37°C and 5% CO_2 to remove transferrin receptors bound to non-fluorescent transferrin in the serum from the plasma membrane Serum starved cells were then rinsed with cold DMEM + 10% FBS + 25 mMHEPES and labeled with 5 μg/ml rhodamine-transferrin for 5 minutes on ice. Cells were rinsed with imaging buffer and shifted to 37°C and 5% CO_2 for 10 minutes. Three rounds of acid stripping was performed on ice by incubating cells with 2 ml of 100 mM glycine, pH 2.0, for 5 minutes and then with HBSS, pH 7.4, for 5 minutes. All acid-stripped samples were subsequently incubated with 37°C HBSS, pH 7.4, for 10 seconds to promote release of remaining surface-bound toxin. Cells were fixed in 3.4 % PFA at room temperature for 15 minutes and rinsed with 1x PBS. Cells were labeled with an anti-GFP primary antibody and an Alexa488 secondary. Samples were mounted in ProLong Gold (Invitrogen).

Quantification of cellular ATP levels

Cellular ATP levels were quantified using the commercially available ENLITEN® ATP assay kit (Promega, Madison, WI). In brief, COS-7 and HeLa cell were split into 12 well plates with their appropriate growth medium. After 2 days, medium was removed and some cells were incubated directly in 500 μl ATP-extraction solution [1% TCA in Tris-Acetate-EDTA (TAE) buffer] to collect base-line ATP readings. The remaining cells were rinsed twice

with ATP depletion media and incubated at 37°C and 5% CO_2. At the indicated times after the initiation of ATP depletion, the depletion media was replaced with 500 μl ATP-extraction solution. Cells were incubated in ATP-extraction solution for 30 minutes at RT, as described before [159]. Aliquots of the cell extract were then moved to 96 well plates and diluted 10 fold in TAE buffer. Reaction reagent containing luciferase was added to each well and the chemiluminescence was read on a Synergy H4 Hybrid Multi-Mode Microplate Reader (BioTek, Winooski, VT).

Imaging

Confocal FRAP experiments were carried out on a Zeiss LSM 510 confocal microscope (Carl Zeiss MicroImaging, Inc., Thornwood, NY) using a 40X 1.4 NA Zeiss Plan-Neofluar objective. Cells were maintained in phenol-red free DMEM containing 1 mg/ml albumin bovine serum and 50 mM HEPES supplemented with the indicated drugs for live-cell imaging experiments. Cells were maintained at 37°C using a stage heater and objective heater. EYFP and Alexa488 were excited using the 488 nm line of a 40 mW Argon laser, and Alexa546, Alexa555, rhodamine, or $DiIC_{16}$ were excited at 543 nm of a HeNe laser and detected using filter sets provided by the manufacturer. For presentation purposes images were exported in tiff format and brightness and contrast was adjusted using Adobe Photoshop, ImageJ or FIJI.

Confocal FRAP

For FRAP measurements, cells were imaged at 4X digital zoom with the confocal pinhole set between 1.01 and 1.99 Airy units. Full frame (512 x 512 pixel) images were collected for FRAP analysis of CTxB, YFP-GL-GPI, YFP-GT46, and STxB. For $DiIC_{16}$ FRAP experiments, the imaging window was reduced to a 4.1 x 8.1 μm rectangle to speed image acquisition. Photobleaching of a circular bleach region 4.1 μm in diameter was performed by repetitively scanning the bleach region 10 times using the 488 nm laser line or both the 488 nm and 514 nm laser

lines at full power. Prebleach and postbleach images were collected at lower laser power (typically 3% transmission or less) with either no line averaging or with line averaging of 2. FRAP measurements were carried out at 22°C, or at 37°C using an objective heater and heated stage insert.

Image processing and data analysis

FRAP analysis

Confocal FRAP data analysis was performed using a recently described method that corrects for diffusion that occurs during the photobleaching event [160] assuming a free diffusion model (as opposed to anomalous diffusion or reaction-diffusion type behavior). FRAP analysis was carried out essentially as described in [161], except that FRAP curves and post bleach intensity profiles were analyzed individually and that prior to fitting, FRAP curves were corrected for photobleaching during imaging by normalizing to the whole cell fluorescence over time as described previously [162]. Datasets in which endocytic vesicles were observed to pass through the bleach region were discarded. Mobile fractions were calculated as described previously [147] using the average of the last three time points as F_∞ and the average of the three prebleach images as F_o. Statistics were calculated with a Student t-test using OriginPro 8.5 (OriginLab Corp; Northampton, MA).

Tubule quantification

To determine the percentage of a population of cells containing invaginations, full field (512 x 512) z-stacks of fields of cells were taken at 1.7x zoom on a 40x objective, with line averaging of 4 and optimal overlay in z direction. Z-stacks were collected consecutively for 50 minutes after labeling with toxin. Cells were then scored by hand as displaying or not displaying invaginations. For cells expressing a plasmid, i.e. CC1-dsRed, the cells were

scored in the CTxB channel with the experimentalist blind to which cells were expressing the plasmid and which were not.

To determine the number and length of invaginations z-sections were taken of individual cells consecutively for 50 minutes after labeling with toxin. The JFilament plugin (Dimitrios Vavylonis and Xiaolei Huang; Lehigh University) for ImageJ was used to trace individual invaginations in 2D. The automated snake tracking feature was used to align the snakes with the invaginations. Tracings were examined and corrected by hand.

Particle tracking

Particle detection and tracking were performed using spot detector and U-tracker software developed by Gaudez Danuser (Harvard University), as previously described [163]. Both programs were run using MatLab 7.11.0 (Mathworks; Natick, MA).

Kymographs

Kymographs were generated using the MultipleKymograph plugin (J. Rietdorf and A. Seitz) for FIJI ImageJ. In brief, line ROI's 5 pixels wide were manually generated by tracing the invaginations. The MultipleKymograph tool then generated the kymograph coinciding with the ROI.

Dose response curves

The HPI-4 dose dependence curve was generated by collecting full field (512 x 512) 16 bit images were taken on a 40x objective with line averaging of 8. ROI's were then drawn around the perinuclear space, flat membrane regions and background in ImageJ. Perinuclear and membrane per pixel fluorescence were correct for background fluorescence and then divided to produce a perinuclear to membrane ratio per cell.

Microscopy-based CTxB binding assay

To produce the cholera toxin binding curve, 1 µM stock of Alexa546-CTxB was first prepared in imaging buffer and lower concentration stocks prepared by serial dilution. Cells were labeled with CTxB for 5 min at room temperature, washed, mounted live in imaging buffer, and visualized at 37°C. Images were taken on a Zeiss LSM 510 confocal microscope (Carl Zeiss Microimaging, Inc, Thornwood, N.Y.) with a 40X 1.4 NA Zeiss Plan-Neofluar objective at 0.7x zoom to acquire multiple cells per field. Fluorescence was excited at 543 nm with HeNe laser and detected with a preset Cy3 channel filter set provided by the manufacturer. The confocal pinhole was set at 2.17 Airy units. 512 x 512 pixel images were collected in 8 bit with line averaging of 8. Laser intensity and detector gain were set near pixel saturation for the 1 µM CTxB labeled cells and left unchanged across all concentrations. For lower concentrations duplicate images of the same field were taken at higher detector gain to validate ROI selection. Individual ROI's were drawn for each cell and for the background region, for images at matched laser intensity and detector gain, and mean pixel intensities in the ROI's collected using ImageJ (NIH, Bethesda, Maryland). Cell fluorescence was background corrected and then the mean and standard deviations computed for all cells at a given concentration.

Statistical analysis

Chi-square tests were performed using Excel (Microsoft). Student t-tests and Mann-whitney U-tests were performed using OriginPro 8.6 (OriginLab; Northampton, MA). All graphs were prepared using OriginPro.

CHAPTER III

MECHANISMS UNDERLYING THE CONFINED DIFFUSION OF CHOLERA TOXIN B-SUBUNIT IN

INTACT CELL MEMBRANES[1]

Introduction

The role of cholesterol-dependent membrane domains have been intensively investigated as a mechanism involved in the regulation of membrane trafficking and signaling in cells [164]. Initially envisioned to exist as stable platforms, such domains are now thought to consist of transient nanoscopic assemblies of proteins, glycolipids, and cholesterol [128]. As such, current models suggest that mechanisms that crosslink components of these domains may be important for facilitating their functions [128], as well as to alter membrane mechanics and deform membranes [165].

Bacterial toxins in the AB_5 family, including Shiga toxin and cholera toxin, are an example of a class of proteins with the intrinsic capacity to crosslink glycolipids via their multivalent membrane binding B-subunits [13, 20, 30, 166-170]. The ability of cholera toxin B-subunit (CTxB) and related molecules such as Shiga toxin B-subunit to cluster glycolipids and organize membrane domains has been linked to their functional uptake into cells by clathrin-independent, cholesterol-dependent endocytic pathways [20, 165, 171, 172]. Recently, it has become evident that the accessibility of glycolipids to toxin binding is itself regulated by cholesterol within both model membranes and cell membranes, as a significant fraction of glycolipids is masked and inaccessible to toxin binding [173, 174]. Thus, a picture is emerging in which the ability of toxin to bind glycolipids is controlled in a cholesterol-dependent manner [173, 174] and the presence of bound toxin itself also leads to changes in underlying membrane domain structure [13, 30, 39, 165, 170].

---

[1] This chapter previously appeared in PLoS One (Day and Kenworthy, 2012)

An important question raised by these findings is how the structure and dynamics of the complex formed upon binding of toxins to the accessible pool of their glycolipids receptors are regulated in cells. For the case of cholera toxin, one striking feature of the CTxB/GM$_1$ complex is that it diffuses extremely slowly within the plasma membrane compared to many other proteins and lipids [34, 36, 68, 147, 172, 175, 176]. This result is surprising given that lipids themselves typically diffuse rapidly in cell membranes, as do many lipid-anchored proteins [57, 147, 177-181]. This suggests that the movement of the CTxB/GM$_1$ complex within the plasma membrane is regulated by fundamentally different mechanisms than those that control the dynamics of other types of cell surface molecules under steady state conditions.

The underlying mechanisms that contribute to the slow diffusion of CTxB are not yet fully understood. However, several factors could potentially account for this behavior. For example, there is some evidence that CTxB is confined by actin-dependent barriers [34]. CTxB could potentially associate with nanoclusters that form via an energy- and actin-dependent process, similar to those reported for other lipid-tethered proteins [66]. CTxB has also been reported to associate with caveolae [7, 182-184], flask-shaped invaginations of the plasma membrane which themselves are immobilized within the plane of the membrane [137, 185]. The intrinsic ability of CTxB to cluster glycolipids could potentially lead to the formation of slowly diffusing CTxB/GM$_1$ complexes. If they became large enough, such complexes could also potentially impact the diffusional mobility of other molecules, by either forming barriers to their diffusion or by trapping them within the same domains [58, 186]. In the current study, we investigated the contributions of these various factors to the confined diffusion of CTxB within the plasma membrane of living cells using confocal FRAP.

Results

Confocal FRAP assay and cell surface markers examined in this study

To measure the diffusion of CTxB on the plasma membrane, we took advantage of a quantitative confocal FRAP-based assay that yields accurate diffusion coefficients for both rapidly and slowly moving molecules [160, 161]. In FRAP, lateral diffusion is described by two parameters, the diffusion coefficient (D), reflecting the average rate of diffusion, and the mobile fraction (M_f), a measure of fraction of molecules that are free to recover over the time course of the experiment.

To quantify the diffusional mobility of CTxB at the cell surface, COS-7 cells were labeled briefly with saturating levels of CTxB (1 μM) (Figure 7B), washed, and shifted onto the microscope stage. We visualized a portion of the plasma membrane, and FRAP measurements were carried out using a circular bleach region (Figure 7A). Although CTxB was endocytosed to the perinuclear region in a time-dependent manner, a substantial fraction of CTxB remained associated with the plasma membrane over time, enabling measurements of its cell surface mobility by confocal FRAP over at least 30 minutes after shifting cells to the microscope stage at 37°C. Care was taken to exclude any FRAP data in which non-surface attached, mobile endocytic vesicles were inside the ROI at any time during the FRAP experiment. The recovery curves were well fit by a pure diffusion model, implying that the recovery process is dominated by lateral diffusion (Figure 7C). In addition, the diffusional mobility of CTxB remained constant over time, suggesting that the properties of the cell surface pool of CTxB do not change significantly even while some of the toxin is being actively endocytosed (Figure 7D).

In order to understand what aspects of the regulation of CTxB's diffusion are specific for molecules that cluster glycolipids, we examined of the diffusional mobility of several additional cell surface markers in parallel in our study: a representative GPI-anchored protein, YFP-GL-GPI [146], a single pass transmembrane protein, YFP-GT46 [145], and a fluorescent lipid analog, $DiIC_{16}$ (Figure 7E). Our rationale for studying these markers was several fold. GPI-anchored proteins are linked to cell membranes via a lipid anchor, and also have been shown to associate with cholesterol-dependent nanoclusters [66, 187] that could potentially organize glycolipids as well. We
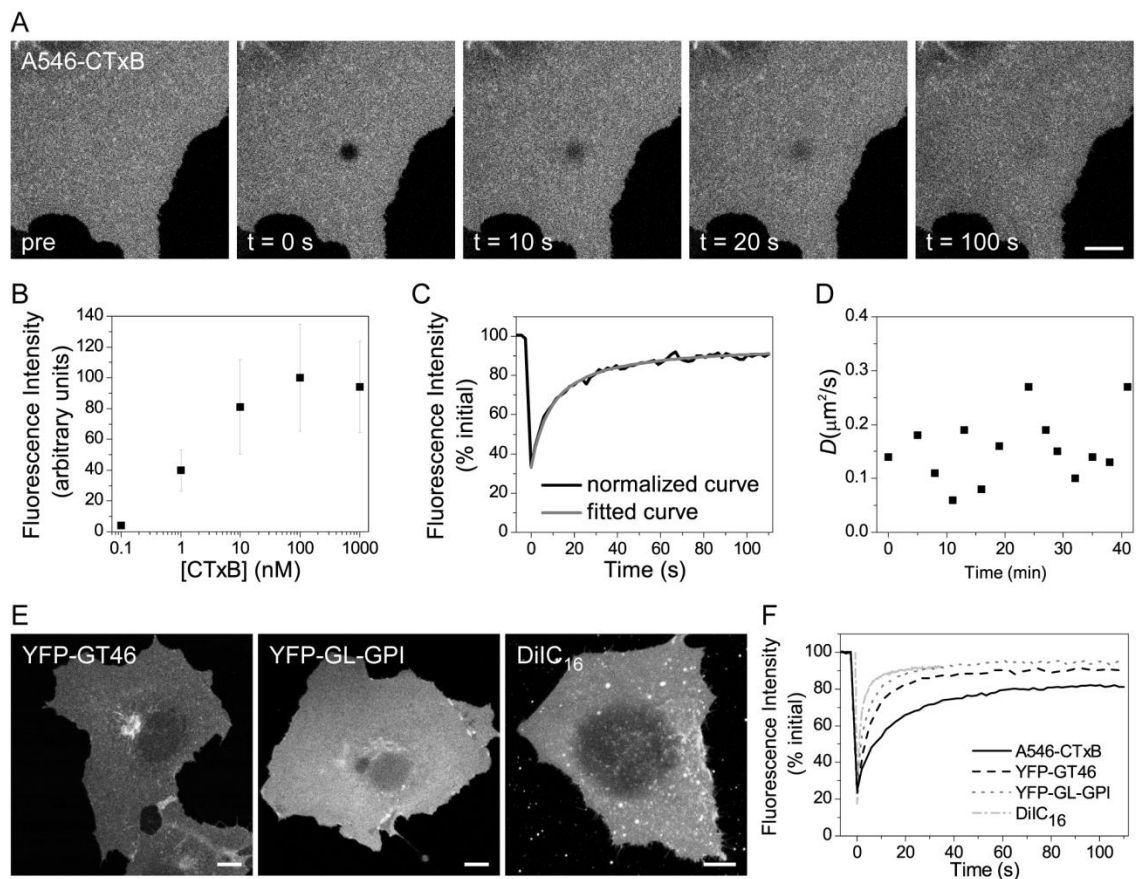
Figure 7. Confocal FRAP assay. COS-7 cells were transfected with the indicated constructs or left untransfected and labeled with Alexa546-CTxB or DiIC16. FRAP was performed at 37uC using a 4.1 μm diameter bleach spot. (A) Representative images of Alexa546-CTxB during a FRAP experiment. Bar, 10 μm. (B) Average fluorescence intensity of Alexa546-CTxB labeling of COS-7 cells incubated with A546-CTxB concentrations ranging from 0.1 nM to 1 μM (mean 6 SD for 59–151 cells). (C) Example of a normalized recovery curve for a cell labeled with 1 μM Alexa546-CTxB after correcting for fluorescence decay during imaging, along with fitted FRAP curve. (D) Representative example of *D* for CTxB as a function of time after labeling. Each value of D was obtained for a different cell on the same coverslip from a single experiment. (E) Representative whole cell images of YFP-GT46, YFP-GL-GPI, and DiIC16 in COS-7 cells. Single confocal slices are shown. The spotty appearance of DiIC16 on the background is due to the presence of dye aggregates. Bar, 10 μm. (F) Representative FRAP curves for Alexa546-CTxB, YFP-GT46, YFP-GL-GPI, and DiIC16 (n = 8–13 cells for each). [32]

chose to study YFP-GT46 because transmembrane proteins are often subjected to different types of constraints to their diffusion than are lipid-anchored proteins [57, 177]. DilC$_{16}$ was selected for these studies to control for the fact that CTxB binds to a lipid receptor at the cell surface. In general, lipids diffuse much more rapidly than proteins do in cell membranes [57, 177-180]. Because CTxB clusters multiple glycolipids, it would not necessarily be expected to behave like a simple reporter of lipid diffusion.

Previous studies have shown that CTxB diffuses significantly more slowly than YFP-GL-GPI, YFP-GT46, and DilC$_{16}$ when directly compared in the same cell line [147, 181]. We confirmed this in control FRAP experiments (Figure 7F). The fastest value of D was measured for DilC$_{16}$ (2.54 ± 0.78 μm^2/s, mean ± SD). D for YFP-GL-GPI (1.18 ± 0.49 μm^2/s) was slower than for DilC$_{16}$ but faster than that of YFP-GT46 (0.54 ± 0.18 μm^2/s), while CTxB diffused the most slowly of all (0.17 ± 0.12 μm^2/s). M$_f$ was ~ 90% for YFP-GL-GPI, YFP-GT46, and DilC$_{16}$, and ~80% for CTxB (Table 1). These data indicate the diffusion of CTxB is selectively constrained at the cell surface relative to these other classes of molecules. We next investigated possible mechanisms underlying the slow diffusion of CTxB. For the purpose of these studies, we focused on understanding the properties of CTxB bound to its accessible pool of glycolipid receptors [173, 174].

CTxB diffusion is confined by the actin cytoskeleton

The actin cytoskeleton is a well-known barrier to the diffusion of a number of cell surface molecules [57, 188-191]. Two previous observations suggest that actin may play a role in controlling the diffusional mobility of CTxB. First, biochemical studies indicate that cholera toxin co-fractionates with actin [192]. Second, CTxB diffusion was shown to be enhanced following actin disruption [34]. However, the latter study did not evaluate how actin disruption affected the mobility of other proteins and lipids, leaving open the question of how specific this effect was. We therefore sought to directly compare the impact of disrupting the actin cytoskeleton on the diffusion of CTxB relative to its effect on other proteins and lipids at the cell surface using latrunculin A (Lat A), which inhibits actin polymerization by sequestering monomeric actin.

Table 1. Mobile fractions of Alexa546-CTxB, YFP-GT46, YFP-GL-GPI, and DilC$_{16}$ following various treatments

	-CTxB		+ CTxB		ATP control	-ATP	Lat A control	+ Lat A	Cav-1$^{+/+}$	Cav-1$^{-/-}$
	20°C	37°C	20°C	37°C	20°C	37°C	37°C	37°C	37°C	37°C
Alexa546-CTxB	NA	NA	NA	NA	79 ± 8 (30)	85 ± 8* (30)	81 ± 8 (23)	84 ± 7 (19)	82 ± 7 (24)	81 ± 7 (26)
YFP-GT46	90 ± 4 (23)	84 ± 6 (22)	92 ± 5 (16)	87 ± 6 (17)	83 ± 9 (24)	77 ± 7** (29)	81 ± 7 (22)	79 ± 7 (19)	85 ± 9 (23)	82 ± 10 (22)
YFP-GL-GPI	88 ± 8 (19)	89 ± 6 (31)	90 ± 6 (19)	91 ± 6 (31)	86 ± 6 (32)	85 ± 9 (32)	85 ± 7 (19)	81 ± 10 (13)	88 ± 7 (37)	85 ± 7 (31)
DilC$_{16}$	89 ± 5 (21)	89 ± 5 (32)	88 ± 5 (20)	90 ± 6 (32)	86 ± 5 (19)	90 ± 5** (24)	88 3 (23)	89 ± 7 (22)	83 ± 7 (47)	83 ± 8 (45)

Values represent mean ± SD. The numbers in parentheses represent sample size.

* 0.05 > p > 0.01; Student t-test against control at the same temperature

** p < 0.01; Student t-test against control at the same temperature

In control experiments, we confirmed that Lat A treatment led to a loss of F-actin within cells as assessed by phalloidin staining of fixed cells, as expected (Figure 8E). Disruption of actin has also been shown previously to lead to the formation of tubular invaginations of the plasma membrane [129]. We verified that similar tubules were apparent in living cells labeled with CTxB or DiIC$_{16}$, as well as in cells expressing YFP-GL-GPI or YFP-GT46 (Figure 8A-D).

Next, we used confocal FRAP to measure the diffusional mobility of CTxB in Lat A-treated and mock-treated cells incubated in media containing DMSO (Figure 8F). For comparison, we monitored the effects of these treatments on the diffusional mobility of YFP-GL-GPI, YFP-GT46, and DiIC$_{16}$ under identical conditions, avoiding regions where plasma membrane tubules were present in these measurements. The results of these experiments showed D for CTxB was significantly increased by LatA treatment from 0.21 ± 0.10 μm^2/s to 0.35 ± 0.18 μm^2/s. In contrast, the diffusion of YFP-GL-GPI, YFP-GT46, and DiIC$_{16}$ was unaffected in the presence of Lat A (Figure 8F). These results suggest the diffusional mobility of CTxB is selectively slowed either directly or indirectly as the result of its interactions with the actin cytoskeleton. However, even in cells in which actin was disrupted, the diffusion of CTxB was considerably slower than that of other cell surface molecules, suggesting additional factors are involved in slowing its lateral diffusion. We therefore asked if the interaction of CTxB with other types of domains might impede its mobility.

Diffusion of CTxB and a transmembrane protein, but not a GPI-anchored protein is enhanced in ATP-depleted cells

Previous studies have reported that certain proteins associate with nanoclusters that maintain a fixed size and a fixed ratio of monomeric to clustered molecules over a wide range of concentrations, implying these domains are actively maintained and require cellular energy for their generation [64, 187]. GPI-anchored proteins are immobilized within these nanoclusters, indicating these domains have the capacity to impact the dynamics of cell surface molecules [66]. It is currently unknown if CTxB associates with actively maintained nanoclusters. We reasoned that ATP depletion might disrupt the interactions of molecules with such structures, thereby leading to
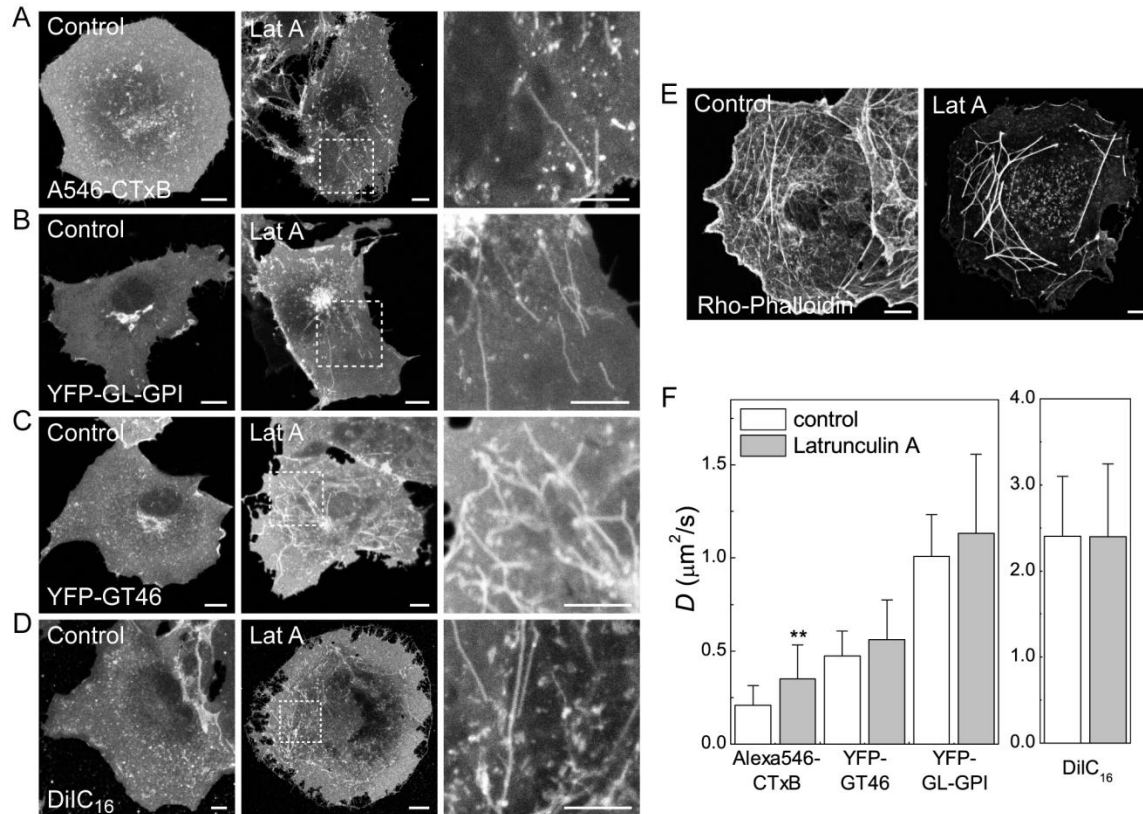
Figure 8. CTxB diffusion is confined by the actin cytoskeleton. (A–D) Subcellular distribution of (A) Alexa546-CTxB, (B) YFP-GL-GPI, (C) YFPGT46 and (D) DilC$_{16}$ in live COS-7 cells under control conditions or following Lat A treatment as described in the Material and Methods. A zoom of the boxed area in Lat A treated cells is shown on the right for each marker. (E) Rhodamine phalloidin staining in fixed COS-7 cells under control conditions or following Lat A treatment. Bar, 10 μm. (F) COS-7 cells were treated with 1 μM Lat A or mock-treated with 0.1% DMSO (''control'') for 5 minutes prior to imaging, and FRAP analysis was performed in the continued presence of Lat A. Diffusion coefficients were measured for Alexa546-CTxB, YFP-GLGPI, YFP-GT46 and DilC16 in control and Lat A treated COS-7 cells at 37°C (mean 6 SD for 13–23 cells). ** p,0.01, Student t-test. [32]

an increase in their overall diffusional mobility. To test this, COS-7 cells were depleted of ATP by a 15 minute

incubation with 0.02 % sodium azide and 50 mM 2-deoxy-D-glucose, or mock-depleted prior to labeling with CTxB.

For comparison, we performed similar experiments in ATP-depleted cells expressing YFP-GL-GPI (which is

predicted to associate with nanoclusters) or YFP-GT46, or labeled with $DiIC_{16}$.

ATP depletion led to several marked changes in the morphology of the plasma membrane and the

underlying cytoskeleton. First, ATP depletion led to the formation of protrusions of the plasma membrane that

were never observed in control cells (Figure 9A-E). Some of these protrusions were localized to the edges of cells

and may represent retraction fibers. Needle-like protrusions were also seen projecting above cells into the media,

as visualized in x-z sections. These protrusions were labeled with CTxB and for the other cell surface markers such

as YFP-GL-GPI (Figure 9B, C, E). Second, in some ATP depleted cells tubular invaginations of the plasma membrane

enriched in CTxB were observed (Figure 9C). Similar invaginations have been proposed to correspond to sites of

clathrin-independent endocytosis induced by Shiga toxin B-subunit binding that tubulate in an ATP independent

manner but whose scission is ATP dependent [20, 169], and have also been reported to form in cells labeled with

CTxB [193]. Tubular invaginations were only observed in cells labeled with CTxB and not other cell surface

markers, although the extent of invagination formation varied between cells. Because ATP depletion has been

previously reported to increase levels of F-actin in cells [194-196], we also examined actin organization under

these conditions by phalloidin staining. We found that F-actin staining was markedly enhanced in ATP-depleted

cells (Figure 10). In addition, the plasma membrane protrusions also appeared to be enriched in actin, suggesting

that the changes in actin organization that occur in response to ATP depletion may be responsible for their

formation.

We next performed confocal FRAP analysis in ATP depleted cells. For these studies, we chose to bleach

ROIs on regions of the plasma membrane that did not include visible membrane protrusions or invaginations. The

results of these experiments showed no change in D for YFP-GL-GPI or $DiIC_{16}$ in ATP depleted versus mock-

depleted cells (Figure 9F). We did note however that the rate of diffusion of $DiIC_{16}$ in both mock ATP depleted and

ATP depleted cells was significantly higher than that of $DiIC_{16}$ under any of the other conditions examined. This

effect was reproducible across days, and therefore likely arises from differences in the media used for various treatments.

In contrast to the lack of effect of ATP depletion on $DiIC_{16}$ or YFP-GL-GPI, CTxB and YFP-GT46 both showed a significant increase in D in ATP depleted cells relative to controls (Figure 9F). We also observed a small but significant increase in M_f for $DiIC_{16}$ and CTxB, and decrease in M_f for YFP-GT46 in ATP-depleted cells (Table 1). Thus, diffusion of CTxB is normally confined by an ATP-dependent mechanism. Because the diffusion of YFP-GL-GPI, which is predicted to associate with nanoclusters, was unaffected under these conditions, it seems unlikely that the increased mobility of CTxB is due to disruption of its association with actively maintained nanoclusters. Instead, the enhanced diffusion of CTxB under these conditions may reflect the substantial changes in the organization of actin that occur in response to ATP depletion (Figure 10), allowing for it to decouple from CTxB.

Diffusion of CTxB and other cell surface molecules is identical in the presence and absence of caveolae

Caveolae are another structural feature of cell membranes with the potential to restrict the diffusion of CTxB. CTxB is sometimes enriched within caveolae, suggesting it has a specific affinity for these domains [7, 182-184]. Since caveolae are immobile within the plane of the membrane [137, 185], even transient interactions of CTxB with caveolae would be expected to constrain its lateral mobility. In agreement with this possibility, several studies have reported that interactions of CTxB with caveolin-1 (Cav-1) itself slow the diffusion of CTxB both at the plasma membrane and within early endosomes at neutral pH [7, 36, 37]. However, these experiments either used a knockdown approach or examined the dynamics of CTxB in enlarged endosomes containing caveolin-1-GFP. Therefore, to more directly assess the effect of caveolae on CTxB mobility, we measured CTxB diffusion in Cav-1$^{-/-}$ and Cav-1$^{+/+}$ mouse embryonic fibroblast (MEF) cells.

All of the markers studied localized correctly to the plasma membrane in the Cav-1$^{-/-}$ cells (Figure 11A). Levels of CTxB binding to the cell surface were also equivalent in the Cav-1$^{+/+}$ and Cav-1$^{-/-}$ MEFs, similar to previous
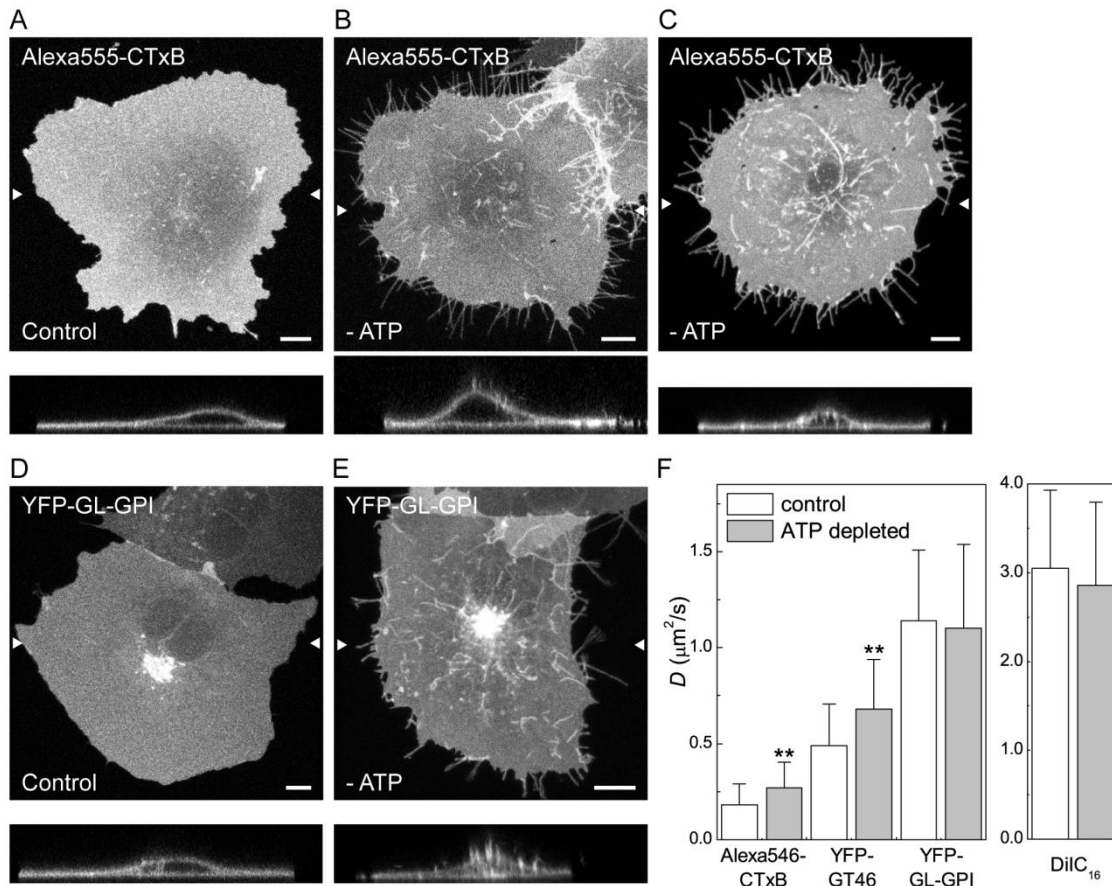
Figure 9. CTxB diffusion is confined by ATP-dependent barriers. (A–E) Subcellular distribution of Alexa555-CTxB and YFP-GL-GPI in control and ATP-depleted COS-7 cells. Images show the projection of a series of confocal slices through live cells. Arrows mark the position of an xz-section (shown below.) Scale bar = 10 μm. (A, D) Typical morphology of cells labeled with Alexa555-CTxB or expressing YFP-GL-GPI under control conditions. (B, E) In ATP depleted cells, in addition to labeling the bulk of the plasma membrane, Alexa555-CTxB and YFP-GL-GPI label protrusions of the plasma membrane found close to the coverslip, as well as protrusions projecting above the surface of the cells into the media. (C) Example of an ATP depleted cell in which CTxB accumulates in tubular plasma membrane invaginations in addition to protrusions. (F) COS-7 cells were ATP depleted or mock-depleted (''control'') for 15 minutes prior to labeling and FRAP was performed in the continued presence of ATP depletion or control medium. Diffusion coefficients were measured for Alexa546-CTxB, YFP-GT46, YFP-GL-GPI or DilC16 (mean 6 SD from 24–32 cells). Cells were labeled with 1 μM Alexa546-CTxB. FRAP was performed at 37°C. ** p,0.01, Student t-test. [32]
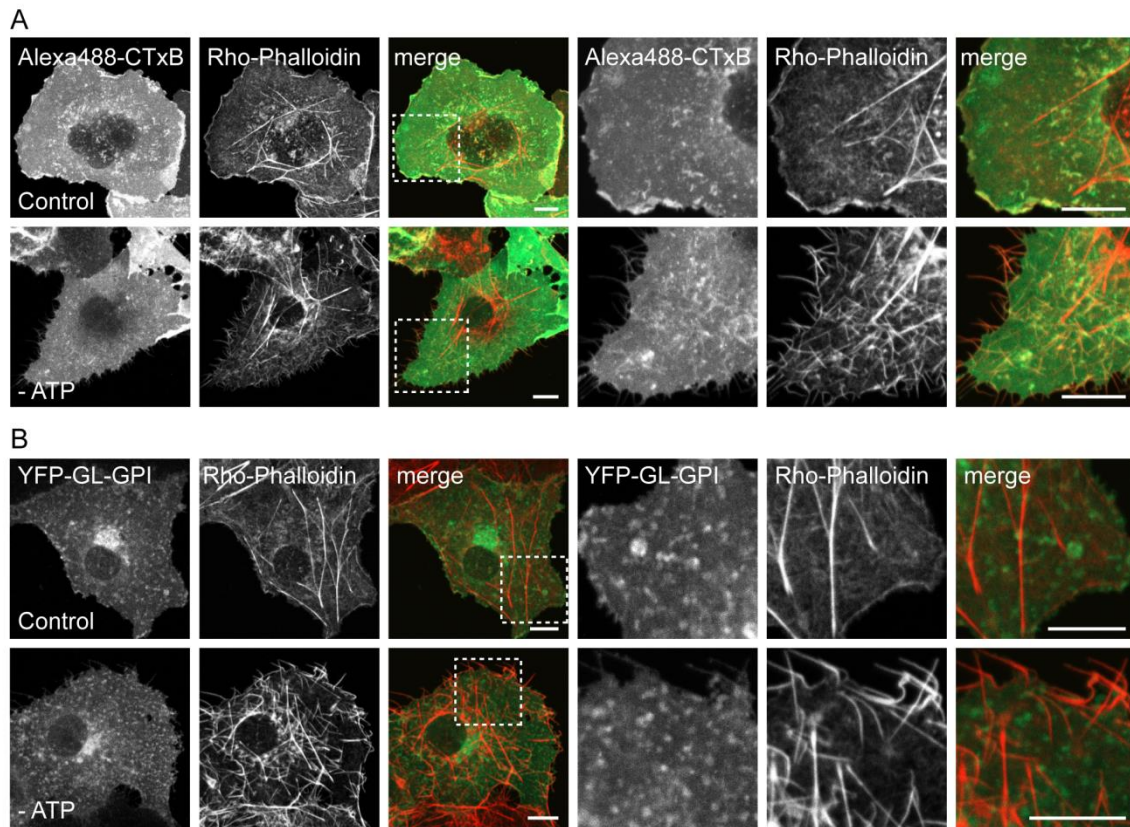
Figure 10. ATP depletion induces actin polymerization. Rhodamine-phalloidin labeling in mock-depleted and ATP depleted COS-7 cells (A) labeled with Alexa488-CTxB or (B) expressing YFP-GL-GPI. A single confocal section is shown for each. A zoom of the boxed area is shown on the right. The merged images show phalloidin staining in red and CTxB or YFL-GL-GPI staining in green. The spotty appearance of CTxB and YFP-GL-GPI is the result of fixation and permeabilization conditions. Scale bar = 10 μm. [32]

reports [108]. Confocal FRAP analysis revealed there was no significant difference in D or M_f between CTxB in Cav-$1^{+/+}$ and Cav-$1^{-/-}$ MEFs, suggesting that CTxB is not diffusionally trapped within caveolae (Figure 11B, Table 1). Furthermore, both the D and M_f values obtained for CTxB in MEFs were similar to those measured in COS-7 cells, which contain abundant caveolae, further suggesting that the slow diffusion of CTxB is not due to its interactions with caveolae. Analysis of the cell surface dynamics of YFP-GL-GPI, YFP-GT46, and DiIC$_{16}$ also showed no differences in Cav-$1^{+/+}$ and Cav-$1^{-/-}$ cells (Figure 11B). These results suggest caveolae do not specifically confine the cell surface dynamics of CTxB, and also do not generally impact the diffusional mobility of other proteins or lipids.

The diffusional mobility of other proteins and lipids at the cell surface is unaffected by the presence of bound CTxB

In the experiments described above, we focused on how structural components of the plasma membrane modulate the dynamics of CTxB. However, binding of CTxB to membranes could itself potentially alter the organization of the plasma membrane organization in a way that influences either its own diffusion, or that of other molecules. For example, binding of CTxB to cells could potentially create crowding effects that cause it to diffuse slowly [197]. Alternatively, the addition of CTxB to cells could lead to the formation of sub-resolution domains that influence the distribution and dynamics of other proteins and lipids, by analogy to its ability to form macroscopic domains in model systems [13, 30]. Cellular proteins with affinity for these domains might become trapped within or transiently interact with these structures, consequently slowing their diffusion as well [186]. Conversely, if such domains were sufficiently abundant and connected, other proteins could potentially become "trapped" within islands surrounded by a cluster of domains formed by CTxB binding [58]. Each of these models predicts that in the presence of CTxB, diffusion of other proteins and lipids should be slowed compared to the absence of CTxB.
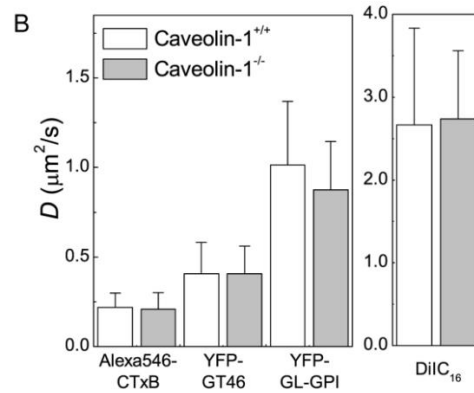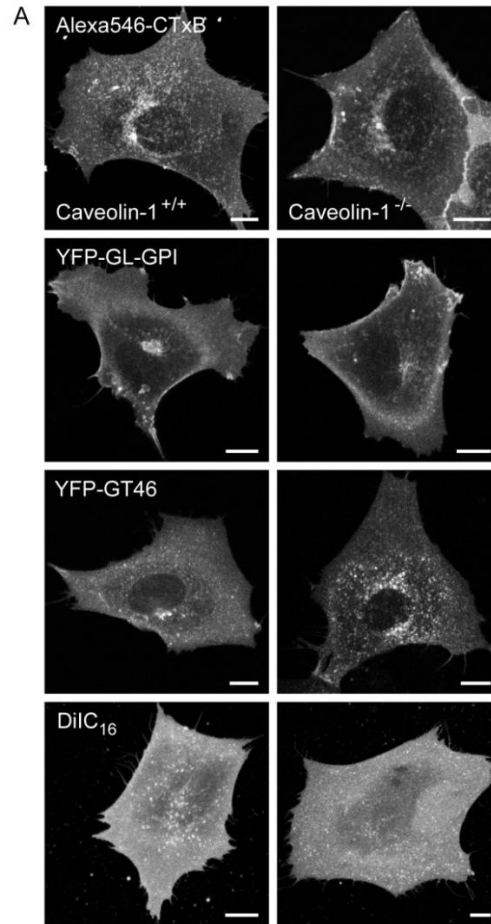
Figure 11. Caveolae have little effect on CTxB diffusion at the cell surface. (A) Subcellular distribution of Alexa546-CTxB, YFP-GL-GPI, YFP-GT46, and DiIC16 in live Cav-1^{+/+} and Cav-1^{-/-} MEF cells. Bar, 10 mm. (B) Diffusion coefficients of Alexa546-CTxB, YFP-GL-GPI, YFPGT46 and DiIC16 in Cav-1^{+/+} and Cav-1^{-/-} MEF cells (mean ± SD from 22–47 cells). Cells were labeled with 1 μM Alexa546-CTxB. FRAP was performed at 37°C. [32]

To test this, we measured the diffusional mobility of DiIC$_{16}$, YFP-GL-GPI, and YFP-GT46 in the presence or absence of saturating levels of CTxB (Figure 12, Table 1). Experiments were carried out at both 22°C and 37°C in order to test for the presence of temperature-dependent membrane percolation threshold [58]. Interestingly, the diffusion of both proteins (YFP-GL-GPI and YFP-GT46) was unaltered by the addition of CTxB at both temperatures. DiIC$_{16}$ diffusion was also unchanged in the presence of CTxB at 37°C, but was significantly increased at 22°C. This implies that if microdomains are formed upon binding of CTxB to the cell surface, they are not sufficiently abundant or large enough to influence the diffusion of our test proteins at physiological temperature. However, they do appear to influence the mobility of DiIC$_{16}$ at lower temperatures, raising the possibility that CTxB binding may impact the viscosity or order of the membrane at lower temperatures, perhaps by perturbing underlying lipid organization [39].

The diffusional mobility of AB$_5$ toxins is not correlated with their capacity to cluster glycolipids

Our findings raise the question of whether the confined diffusion we observed for CTxB is a general feature of proteins with the intrinsic ability to cluster glycolipids. The B subunit of Shiga toxin (STxB) is another example of a bacterially derived toxin with a homopentameric structure that binds a glycolipid receptor (in this case, Gb3) [166]. While there is no apparent similarity in the amino acid sequences of these two proteins, their structures are highly homologous [166]. Importantly, STxB can bind up to 15 Gb$_3$ molecules per homopentamer [198]. We therefore predicted that STxB would diffuse even more slowly than CTxB if the extent of glycolipid clustering is a major determinant of their cell surface dynamics.

To test this, we initially sought to measure the diffusional mobility of STxB in the plasma membrane of unperturbed COS-7 cells. We found that COS-7 cells normally label poorly with STxB. Therefore, to enable STxB binding, COS-7 cells were transfected with Gb3 synthase [149]. We next attempted to perform FRAP analysis of STxB at the cell surface. However, within minutes after labeling, STxB was rapidly internalized from the cell surface into numerous small, rapidly moving vesicles and tubular structures (Figure 13A), precluding FRAP analysis. We therefore took advantage of the fact that ATP depletion, a condition we used to study the regulation of the
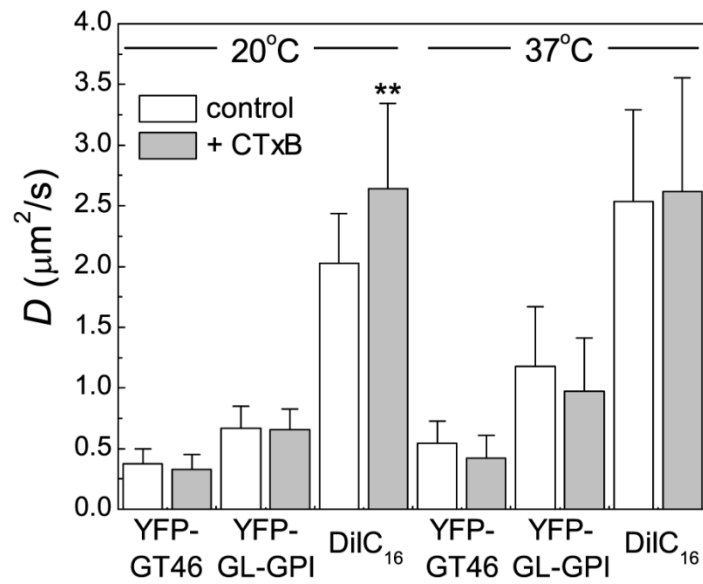
Figure 12. CTxB binding has little effect on the diffusion of other cell surface molecules. COS-7 cells expressing YFP-GL-GPI or YFPGT46, or stained with DilC$_{16}$ were labeled with 1 μM Cy5-CTxB (YFP-GLGPI and YFP-GT46) or Alexa488-CTxB (DilC$_{16}$) for 5 minutes at room temperature and washed prior to FRAP studies. Diffusion coefficients were measured for YFP-GL-GPI, YFP-GT46, and DilC16 in the presence and absence of 1 μM Cy5 CTxB (mean 6 SD for *n* = 16–32 cells). FRAP data were collected at both 20°C and 37°C. ** *p*,0.01, Student *t*-test. [32]

diffusion of CTxB (Figure 9), inhibits the internalization of STxB [20] and CTxB (this study) as a way to compare the dynamics of CTxB and STxB on the plasma membrane.

For these experiments, COS-7 cells expressing Gb_3 synthase were preincubated in ATP depletion medium for 15 min prior to labeling with Alexa 488-STxB and subsequently imaged in the continued presence of ATP depletion medium. In ATP depleted cells, STxB often accumulated in tubular plasma membrane invaginations (data not shown), similar to those reported previously [20]. In some cells, STxB could also be found in protrusions induced by ATP depletion (data not shown), similar to those observed for other cell surface markers. Importantly, under these conditions, a substantial fraction of STxB remained trapped at the cell surface, enabling us to use confocal FRAP to assess the dynamics of the plasma membrane pool of the toxin. Remarkably, the cell surface pool of STxB diffused significantly faster than CTxB, with a characteristic D of ~0.5 μm^2/s and M_f of 81±7%. In fact, this was significantly faster than the diffusion of CTxB under any of the conditions we examined. These data indicate that confined diffusion is not a general property of glycolipid binding toxins, and suggest that in cells, the diffusional properties of CTxB and STxB are not correlated in a simple way with their capacity for clustering multiple glycolipids.

DISCUSSION

In contrast to the highly dynamic properties of native lipid rafts, rafts stabilized by binding of CTxB to the plasma membrane of living cells diffuse extremely slowly. In the current study, we used confocal FRAP to analyze the regulation of the dynamics of CTxB, with the goal of identifying mechanisms that confine its lateral diffusion. FRAP is an ensemble technique which reports on the average rate of diffusion of a large populations of particles across micrometer distances. This is in contrast to single particle tracking and fluorescence correlation spectroscopy which report on the short range diffusion of a small number of particles at one time. In certain
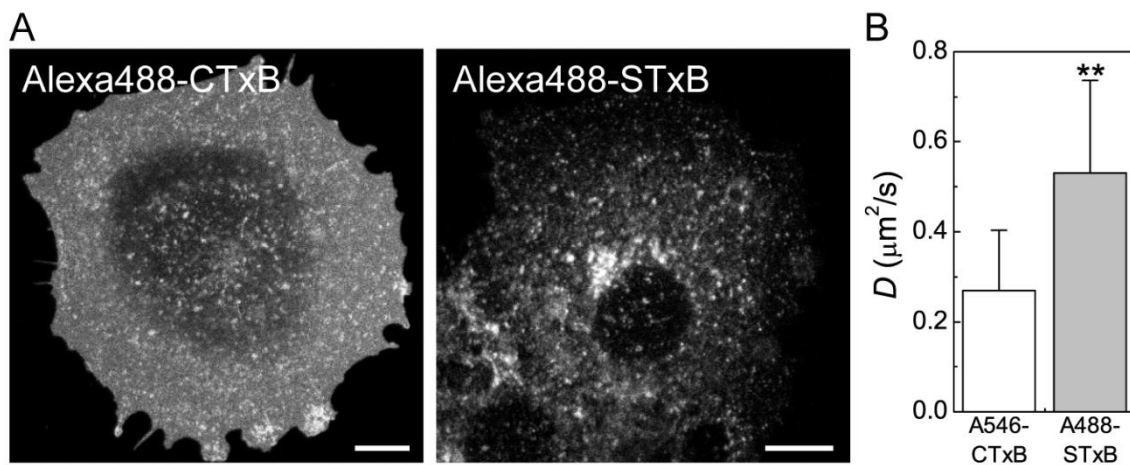
Figure 13. STxB, another homopentameric glycolipid-binding toxin, diffuses more rapidly than CTxB. (A) Subcellular distribution of CTxB and STxB in control cells approximately 5 minutes after labeling and shifting to 37°C. (B) Diffusion coefficients of STxB vs. CTxB in ATP depleted COS-7 cells (mean 6 SD from 30 and 28 cells, respectively). Cells were labeled with 1 μM Alexa546-CTxB or 75 nM A488-STxB. FRAP was performed at 37°C. ** *p*,0.01, Student *t*-test. [32]

instance the ability of measure a few particles at once is useful as it allows for easy separation of populations having distinct diffusional behaviors. However, in our current study all FRAP data was well fit by a single component diffusion model, indicating that alternative techniques are not necessary to understand the slow diffusion of CTxB. Similarly, we have performed fluorescence correlation spectroscopy on CTxB in COS-7 cells at steady state and this data also fits a single component diffusion model (not shown). Finally, previous diffusion measurements of CTxB collected by FRAP, fluorescence correlation spectroscopy, and single particle tracking have all reported that the diffusion of CTxB is highly confined [33, 34, 36, 68, 172, 175, 176], indicating that the barriers that restrict the long range motion of CTxB are likely conserved over the smaller spatial scales observed by fluorescence correlation spectroscopy and single particle tracking.

Our results highlight several important differences in how the cell surface dynamics of CTxB are regulated compared to classical markers of lipid rafts such as GPI-anchored proteins, as well as other general classes of molecules such as transmembrane proteins or lipid probes. For example, although previous studies have indicated that the dynamics of many raft-associated molecules are unaffected by disruption of the actin cytoskeleton [57], actin plays an important role in constraining the diffusion of CTxB. The dependence of CTxB diffusion on actin organization may seem surprising given that CTxB binds a glycolipid receptor and thus lacks the ability to directly couple to actin. However, the CTxB/GM_1 complex could potentially interact indirectly with actin in several ways. The diffusion of CTxB could be impeded by the presence of transmembrane "post" proteins that are attached to actin-based corrals [188, 199]. Alternatively, crosslinking of GM_1 by CTxB could initiate signaling events that in turn transiently connect the CTxB/GM_1 complex to actin with the help of currently unknown transmembrane proteins, by analogy to how crosslinked GPI-anchored proteins are thought to interact with actin [200-203]. The formation of a "textured" lipid phase in response to CTxB binding may contribute to signaling across the bilayer leaflets [39]. There is also evidence from freeze-fracture immunolabeling electron microscopy that GM_1, the high affinity glycolipid receptor for CTxB, associates with actin-dependent clusters in cells [204]. Thus, GM_1 itself may be coupled to actin, providing an indirect link between CTxB and the cytoskeleton.

Our results also indicate the diffusion of CTxB is normally confined by ATP-dependent processes. Initially, we set out to test the effects of this treatment as a way to assess the possible interaction of CTxB with actively

maintained nanoclusters, a class of domains previously shown to lead to the local enrichment and immobilization of GPI-anchored proteins [66]. Despite the known interaction of GPI-anchored proteins with such structures, ATP depletion had little influence on the overall mobility of a representative protein, YFP-GL-GPI. We speculate this may be the case because only a relatively small fraction of GPI-anchored proteins associates with these domains [66]. However, ATP depletion also had a profound effect on actin organization and membrane structure. In particular, we observed a dramatic increase in F-actin staining close to the plasma membrane in response to ATP depletion, accompanied by the formation of needle-like protrusions. Based on these observations, we propose remodeling of actin to form longer filaments may increase the dimensions of the actin-defined compartments that normally confine protein and lipid diffusion at the cell surface [70], therefore increasing the mobility of CTxB in response to ATP depletion. This model might explain why ATP depletion and LatA treatment have similar effects on CTxB dynamics, even though they have much different effects on overall actin organization. Other changes in membrane structure and composition known to occur in response to ATP depletion, including inhibition of phosphoinositide synthesis and the release of some small GTPases from the plasma membrane [205], could also contribute to the shift in CTxB diffusion. This multiplicity of effects of ATP depletion may also explain why diffusion of the transmembrane protein YFP-GT46 was enhanced following ATP depletion, but unaffected by actin disruption following LatA treatment.

Caveolae have been shown to become enriched in and internalize CTxB, although they are not required for its endocytic uptake into cells [108]. We therefore tested for a potential role of caveolae in controlling the overall diffusion of CTxB at the cell surface. We found that the absence of caveolae had no effect on the diffusion of CTxB, or for that matter on any of the other cell surface markers examined. *D* was also very similar for all the molecules examined in COS-7 cells (which contain caveolae) and in caveolin-1$^{-/-}$ MEFs, further indicating that caveolae per se do not strongly influence the mobility of the molecules examined here. Taken together, we conclude from these studies that caveolae are not a major barrier to the diffusion of CTxB, and also do not function as general regulators of protein or lipid diffusion. This does not rule out the possibility that specific proteins or lipids interact with caveolae, especially following crosslinking [202]. Caveolae could also potentially become saturated with CTxB, as CTxB has been reported to be selectively taken up by caveolae when present at very low

labeling concentrations [7]. The effects of caveolae and caveolin-1 on the diffusion of proteins like CTxB may also not necessarily be identical, since caveolin-1 can exist at the cell surface as small oligomers under conditions where caveolae per se are not present [36]. This may explain the difference between our current results and those of a previous study examining the effects of caveolin-1 on CTxB diffusion utilizing a knock down approach,that may have left these residual caveolin-1 oligomers on the cell surface [36, 37]. However, it is also formally possible that the role of caveolae and caveolin-1 in modulating the diffusion of CTxB are different in adipocytes and mammary tumor cells [36, 37] than in MEFs.

For purposes of this study, caveolae are the only nascent endocytic vesicles we chose to examine, as previous work had identified caveolin-1 as a factor impacting CTxB diffusion [36, 176]. However, caveolar endocytosis is not the only endocytic pathway utilized by CTxB [88, 91-93, 193]. To the best of our knowledge the impact that these other pathways on the diffusion of CTxB has not yet been examined, and studies into the role of these pathways on CTxB dynamics are ongoing in our lab. Among these pathways, the possibility that CTxB diffusion is regulated by flotillin appears especially promising as flotillin has been shown to modulate the diffusional mobility of other sphingolipid-binding molecules [206].

Because CTxB binding itself can potentially alter the organization of the plasma membrane, we investigated its effects on the diffusion of other proteins and lipids. The results of these experiments showed very little change in protein or lipid diffusion in the presence of bound CTxB at physiological temperature. This result immediately rules out the possibility that CTxB binding causes crowding effects that slow its own diffusion [197]. They further imply that if CTxB forms small domains in intact cells, these domains do not incorporate other classical "raft"-associated proteins [186], and also are not sufficiently large to form barriers to the diffusion of non-raft proteins or lipids [58]. Our observation that CTxB binding does not alter the diffusion of YFP-GL-GPI is consistent with a recent near field scanning microscopy study showing that GPI-anchored proteins are in close proximity to CTxB, but do not directly colocalize with CTxB-enriched domains [207]. They somewhat differ, however, from data reported by Pinaud and colleagues [208]. In that study, the effects of CTxB on the diffusional mobility of an artificial GPI-anchored protein consisting of avidin attached to the membrane via a GPI-anchor, Av-GPI, were investigated in some detail using single quantum dot tracking [208]. A modest decrease in mobility of a

slowly diffusing population of Av-GPI was reported to occur in cells labeled with CTxB. However, under steady state conditions, even the "fast" values of D reported for Av-GPI are almost two orders of magnitude slower than our measured D for YFP-GL-GPI (0.038 μm^2/s for Av-GPI versus ~1 μm^2/s for YFP-GL-GPI). It thus seems likely that Pinaud et al. detected interactions of CTxB with a subset of partially immobilized GPI-anchored proteins, rather than a freely diffusing population of GPI-anchored proteins.

Since hydrodynamic radius is a key regulator of diffusion within membranes we compared the diffusion of CTxB to that of STxB. Given that STxB has the capacity to bind up to 15 Gb_3 lipids, compared to CTxB's 5 GM_1 binding sites, it could be predicted that STxB will experience more drag from its lipids which could lead to even slower diffusion than CTxB. However, in ATP depleted cells we found that the diffusion of STxB is, in fact, significantly faster than that of CTxB, suggesting that the absolute number of lipid binding sites is not correlated with the cell surface mobility of either toxin. This lack of correlation between the number of bound lipids and the rate of diffusion between these toxins, mirrors a previous study from our lab examining the role of cross-linking by comparing the diffusion of wild type CTxB to that of chimeric CTxB, made of a mixed population of toxins with one or two functional binding sites for GM_1 [172]. In that study, we found no significant difference in the rate of diffusion between wild type and chimeric CTxB's on the plasma membrane of COS-7 cells at steady state. From these two studies it appears that the number of gangliosides crosslinked by CTxB has very little effect on the diffusion of the toxin.

A number of hypothesizes could be put forward to explain the lack of direct scaling between the number of gangliosides bound by AB5 toxins and the rate of diffusion of the toxins. One such possibility is that CTxB may be recognizing alternative binding partners. While GM_1 is the highest affinity binding partner identified for CTxB, it is well documented that CTxB also has a high affinity for other ganglioside species [24-26]. Furthermore, live cell studies have indicated that CTxB may recognize alternate binding partners in the plasma membranes of live cells [209, 210]. If one of these alternate binding partners were a glycosylated protein, this would explain the apparent disconnect between hydrodynamic radius of the toxin and diffusion. Furthermore, this occurrence could explain both the slow diffusion of the toxin and would also lay out a clear model for the mechanism by which CTxB diffusion is sensitive to cortical actin.

Another possible factor that could be contributing to the slow diffusion of CTxB may be related to the subresolution topology of the cell surface. It is well documented that certain membrane components localize to, or are excluded from, specific membrane regions based on the intrinsic curvature of that membrane region [211-213]. Furthermore, the complex topology of the plasma membrane can impact the apparent diffusion of various markers [214]. To control for potential effects of membrane topology on diffusion, we endeavored to avoid photobleaching visible protrusions or invaginations produced by ATP depletion and Lat A treatment. We cannot fully exclude the possibility that there may have been subresolution protrusions and invaginations in our bleach regions. However, with the exception of plasma membrane invaginations formed in response to ATP depletion, which were selectively enriched in CTxB, all of the markers examined appeared to label membrane invaginations in LatA treated cells, protrusions in ATP depleted cells, and "flat" regions of the membrane to similar degrees. This suggests that these markers have roughly equivalent affinities for convex, concave and flat plasma membrane regions. Therefore, it seems unlikely that potential subresolution changes in cell surface topology accounted for the changes we observed in diffusion following these treatments; rather, we propose these differences in diffusion were the result of lateral heterogeneity not related to cell surface topology. Further work is certainly needed to examine the interplay between membrane topology and lateral heterogeneity, as well as membrane topology and diffusion.

Finally, it has been reported that many gangliosides in the plasma membrane are shielded against toxin binding. This is supported by the observation that cholesterol depletion increases the level of CTxB binding to cells [215]. From this observation it may be argued that the raft associated glycolipids are the ones that are most heavily masked and therefore that CTxB is not reporting on lipid rafts. However, treatments such as cholesterol depletion have multiple effects on membranes. For example, in our own previous work we showed that cholesterol depletion leads to a systematic slowing of the diffusion of multiple cell surface markers, including CTxB [33]. Furthermore, it is worth noting that the only the propensity of CTxB to bind cells following cholesterol depletion has been examined. This says nothing of the state of GM_1 after CTxB binding and therefore, it remains unclear if GM_1, once bound by CTxB, then interacts with cholesterol. Therefore, while the observation that cholesterol depletion increases cholera toxin of cells is an interesting one, further work is required to regarding the

effects of cholesterol on toxin binding and also on the implications of ganglioside masking, if any, upon toxin organization and dynamics.

In summary, our results are consistent with a model in which in cells, the diffusional mobility of CTxB/GM$_1$ complexes is restricted by F-actin dependent as well as ATP-dependent processes, which may also be linked to the maintenance of actin organization. Coupling of these complexes to actin could potentially occur either with the help of currently unidentified transmembrane proteins, or by trapping of small CTxB-enriched domains within actin-defined corrals. Indirect interactions of CTxB with the cytoskeleton could in turn provide a mechanism that facilitates toxin uptake by clathrin-independent endocytic mechanisms [169, 192]. This working model should provide a useful framework for evaluating the role that both crosslinking and the cytoskeleton play in assembling functional toxin-stabilized domains.

CHAPTER IV

DYNIEN PROVIDES MECHANICAL FORCE FOR MEMBRANE TUBULATION IN CLATHRIN-

INDEPENDENT ENDOCYTOSIS

Introduction

Multiple clathrin-independent endocytic mechanisms are known to exist [86]. The physical mechanisms that deform the plasma membrane and give rise to endocytic vesicles in these pathways are poorly understood. One prominent model for the formation of clathrin independent endocytic vesicles states that these vesicles are mechanically generated by multivalent lipid binding toxins, including Shiga toxin and cholera toxin, in what is known as "toxin-induced endocytosis".

This model is supported by the observation that fluorescently conjugated STxB and CTxB accumulate in long (multiple micrometer) invaginations of the plasma membrane under ATP depletion [20, 40].   As cellular machinery is thought to be in rigor under these conditions, the prominent thinking is that the toxins are imparting curvature on the membrane, an interpretation consistent with reports of AB5 toxins having the capacity to deform model membranes [20, 40]. The current model states that endogenous proteins appear to be function only in the scission of these invaginations, since induction and growth of these invaginations persist under ATP depletion.

Utilizing quantitative fluorescence microscopy approaches, we have further characterized the mechanisms that drive membrane deformation in toxin-induced endocytosis. Employing a chimeric cholera toxin with a reduced number of functional GM_1 binding sites, we tested the importance of receptor cross-linking on the production of CTxB enriched membrane invaginations under ATP depletion, and found that receptor cross-linking has very little effect on the formation of invaginations. Furthermore we identified, for the first time, an

endogenously expressed membrane marker, HRas, colocalizing with CTxB on the invaginations. Using GFP-HRas we uncovered that the membrane tubulation previously described as toxin-induced is in fact generated by an endogenous process, as the tubules could be identified in the absence of AB5 toxins. While disruption of the actin polymerization and depolymerization cycle appears critical for the formation of long invaginations, actin- and actomyosin-based processes are not providing the force to deform the plasma membrane. Alternatively, perturbations of microtubules and disruption of the dynactin complex significantly inhibited tubulation of the plasma membrane. Using both a small molecule inhibitor of dynein's ATPase activity to block membrane tubulation and particle tracking of lysosomal movements under ATP depletion, we confirmed that some dynein motor activity persists under previously published ATP depletion conditions. Together, this research implicates microtubules, dynein and dynactin as capable of generating plasma membrane curvature as a precursor to endocytic vesicle formation.

Results

Tubule formation is not dependent on receptor cross-linking

We took advantage of a previously described assay in which STxB and CTxB can be trapped in surface attached tubular invaginations under conditions that are permissive for tubule growth but that inhibit tubule scission [20]. In a recent study we confirmed that CTxB accumulates in surface-attached tubular invaginations in cells following actin disruption or ATP depletion [32]. However, actin disruption also led to the formation of plasma membrane tubules by a toxin-independent mechanism [32]. We therefore utilized ATP depletion as a model for stabilizing putative toxin-induced tubular invaginations in the current study (Figure 14, Figure 15). We previously observed that ATP depletion also induces the formation of membrane protrusions that bear superficial resemblance to invaginations in single confocal sections (Figure 9) [32]. To differentiate between protrusions and invaginations in our experiments, we collected confocal z-stacks (Figure 14B, C). Tubules labeled with low concentrations of red Alexa555-CTxB, quickly filled with green Alexa488-CTxB, indicating that the tubule

membrane is continuous with the plasma membrane (Figure 16). Furthermore, the invaginations did not remain intact following fixation, so all experiments were carried out in living cells.

First, we needed to verify that the CTxB-positive tubules were in fact, plasma membrane attached. To do this ATP depleted cell were labeled with a low concentration Alexa555-CTxB and incubated on the scope until the toxin was readily observed in tubules. A high concentration of A488-CTxB was then added and the rate of accumulation of this toxin in invaginations was recorded in real time. Tubules acquired the A488-CTxB at a rate too fast to be the result of intracellular trafficking and more consistent with that of CTxB diffusion across the membrane, indicating that the tubule membranes are continuous with the plasma membrane (Figure 16).

To test if toxin binding caused plasma membrane tubulations by compaction or reorienting multiple glycosphingolipids into a curved surface, we prepared a mixture of chimeric cholera toxins (CTx chimera) that bind 0, 1, or 2 glycosphingolipid receptors (ganglioside GM_1) instead of the usual 5 [172]. The 1- and 2-GM_1 binding site mutants still bind to cell membranes, undergo GM_1-mediated endocytosis, and caused intoxication, albeit with substantially decreased efficiency compared to wild type cholera toxin [172]. We hypothesized that the CTx chimera mutants should be defective in bending the plasma membrane if receptor crosslinking is essential for this process to occur. We studied the uptake of the fluorescently-labeled CTx chimera in 3-dimensions by confocal microscopy of live cells and compared this to the uptake of wild type CTxB, which can bind five gangliosides at once. Unexpectedly, we found that the mutant toxin was readily observed in tubular invaginations (Figure 17A). Compared to wild type CTxB, the mutant cholera toxin accumulated in invaginations in a slightly smaller percentage of cells (Figure 17B). However, the average number of invaginations per cells and length of the invaginations were essentially identical (Figure 17C, D). Thus, binding of cholera toxin to only 1 or 2 GM_1 molecules is sufficient to target the protein to tubular invaginations, implying that extensive crosslinking of its glycolipid receptor is not required for this process to occur.
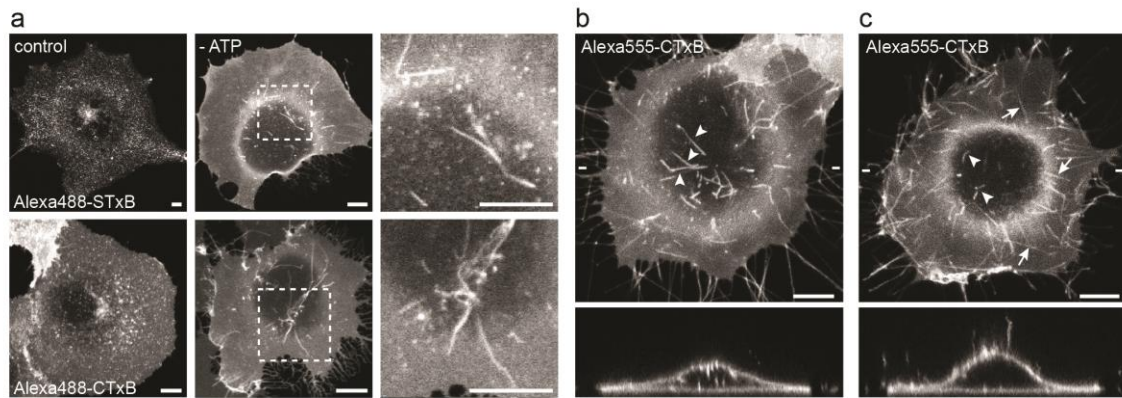
Figure 14. **CTxB accumulates in plasma membrane-derived tubular invaginations.** (A) Subcellular distribution of CTxB and STxB in control and ATP depleted COS-7 cells. (B-C) Confocal sectioning of ATP depleted COS-7 labeled with 100 nM Alexa555-CTxB show that CTxB accumulates in membrane derived invaginations and protrusions. Examples of invaginations are marked with arrowheads and protrusions with arrows. Invaginations and protrusions can also be distinguished in x-z-sections (below). X-Z-sections shown were taken between the dashes in the above image. Bar equals 10 μm.
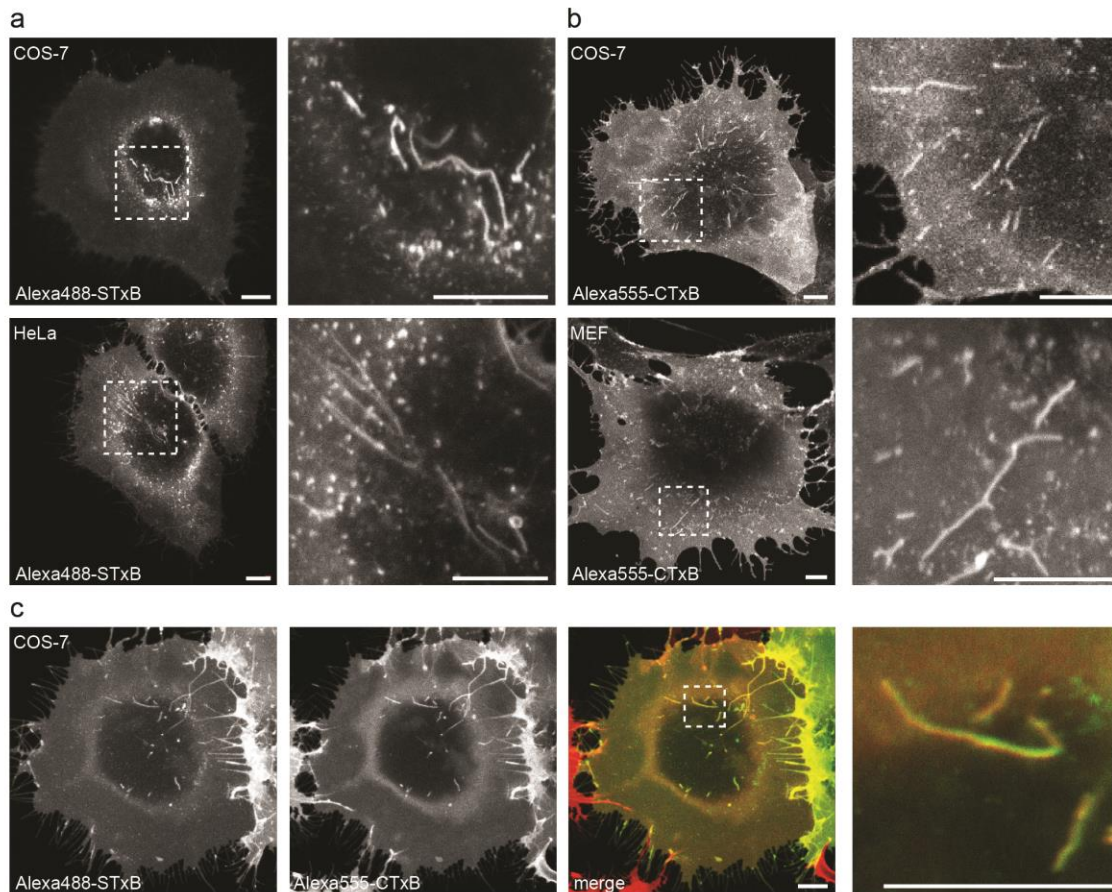
Figure 15. CTxB and STxB label tubular invaginations in multiple cell types. (A) Alexa488-STxB accumulates in invaginations in ATP depleted COS-7 expressing Gb$_3$ synthase and also in HeLa cells, which naturally express Gb3. (B) Alexa555-CTxB labels plasma membrane invaginations in ATP depleted COS-7 and MEF cells. (C) Alexa488-STxB and Alexa555-CTxB accumulate in the same plasma membrane invaginations in ATP depleted COS-7 expressing Gb$_3$ synthase. Bar equals 10 μm.
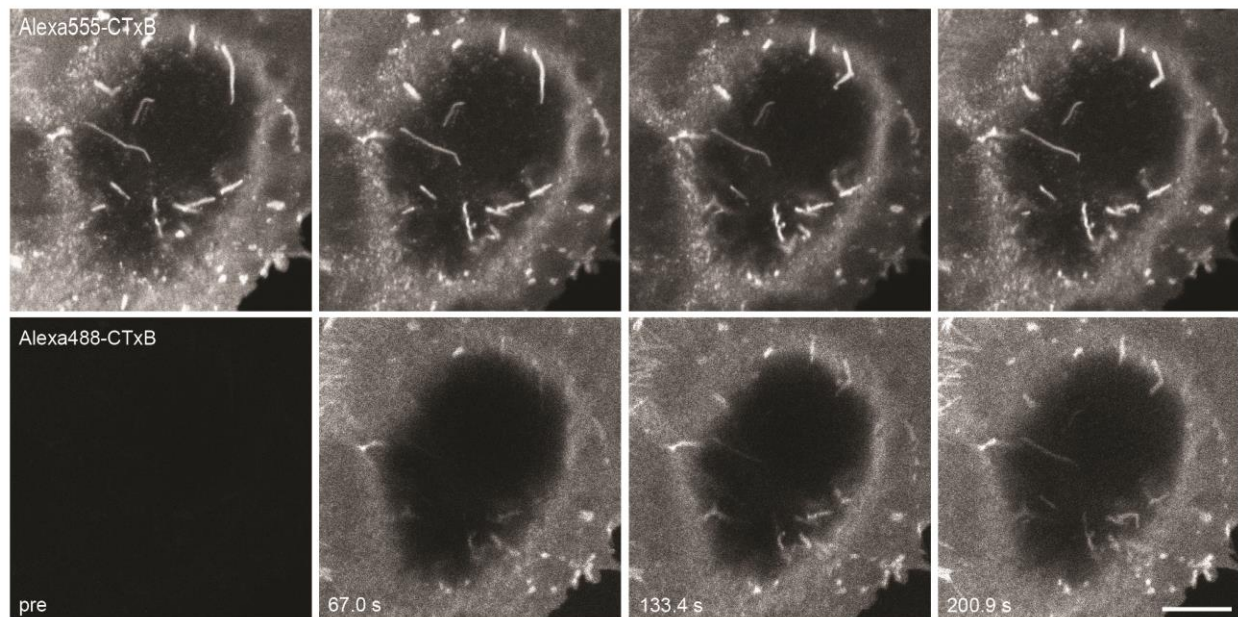
Figure 16. CTxB positive invaginations are readily accessible to new toxin. Live, ATP depleted COS-7 cells were labeled with 25 nM A555-CTxB and incubated on the microscope at 37°C. Following the visible formation of tubules containing A555-CTxB, a highly concentrated dose of A488-CTxB bringing the A488-CTxB concentration in the media to 50 nM. The A488-CTxB quickly gains access to the tubules.
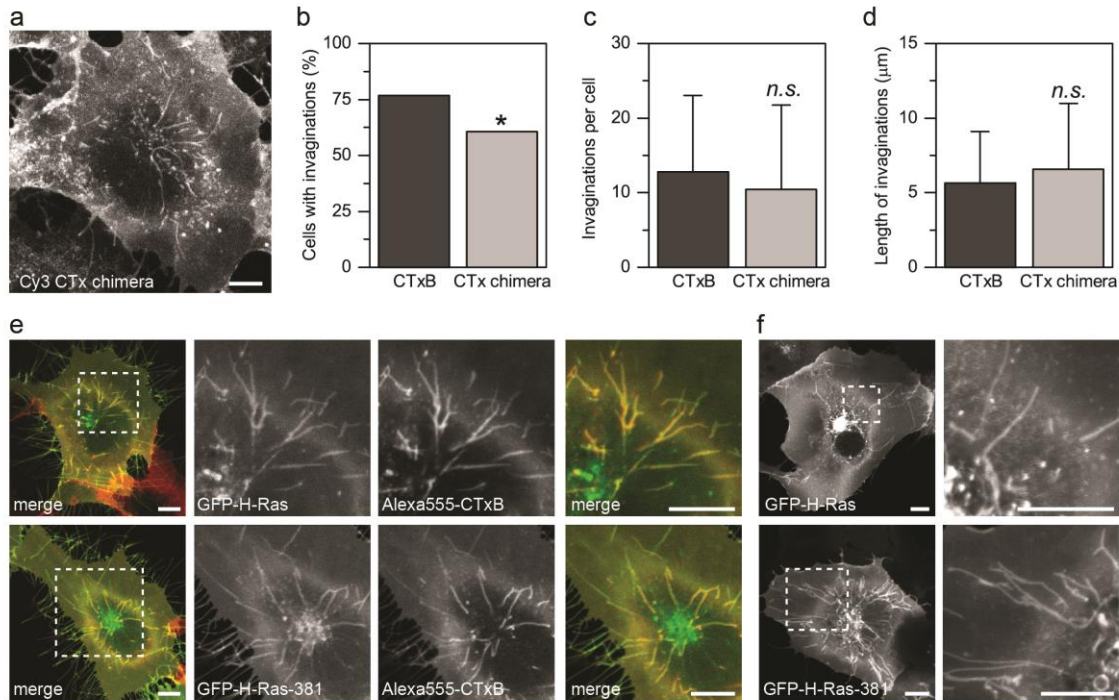
Figure 17. 1 or 2 GM$_1$ binding sites are sufficient to target cholera toxin to plasma membrane invaginations, and toxin binding is not required for tubular invaginations to form. (A) ATP depleted COS-7 cells labeled with chimeric CTx, comprising a mixed population of toxins with only 1 or 2 function GM1 binding sites. Cells were labeled with 500 nM Cy3-CTx chimera. (B) Fewer cells labeled with CTx chimera displayed invaginations as compared to those labeled with wild type CTxB (mean ± SD from 117-119 cells). * $p<0.05$, chi-squared test. (C) Cells labeled with Cy3-CTx chimera or Alexa555-CTxB show no difference in the average number of invaginations per cell (mean and SD of 42-46 cells). *n.s., p*>0.05; Student t-test. (D) Invaginations positive for Cy3-CTx chimera or Alexa555-CTxB show no difference in length (mean ± SD from 219-332 invaginations). *n.s., p*>0.05; Student t-test. (E) GFP-HRas and a construct containing only the C-terminal 10 amino acids of HRas, GFP-HRas-381, both colocalize with A555-CTxB in plasma membrane invaginations in ATP depleted cells. (F) In the absence of CTxB, GFP-HRas and GFP-HRas-381 label membrane invaginations under ATP depletion. Bar equals 10 μm.

Membrane tubulation occurs in the absence of toxin

An alternative hypothesis that could explain why STxB and CTxB accumulate in tubular invaginations is that tubules are generated through the action of endogenous cellular machinery and toxin is subsequently sorted into them. This model predicts that it should be possible to visualize the presence of cellular plasma membrane markers in invaginations in the absence of bound toxin. Consistent with this, we made the observation that the plasma membrane protein GFP-HRas strongly associated with tubular invaginations in ATP depleted cells either in the presence or absence of bound CTxB (Figure 17E, F). The formation of these structures was not dependent on the GTPase activity of overexpressed HRas, as a construct consisting of GFP appended to the C-terminal 10 amino acids of HRas also associated with tubular invaginations in ATP depleted cells (Figure 17E, F). Because these tubular invaginations do not require toxin binding to form, we conclude that endogenous cellular machinery must be responsible for mechanically deforming the plasma membrane under these conditions.

Actin-mediated mechanisms are not providing the force for membrane tubulation

It has previously been reported that STxB positive invaginations produced under ATP depletion align with F-actin in mCherry-Lifeact expressing HeLa cells [169]. Furthermore, we have observed that ATP depletion induces the formation of long F-actin filaments, many of which are oriented perpendicular to the plane of the plasma membrane (Figure 10) [32]. Based on these two observations we examined the possibility that an actin-based mechanism may be providing the force for membrane tubulation. Initially, we quantified the percentage of ATP depleted cells showing CTxB positive protrusions or invaginations as a function of time after labeling and shifting the cells to 37°C. This analysis revealed that the formation of protrusions is not correlated in time with the appearance of invaginations (Figure 18); indicating that these two events may not be related. To further test the role of actin polymerization in membrane tubulation, ATP depletion induced polymerization of actin was inhibited by treating COS-7 cells with 250 nM Jasplakinolide to stabilize actin prior to ATP depletion. Cells were then labeled with Alexa555-CTxB to assess plasma membrane topology. While cells that had undergone ATP depletion with DMSO pretreatment displayed plasma membrane protrusions, those pretreated with Jasplak did not (suggesting

that Jasplak treatment had stabilized F-actin) (Figure 19). Furthermore, actin stabilization did not prevent the formation of plasma membrane invaginations. In fact, a significantly higher percentage of cells which had been pretreated with Jasplakinolide developed invaginations as compared to those which had only been ATP depleted.

To confirm that actin filaments were not providing the force for membrane tubulation we next examined the alignment of toxin containing invaginations with F-actin under ATP depletion. As fixation did not preserve tubules formed under ATP depletion, these experiments had to be performed in live cells expressing F-actin reporters. COS-7 cells were transiently transfected with a plasmid encoding with either GFP-F-tractin or GFP-UtrCH, both of which bind F-actin but not G-actin [151, 152]. The vast majority of Alexa555-CTxB-positive tubules did not appear to align with F-actin filaments in COS-7 cells expressing GFP-tractin or GFP-UtrCH. To quantify this result, JFilament for ImageJ was used to generate 3D tracing of invaginations in the Alexa555-CTxB image channel. These tracings were then overlaid on the F-tractin channel and scored as having no alignment, partial alignment, or full alignment with F-tractin positive F-actin. This method revealed that only 2.4 % of CTxB positive invaginations were aligned with F-actin, while 79.8 % showed no alignment. Furthermore, repeating this analysis for F-actin in membrane protrusion we found that 92.4 % of protrusions were fully aligned with F-actin (Figure 20); consistent with our previous observations that protrusions are actin rich (Figure 10) [32]. Similarly, very small fraction of STxB-positives invaginations visually aligned with F-tractin positive actin filaments in HeLa cells (data not shown).

Plasma membrane tubule formation is microtubule dependent

We noticed that tubular invaginations often were directed toward the center of the cell in an orientation similar to that of the microtubule network (Figure 14A, 14B, 17A, 17E, 17F). Furthermore, CTxB has previously been found to localize within tubular invaginations whose formation is dependent on microtubules [93, 130]. We therefore considered the possibility that tubulation of the plasma membrane in ATP depleted cells is facilitated by a microtubule dependent process. To test this, we first asked whether the microtubule network is maintained under the conditions of our experiments. In agreement with earlier studies [216], intact microtubules could be visualized in ATP-depleted cells (Figure 21A, 22). Next, we asked if an intact microtubule network is required for
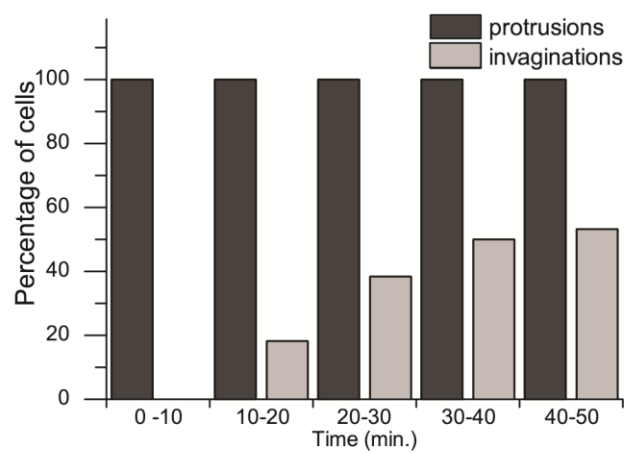
Figure 18. Time course of protrusion formation is distinct from that of invaginations. COS-7 cells were ATP depleted and labeled with 100 nM A555-CTxB at room temperature. Cells were then shifted to 37°C. Z-stack collected to identify protrusions and invaginations as a function of time after the temperature shift (n = 15 – 32 cells).
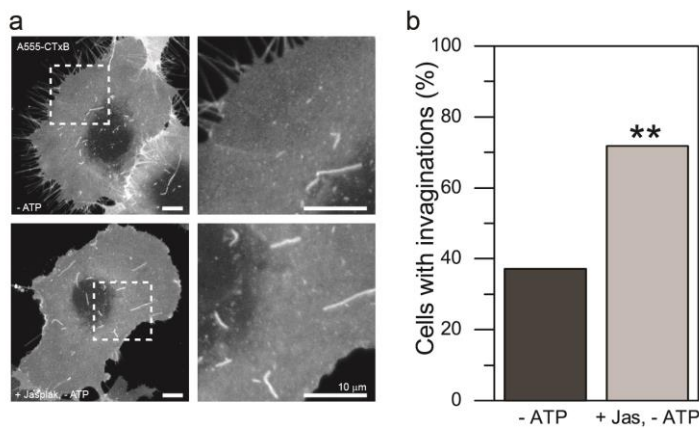
Figure 19. Actin stabilization prevents ATP depletion induced actin polymerization, but does not block the formation CTxB positive invaginations. (A) CTxB positive plasma membrane invaginations are evident COS-7 under ATP depletion and in COS-7 cells which were treated with 250 nM Jasplakinolide prior to ATP depletion. (B) More cells pretreated with Jasplakinolide displayed invaginations as compared to those which had only been ATP depleted (mean ± SD from 55-65 cells). ** $p<0.01$, chi-squared test.
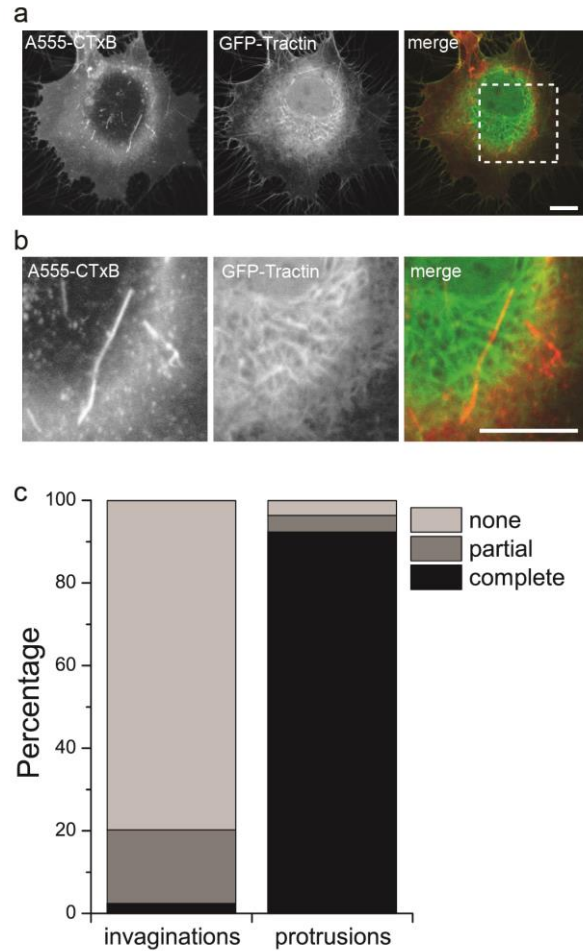
Figure 20. Membrane protrusions, but not invaginations, align with actin filaments. (A, zoom in B) A555-CTxB is enriched in membrane protrusions and invaginations in COS-7 cells, expressing the F-actin marker, GFP-tractin. (C) Classifying the protrusion and invaginations based on their alignment with F-tractin position actin filaments (n = 84 invaginations and 276 protrusions).
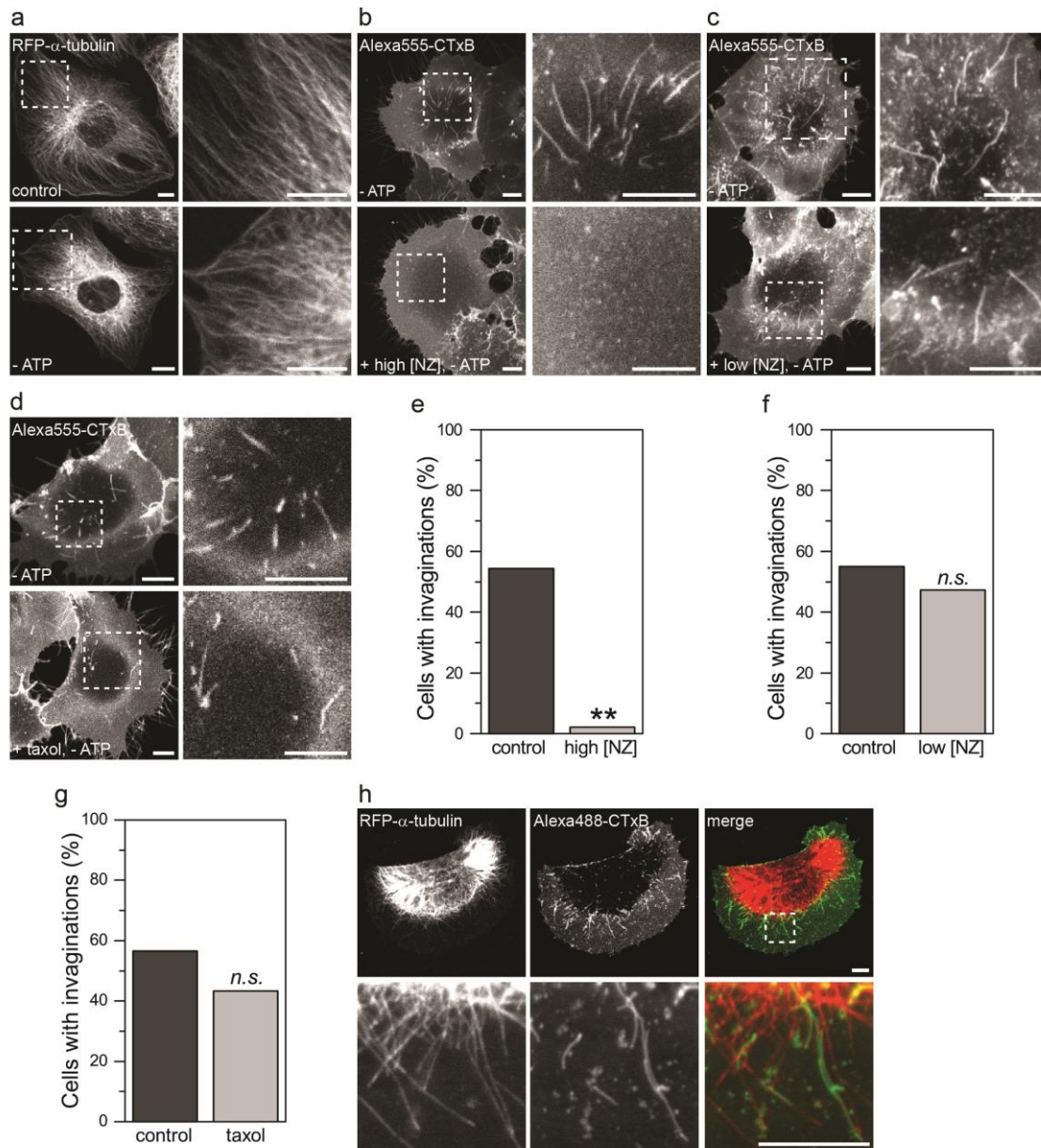
Figure 21. An intact microtubule network is required for the formation of tubular invaginations. (A) Microtubules incorporating mCherry-tubulin persist in COS-7 cells following ATP depletion. (B-G) Microtubule disruption but not microtubule stabilization prevents the formation of tubular invaginations. (B, E) Pretreatment of cells with 16.7 μM nocodazole prior to ATP depletion blocks the formation of plasma membrane invaginations (mean ± SD from 74 cells). ** $p<0.01$, chi-squared test. (C, F) Stabilizing microtubules by pretreatment with 150 nM nocodazole prior to ATP depletion has no effect on the formation of plasma membrane invaginations. (mean ± SD from 135-169 cells). *n.s. p>0.05*, chi-squared test. (D, G) Stabilizing microtubules by pretreatment with 1 μM taxol prior to ATP depletion has no effect on the formation of plasma membrane invaginations. (mean ± SD from 115-127 cells). *n.s. p>0.05*, chi-squared test. (F) CTxB positive invaginations align with taxol stabilized microtubule tracks in stably expressing RFP-tubulin HeLa cells under ATP depletion. Bar equals 10 μm.

75

tubular invaginations to form. Remarkably, disruption of microtubules with nocodazole prior to toxin labeling led to essentially a complete loss of extended tubular invaginations (Figure 21B, E). These findings establish a requirement for an intact microtubule network for growth of the invaginations to occur.

We next considered how microtubules support tubulation of the plasma membrane. One potential model is via a "search-and-capture" type mechanism [217, 218] in which the nascent plasma membrane invaginations are captured by dynamic microtubule plus ends. Such a mechanism has previously been shown to drive the movement of organelles [219, 220]. This model predicts that both plus-end binding proteins and microtubule dynamics would be important for tubule formation to occur.

To examine this possibility, we first used a GFP-EB3 construct to ask whether the plus-end binding protein EB3 remain associated with microtubule plus ends under the conditions where tubule growth occurs using a GFP-EB3 construct [153]. Unlike in control cells where GFP-EB3 associated with rapidly moving microtubule plus ends (Figure 22), in ATP-depleted cells GFP-EB3 was no longer concentrated at the tips of microtubules, instead accumulating along their length (Figure 22).   These findings indicate that the enrichment of end binding proteins at the plus ends is not important for plasma membrane tubulation to occur. They further suggested that microtubule dynamics might not be required for the formation of tubular invaginations. We tested this possibility by inhibiting microtubule dynamics using taxol [221] prior to ATP depletion. Taxol pretreatment had no effect on the percentage of cells positive for invaginations compared to mock-treated cells incubated with carrier (Figure 21D, G). Using short (5 minute) incubations with 150 nM Nocodazole to stabilize microtubules prior to ATP depletion, similarly had no effect on the prevalence of membrane invaginations (Figure 21C, F). Furthermore, tubules often aligned with taxol-stabilized microtubules, as visualized in cells expressing mCherry-tubulin (Figure 21H). We conclude that microtubule dynamics are dispensable for the growth of tubular invaginations.

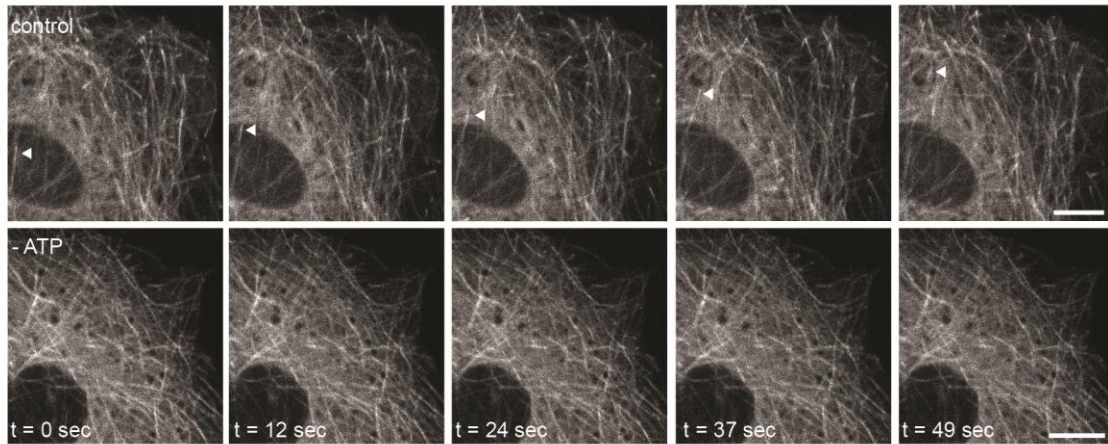**Figure 22. ATP depletion stalls microtubule polymerization.** COS-7 cells expressing GFP-EB3 were imaged at 37°C under control conditions or under ATP depletion.   The + TIP marker, GFP-EB3, is enriched at the microtubule + TIP and can be seen tracking with tip as the microtubule grows. Under ATP depletion, GFP-EB3 is dispersed along the length of the microtubules and no microtubule motion is present. Bar equals 10 μm.

Cytoplasmic dynein provides the pulling force to generate plasma membrane invaginations under ATP depletion

Another mechanism by which microtubules could contribute to the growth of tubular invaginations is through the activity of microtubule-based motors [144, 222], for example via a sliding mechanism similar to that utilized to tubulate the endoplasmic reticulum [223]. Microtubule-based motility involves two classes of motor proteins, dynein and members of the kinesin family [142, 224]. Given that tubular invaginations often were oriented toward the center of the cell where microtubule minus ends are located, the minus-end direct motor dynein appeared was a likely candidate for contributing to the tubulation process.

Because dynein is an ATPase [224], at first glance it seemed unlikely that dynein's motor is active under conditions where cellular ATP is depleted. However, recent results indicate that only a few dyneins are required to support long range endosomal motions [225]. Moreover, motor copy number is not thought to be a major determinant of motility [226]. These findings suggested that even a small number of active motors could contribute to the formation of tubular invaginations. As an initial test of this model, we performed control experiments examining the trafficking of lysosomes, a dynein-dependent process [227], in cells expressing mCherry-LAMP1. The motion of LAMP1-positive structures was substantially attenuated in ATP depleted cells compared to controls (Figure 23), consistent with the finding that ATP levels were decreased to approximately 2-3% of control levels under these conditions (Figure 24). However, a few long-range motions could be observed (Figure 23A), indicating that at least a fraction of motors remain active in ATP depleted cells.

Based on these results it seemed possible that dynein might contribute to the formation of extended tubular plasma membrane invaginations in ATP-depleted cells. To test this idea, we visualized the formation of tubular invaginations containing CTxB over time (Figure 23H-Q). Toxin containing tubules most often underwent preferential growth toward the nucleus (Figure 23H,K), but they were also observed to pause, or to undergo bi-directional motions (Figure 23I,N-P) and branching events (Figure 23J,Q), suggesting they can switch tracks. Overall, the dynamics of the growth of CTxB tubular invaginations revealed complex motions consistent with the expected activity of membranes transported by microtubule motors.

a mCherry-LAMP-1
ATP depleted

b 0:00 0:16 0:32 0:47
   1:03 1:19 1:34 1:50

c Distance (μm)
   Distance (μm)

d mCherry-LAMP-1
control

e Distance (μm)
   Distance (μm)

f mCherry-LAMP-1
PFA fixed

g Distance (μm)
   Distance (μm)

h Alexa555-CTxB

i Alexa555-CTxB

j Alexa555-CTxB

k 00:00 01:00 02:08 03:13 04:20 05:26

l 05:26

m time
   distance

n 00:00 01:50 03:40 05:31 07:21 09:11 11:01

o 11:01

p time
   distance

q 00:00 00:40 01:19 01:58 02:38 03:17 03:56 04:36

79

Figure 23. Live cell imaging of tubular invaginations in ATP depleted cells reveals complex motions including bidirectional motility and branching events. (A-C) A subset of lysosomes labeled with mCherry-LAMP-1 display long range directed motions in ATP depleted COS-7 cells. (B) Time lapse of zoomed in region of the cell in panel A. An example of a lysosome undergoing long-range directed motion is marked with the arrowhead. (C) Tracings of lysosome movement as detected by particle tracking analysis of the boxed region shown in panel B. Each track is indicated by a different color. (D-E) mCherry-LAMP-1 positive lysosomes display frequent long-range directed motions in COS-7 cells under control conditions. (E) Tracings from particle tracking analysis of lysosome movement in the boxed region shown in panel D. (F-G) mCherry-LAMP-1 positive lysosomes are immobile in PFA fixed COS-7 cells. (G) Tracings of lysosome movement as detected by particle tracking analysis of the boxed region shown in panel F. The total observation times were 1960 s for the trajectories in C and 470 s in E and G. (H, K, L, M) CTxB-positive invaginations often grow in fluid directed motions. K shows frames from a time series zoomed in on the boxed region in panel I. L shows the ROI used to generate the kymograph in M. (I,N,O,P) CTxB-positive invaginations also extend, retract, and regrow along the same axis. N shows frames from a time series of the boxed region in panel I. O shows the ROI used to generate the kymograph in P. (J,Q) Occasionally, the CTxB positive tubules undergo branching events. Q shows a zoom of the boxed region in J. Time stamps are in minutes:seconds. Bar equals 10 μm.
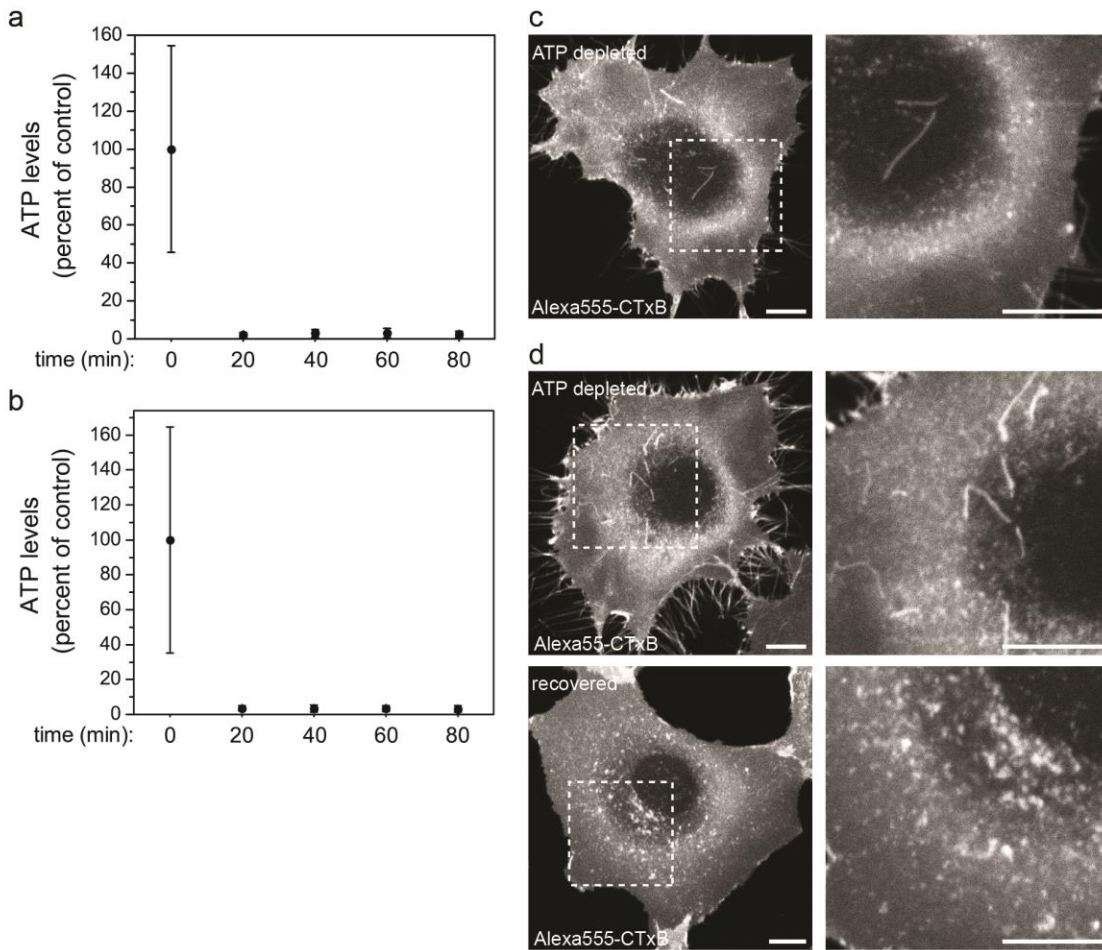
Figure 24. ATP depletion results in an over 90% reduction in cellular ATP levels and is reversible. (A-B) Incubation in ATP depletion media (50 mM 2-deoxy-D-glucose and 0.02% sodium azide) results in a greater than 90% decrease in cellular ATP levels from control (time 0) in COS-7 (A) and HeLa (B) cells. **(C)** Alexa555-CTxB labels tubular invaginations after being ATP depleted for 45 minutes. **(D)** To test the reversibility of ATP depletion, after 45 minutes in ATP depletion media, media was replaced in with fresh ATP depletion media or control media and incubated for an additional 15 minutes at 37°C. In the ATP repleted cells, CTxB was trafficked to perinuclear compartments, indicating the treatment is reversible. Bar equals 10 μm.

Having provided indirect evidence that residual motor activity is retained in ATP depleted cells, we next examined the requirements for dynein's motor activity more directly. In particular, we predicted that even in ATP depleted cells, the ATPase activity of dynein would be required for tubule formation. To test this we took advantage of a newly described small molecule inhibitor of dynein, HPI-4 [228]. We first performed control experiments to establish conditions under which HPI-4 inhibits dynein-based trafficking in cells (Figure 25). Additionally, we utilized the knowledge that endosomal positioning is maintained by opposing forces of dynein and kinesins upon the endosomal membrane. Therefore, inhibiting dynein would be predicted to reposition endosomes near the cell surface. Using mCherry-Rab11 as a marker of the perinuclear recycling endosomes, we confirmed that dsRed-CC1, p50-GFP and HPI-4, each inhibited cytoplasmic dynein, allowing for repositioning of Rab11 positive endosomes (Figure 26). We next assayed for tubule formation in ATP-depleted cells pretreated with HPI-4. We observed a decrease in the presence of tubular invaginations in cells treated with HPI-4 but not in control cells treated with carrier alone, suggesting that the ATPase activity of dynein is indeed necessary for the formation of tubular invaginations (Figure 27A, B).

It is well established that dynein requires the dynactin complex for its function [224, 229]. We perturbed dynactin in two different ways as a further means to test for a role of dynein in tubulation of the plasma membrane. First, we interfered with dynein/dynactin binding by overexpression of a dsRed-tagged form of the N-terminal coiled coil regions of the dynactin p150 subunit, CC1 [229] (Figure 27C, D). Second, we overexpressed a GFP-tagged form of p50/dynamitin, which disrupts the dynactin complex [229] (Figure 25C, 26B). Expression of either protein strongly inhibited the formation of tubular invaginations compared to surrounding untransfected cells or cells expressing GFP alone (Figure 27C-E). We conclude that the dynactin complex is required to support tubulation of the plasma membrane (Figure 28), further implicating dynein in this process as well.
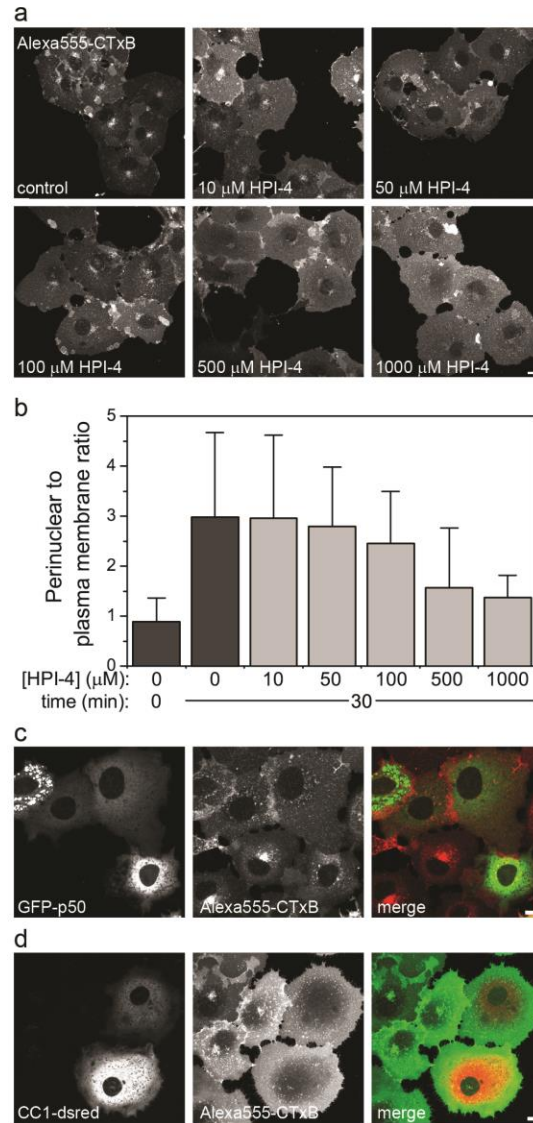
Figure 25. HIP-4, CC1 overexpression, or p50 overexpression disrupt delivery of CTxB to perinuclear compartments. (A) In COS-7 cells, CTxB normally accumulates in perinuclear compartments after 30 minutes of uptake at 37°C. However, pretreatment with 500µM HPI-4 results in a dramatic reduction of the perinuclear delivery of CTxB. (B) The accumulation of CTxB in the perinuclear space in inhibited in a dose dependent manner by HPI-4. Cells were pretreated with HPI-4 for 1 hour then allowed to uptake CTxB for 30 minutes prior to fixation. The extent of CTxB delivery to the perinuclear region was quantified as the ratio of the mean pixel intensity of an ROI in the perinuclear region to the mean pixel intensity of an ROI centered on the plasma membrane. n = 36-108 cells and error bars are standard deviations. Bar equals 10 µm. (C) Cells expressing GFP-p50 showed a block in the delivery of Alexa555-CTxB to perinuclear compartments after 30 min of uptake at 37°C compared to non-GFP-p50 expressing cells. (D) Likewise, expression of CC1-dsRed resulted in reduced Alexa488-CTxB accumulation in perinuclear compartments as compared to non-expressing cells. Bar equals 10 µm.
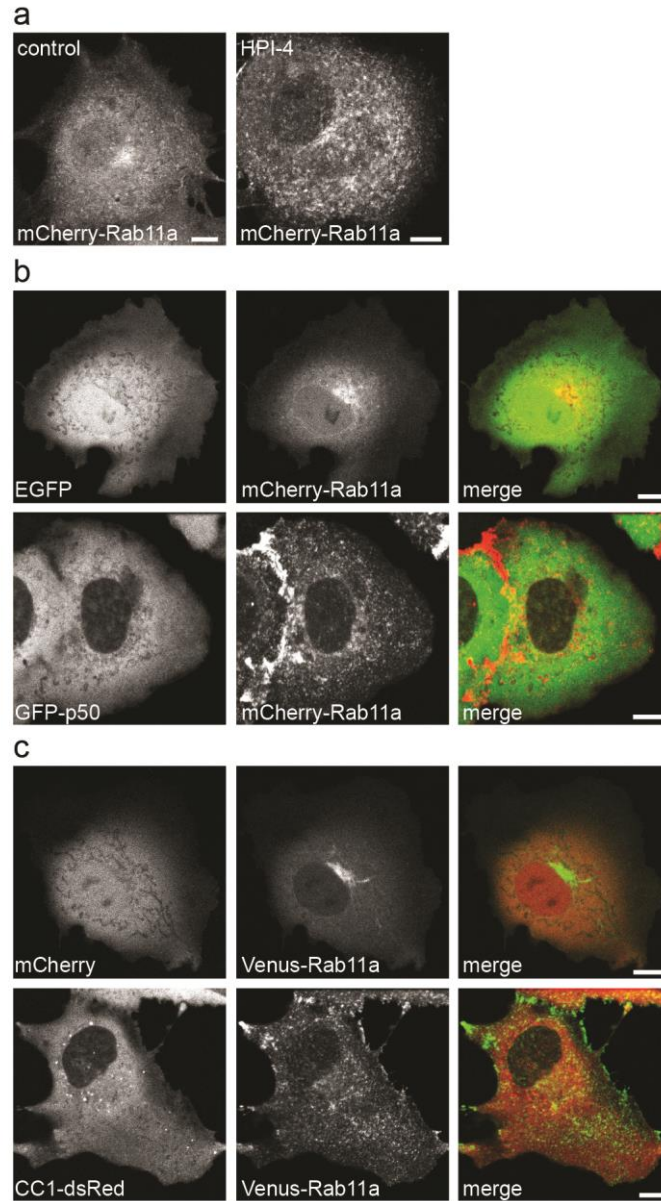
Figure 26. Control experiments demonstrate that HPI-4, CC1 overexpression, or p50 overexpression cause redistribution of recycling endosomes in COS-7 cells. (A) One hour incubation in 500 μM HPI-4 causes the redistribution of mCherry-Rab11a from the perinuclear space to the cell periphery. (B) In EGFP expressing cells the mCherry-Rab11a positive recycling endosomes are located in the perinuclear region. However, disruption of dynactin by GFP-p50 overexpression results in redistribution of recycling endosomes to the cell periphery. (C) Venus-Rab11a positive recycling endosomes localize near the nucleus in mCherry expressing cells, but are found near the cell surface in CC1-dsRed expressing cells. Bar equals 10 μm.
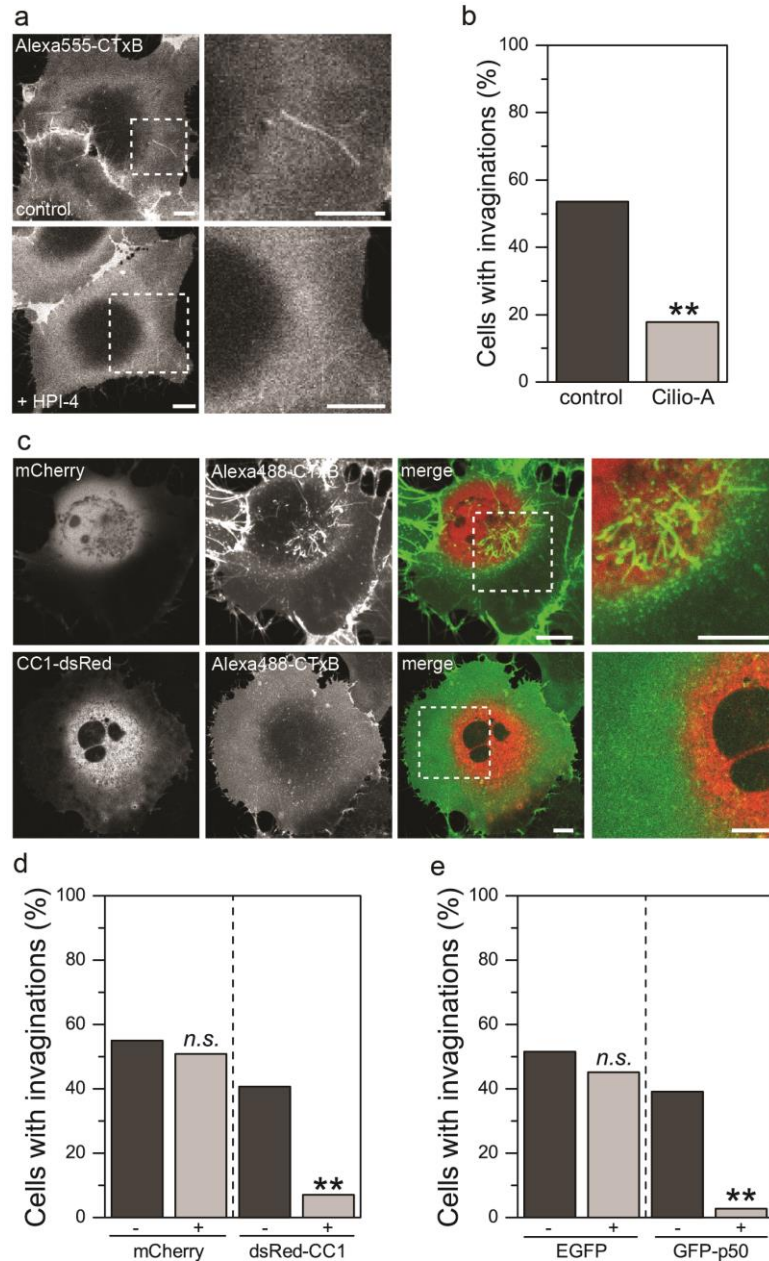
Figure 27. The ATPase activity of dynein and an intact dynactin complex are required for the formation of tubular invaginations. (A-B) Inhibition of dynein ATPase activity with 500 μM HPI-4 significantly reduces the percent of cells displaying tubular invaginations. (mean ± SD from 95-122 cells). ** *p*<0.01, chi-squared test. (C-D) Expression of the dynactin disrupting protein, CC1-dsRed, significantly reduces the percent of cells with CTxB positive invaginations as compared to untransfected cells. Bar equals 10 ▯m. (mean ± SD from 40-64 cells). *n.s., p*>0.05; ** *p*<0.01, chi-squared test. (E) Similarly, expressing of a second dynactin disrupting protein, GFP-p50, reduced the prevalence of cells with invaginations as compared to untransfected cells. (mean ± SD from 42-101 cells). *n.s., p*>0.05; ** *p*<0.01, chi-squared test. (F) Previously proposed model in which toxin-driven compaction of glycolipid headgroups drives bending and tubulation of the plasma membrane. (G) Working model based on our current findings. In this model, CTxB positive invaginations do not require the toxin to form. Instead, the driving force for tubule formation is supplied by the microtubule motor dynein.
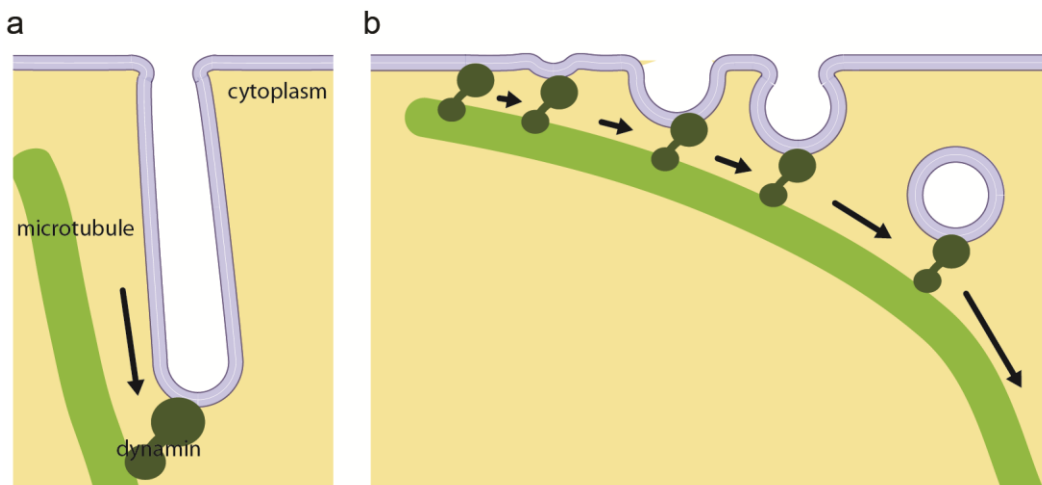
Figure 28. Models of dynein function in endocytosis. (A) Our data indicates that cytoplasmic dynein pulls at the plasma membrane leading to the membrane tubulation under inhibition of scission by ATP depletion. (B) Furthermore, this provides evidence that cytoplasmic dynein has the capacity to aid in the formation of vesicles by deforming the plasma membrane in addition to facilitating the early movement of vesicles away from the plasma membrane.

Discussion

Although the role of microtubules and motors in tubulating model membranes and intracellular compartments such as endosomes and the TGN is well recognized, until this report there has been little evidence that they can act at the plasma membrane directly [222, 230-236]. Based on our results, we propose a model wherein dynein and dynactin on the plasma membrane can interact with microtubules close to the cell surface to allow tubule extension (Figure 28). Dynein might drive tubule formation by sliding the membrane along microtubules, albeit only slowly under conditions where ATP is limiting. Alternatively, the plasma membrane may be locked onto microtubules using dynein/dynactin as a tether, and slow microtubule depolymerization or rearrangements within the cell may cause the tubules to form. Other minus end directed motors such as kinesins-14 might also contribute to these processes. These microtubule-based mechanisms may function cooperatively with the membrane reorganizations and bending induced by the AB5 toxins binding to their sphingolipid receptors [20, 40], but this is not required. Motor-driven tubulation of the plasma membrane may additionally facilitate recruitment of curvature-sensing proteins [237], including curvature-sensitive cargo molecules such as CTxB itself [238].

The exact mechanism by which the combination of dynein and dynactin bind the plasma membrane and how this process is regulated remains to be determined. This could potentially involve recruitment to sites of local membrane bending induced by endogenous cellular factors, similar to that previously described for retromer [233]. The mechanism of attachment of dynein/dynactin to the plasma membrane may alternatively be related to those involved in positioning of the mitotic spindle [239]. Indeed, microtubule-dependent plasma membrane invaginations have been reported to form in *C. elegans* embryos at cortical sites where spindle poles are tethered [240]. Caveolae could also potentially serve as a preferential site for dynein/dynactin recruitment to the plasma membrane, as caveolin-1 has been observed in long, toxin-positive tubules under conditions that inhibit endocytosis [76, 241].

In our experiments, ATP depletion was used as a tool to inhibit membrane scission and facilitate trapping of CTxB in surface-attached tubules. Although it is not yet entirely clear why ATP depletion is permissive for tubule growth, dynamic cycling between F- and G-actin is thought to be necessary for their scission [169], suggesting that alterations to actin dynamics may allow for tubule elongation. Consistent with this possibility, we previously observed that ATP depletion induces substantial cortical actin rearrangements [32]. Changes in cortical actin may also decrease plasma membrane tension, favoring the formation of long invaginations by microtubule-dependent pulling. Alternatively, cortical actin may act as a physical barrier between microtubules and the cell surface.

Reorganization of cortical actin either through endogenous processes or in response to actin perturbing agents [129] may then permit microtubules access to the plasma membrane and thus upregulate membrane tubulation.

Importantly, microtubule-dependent plasma membrane tubules containing CTxB have also been observed under basal physiological conditions [93], suggesting this is a normal cellular phenomenon and not an artifact of ATP depletion. Microtubules, dynein and dynactin may thus contribute in a significant way to the induction of curvature and general reshaping of the plasma membrane that allows for the formation of clathrin-independent endocytic carriers.

CHAPTER V

CONCLUSIONS

Summary

Cholera toxin has become a popular tool for the study of cell biology both as a putative raft marker and cargo molecule for clathrin-independent endocytic pathways; two phenomena which have not been well characterized. The lipid raft hypothesis states that the plasma membrane is organized into domains through lipid-lipid interactions. While model membrane studies provide compelling evidence for existence of lipid rafts, identifying them in live cells has proven challenging. One technique cell biologist have turned to is diffusion studies, as clear predictions can be made regarding the impact of rafts on lateral diffusion at the plasma membrane. However, rafts are not the only mechanism that may perturb diffusion at the cell surface.

Using confocal FRAP on live cells I sought to elucidate the cause of the slow diffusion of CTxB at the plasma membrane; which has previously been proposed to be the result of CTxB confinement in laterally immobilized, toxin-stabilize rafts [30, 36, 37]. My work in this area revealed no evidence to support raft cross-linking or raft mediated slowing of CTxB diffusion, although that possibility cannot be fully ruled out. Furthermore, I uncovered a role for actin in restricting the diffusion of CTxB. This was unexpected as CTxB is bound to lipids on the outer leaflet of the membrane and therefore cannot come in direct contact with actin. Precisely how actin inside the cell could be sensed by CTxB on the outer leaflet remains unclear.

CTxB was one of the first cargo molecules identified entering cells through clathrin independent endocytic mechanisms. Much about these pathways is not well understood, including how the membrane is deformed to generate the endocytic vesicles. Through live cell studies of cholera toxin, I tested a model from the literature for

a specific mode of endocytosis which proposes that SV40, STxB, and CTxB mechanically deform the plasma membrane to generate clathrin and caveolin independent endocytic invaginations at the plasma membrane. Using a mutant form of the toxin, predicted to be highly impaired in its ability to bend membrane, I uncovered evidence that the toxin may not be bending the membrane. This finding was supported by the identification of HRas on tubular intermediates of toxin-induced endocytosis; where it is found in both the presence and absence of toxin. The presence of HRas on these tubules in the absence of bound CTxB indicates that these tubules form by disruption of an endogenous process, as well as helps shed light on possible connections between the supposedly "toxin-induced" endocytosis and other endocytic pathways.

The most important finding to come out of my research is not that the previous model was incorrect, but rather that cytoplasmic dynein can tubulate the plasma membrane to aid in clathrin-independent endocytosis. Currently, the formation of endocytic vesicles and early trafficking events are seen as two distinct events. Vesicles are thought to form primarily by the deformation of the membrane by proteins whose primary function is to bind membranes such that they may induce and stabilize curvature. Once endocytic vesicles have formed, they are moved away from the plasma membrane by actin-mediated processes. Yet our data suggests that both steps in the biogenesis of endocytic vesicles can be facilitated by a single protein, cytoplasmic dynein. Dynein and microtubules are already known to be capable of tubulating membranes in intracellular compartments such as endosomes and the trans-Golgi network [144]. The involvement of cytoplasmic dynein in endocytosis is a novel finding for the field as demonstrated in a recent review which states "Microtubule motors assist in carrier biogenesis, with the exception of endocytic carriers" [144]. Therefore, the finding that microtubule motors are involved in the biogenesis of endocytic vesicles will mark an important advancement our understanding of endocytosis.

Future directions

Mechanisms for confined CTxB diffusion

My work with membrane dynamics revealed no direct evidence to support the model of CTxB cross-linking lipid rafts (Figure 12). Alternatively, CTxB diffusion could be slowed by transient confinement within docked endocytic vesicles at the plasma membrane. Such a model has been proposed previously for CTxB confinement within caveolae [36, 37]. My research tested this model, and found no effect of caveolin-1 on CTxB diffusion in MEF cells (Figure 11). However, other classes of endocytic vesicles may confine diffusion of particle at the plasma membrane [206]. These forms of confinement were not examined but may be worth testing in future studies. While CTxB diffusion was insensitive to Cav-1 expression, the diffusion of CTxB was sensitive to actin disruption by Lat A (Figure 8). Furthermore, ATP depletion increased the rate of CTxB diffusion (perhaps because of the actin remodeling that ATP depletion induces) (Figure 9, 10). How CTxB, which is bound the extracellular leaflet of the plasma membrane by lipid, can sense actin is not immediately clear. Also the effect of actin, while significant, appears to be too small to fully account for the diffusion of CTxB, suggesting other mechanisms are also contributing to slow CTxB diffusion.

One hypothesis that we did not explore is that CTxB binding to the plasma membrane may not be specific for GM_1. Ganglioside GM_1 is the highest affinity receptor for CTxB known. Yet CTxB may be binding more than just GM_1 in live cells, as FACS sorting of mouse embryonic neuroepithelial cells by CTxB surface density found that CTXB binding did not coincide with GM_1 expression levels, suggesting alternative receptors are present [210]. This alternative receptor may be another ganglioside as surface plasma resonance (SPR) studies have found that CTxB has affinities for the lipids GM_2 and GD_{1a} $1:10^{th}$ that of CTxB's affinity for GM_1 [24]. Additionally, this and other studies have found that CTxB has an affinity for many additional gangliosides species [24-26]. This is an especially important observation given that CTXB is often used in cell biology studies at concentrations at or near the saturation of the plasma membrane.

While it is not immediately clear how the binding of CTxB to lipids other than GM_1 may account for the slow diffusion, but if CTxB is binding a glycoprotein this could easily explain many of the characteristics of CTxB diffusion. For, example, transmembrane proteins generally diffuse much slower than lipid anchored proteins. In fact, the rate of CTxB diffusion is consistent with the rate of diffusion of many transmembrane proteins [33]. Furthermore, anchorage to transmembrane proteins, would provide a mechanism for the sensing of cortical actin by CTxB, as indicated in my own research [32]. While GM_1 is commonly accepted as the only receptor for CTxB, biochemical evidence is beginning to emerge to support the existence of glycoprotein receptor as well.

At least one study suggests that CTxB is binding a glycoprotein at the cell surface [209]. In this study the binding of CTxB to T cells was only partially inhibited in cells that had been treated with a small molecule inhibitor of GM_1 synthesis. Interestingly, trypsin incubation significantly reduced CTxB binding, suggesting that CTxB is binding to a protein [209]. And an earlier paper found that CTxB could bind a protein known a sucrose-isomaltase [242]. Additionally, Jennifer Kohler's lab at UT Southwestern has isolated both GM_1 and a glycoprotein as binding partners of CTxB in T-84 and Caco cells (unpublished). Ongoing work in her lab is aimed at identifying the protein and determining its impact on lateral diffusion of CTxB in the plasma membrane (personal communication with Jennifer Kohler).

My published FRAP data [32] was collected at labeling concentrations of CTxB above saturation for the receptor(s) at the cell surface. However, I did examine the diffusion of CTxB as a function of concentration in COS-7 cell (Figure 29) and found a strong inverse correlation between CTxB labeling concentration and the rate of diffusion. One possible explanation for this concentration dependence is that that CTxB is binding distinct species with different binding affinities. The binding affinity of CTxB for GM1 is extremely high [25]. If CTxB has a second binding partner, say a glycoprotein, for which CTxB affinity is lower than that of CTxB for GM_1, this would explain why at low labeling concentrations CTxB diffuses quickly and slows to a rate consistent with that of transmembrane proteins at high labeling concentrations. An alternative explanation for concentration dependent diffusion is that CTxB cross-linked rafts grow in size as a function of concentration. In this case as the lipid rafts expand in size they become increasingly trapped in actin defined corrals. Both models are consistent with the actin dependent diffusion we reported [32], since transmembrane proteins could directly come in contact with

92

actin and large rafts have been predicted to become trapped inside actin corrals [243]. Therefore, at this time I cannot determine which model is more compelling, but the observation of concentration dependence for CTxB is novel and in fact showed the strongest effect on diffusion of any of the variables I examined. Therefore this is an avenue of research that I think is very promising.

Role of ATP depletion and actin disruption on diffusion

My FRAP work indicates that ATP depletion and actin disruption both lead to an increase in CTxB diffusion at the plasma membrane. Additionally, both perturbations allow for the formation of plasma membrane invaginations. The formation of invaginations may or may not be related to altered diffusion under these treatments, although it is an interesting coincidence. (The possible mechanism through which actin could be involved will be discussed in detail elsewhere.)

How actin disruption could be having the same effect on CTxB diffusion as ATP depletion, which leads to actin polymerization, is an interesting problem. Two possible explanations come to mind. First, as established in my PLoS One paper [32], ATP depletion triggers massive polymerization of actin near the plasma membrane (Figure 10). However, phalloidin staining of these cells indicates that many small actin filaments are being replaced by a small number of long filaments. This indicates that actin corrals are becoming larger under ATP depletion. Additionally, I have observed that over time the protrusions formed by actin polymerization under ATP depletion become floppy and the cell body begins to ball up. Both observations are consistent with breaks in the actin filaments at later time points after ATP depletion, an observation previously characterized [244]. If this is occurring it would mean that the longer the cells are maintained in ATP depletion media the more breaks in the actin corrals occur and the faster CTxB could diffuse.
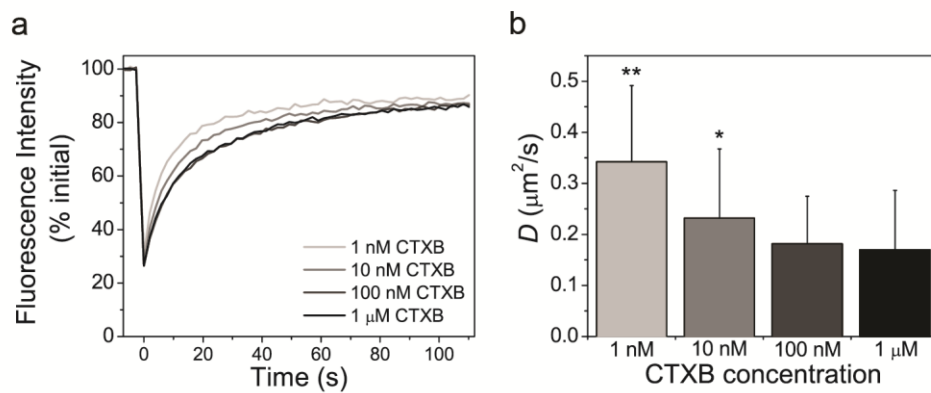
93

Figure 29. A555-CTxB diffusion is dependent on cell labeling concentration. (A) Averaged FRAP curves of Alexa555-CTXB at different labeling concentrations in COS-7 at 37°C. (B) Diffusion coefficients of Alexa555-CTXB at different labeling concentrations. (Bars are averages and standard deviations of 22-26 samples; ** $p < 0.01$; * $p < 0.05$; Student *t*-test).

Comparison of tubular invaginations across perturbations

As part of my dissertation research, I tested a model for the endocytosis of CTxB and STxB, known as "toxin induced endocytosis." This putative form of endocytosis is commonly studied under perturbations allow for the tubulation of what are presumably trapped nascent vesicles at the plasma membrane. The initial paper proposing the toxin induced endocytosis model used four methods to trap membrane tubules, namely, cholesterol depletion, dynamin inhibition, actin disruption, and ATP depletion [20]. In a follow up paper from the same group, actin stabilization was added to the list of perturbations under which tubular invaginations form [193]. While it is strongly implied in these papers that the tubules formed under each treatment represent the same class of structures, I find no experimental evidence in the literature to support that idea. This is a major drawback to the toxin induced model and an assumption that I think deserves considerable attention. In the course of my research I have tested all five treatments (cholesterol depletion, dynamin inhibition, actin disruption, ATP depletion, and actin stabilization) previously reported to induce membrane tubulation. While I cannot completely dismiss the idea that they are all the same, in my hands I see distinct differences between the tubules formed by some of the treatments, leading me to believe that they are not all equivalent structures.

Using MβCD to deplete cellular cholesterol prior to CTxB labeling, we see almost no toxin positive tubules. Under this treatment the cell bodies retract and most of the toxin remains trapped at the cell surface as endocytosis and cellular trafficking are clearly impaired by cholesterol depletion (Figure 30). The small amount of CTxB which is endocytosed accumulates in bright puncta (resembling early endosomes) around the cell periphery and never reaches the Golgi complex.

I am also not convinced that the tubules I observed under dynamin inhibition are the same as those formed by ATP depletion, actin disruption and actin stabilization. In the study by Romer et al. STxB positive plasma membrane invaginations were identified in HeLa cells when dynamin 2-mediated membrane scission had been blocked with either the small molecule dynamin inhibitor, dynasore, or with the dominant negative mutant dynamin 2 K44A [20]. I have not worked with dynamin K44A, but I did perform a large number of experiments with dynasore. In COS-7 cells which had been treated with dynasore prior to CTxB labeling, I observed the

formation of CTxB positive tubules (Figure 30). Visually, these tubules appeared to originate inside the cell and not at the plasma membrane. Furthermore, their dynamics were very distinct from that of the tubules formed under all other treatments. Tubules which appear under dynamin inhibition wave back and forth at their leading tip as they elongate. This waving continues until the leading edge of the tubule makes contact with another tubule and stops growing. Through this process tubules became highly branched until they appeared to assemble a single branching network throughout the cytoplasm. The experiment was repeated Cy3-STxB in HeLa cells and the same types of tubules were seen. These structures did not resemble the STxB positive invaginations shown in Romer et al [20]. However, another paper out of Rob Parton's lab has reported the formation of CTxB positive tubules under dynamin inhibition [108]. These structures were proposed be formed from GEEC's and ARF6 related endosomes. Since the tubules reported in this paper are highly branched, it seems most likely that the structures I observe using dynasore are the same as those observed by the Parton lab.

As demonstrated in Chapters III and IV, we were able to observe tubular, CTxB positive structures under ATP depletion, actin disruption (with Lat A) and actin stabilization (with Jasplak). While we cannot at this time be confident that all three treatments were tubulating the same class of structures, multiple lines of evidence suggest that that they are comparable. First, tubules formed under each of these three treatments treatment were morphologically very similar. In each case, they were many micrometers in length with few branches (particularly as compared to highly branched structures formed under dynamin inhibition).

Furthermore, tubules formed under ATP depletion, actin disruption and actin stabilization all appear to originate at the plasma membrane (Figure 30). However, I must acknowledge that I have only tested surface accessibility for tubules formed under ATP depletion (Figure 16). It is important to acknowledge that some of the tubules formed under Jasplak and to perhaps a greater extent under Lat A are mobile. In both cases, the tubules appear to elongate from the plasma membrane before scissioning and moving towards the center of the cell while retaining their tubular shape. Tubules formed under ATP depletion elongated over time but were almost never
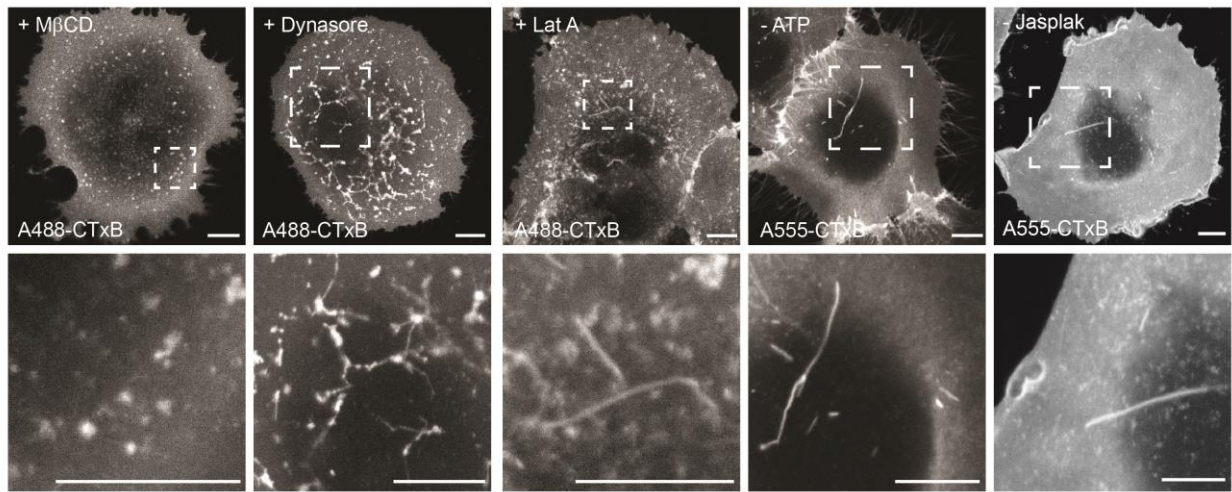
Figure 30. **Comparative morphology of CTxB positive structures under cholesterol depletion, dynamin inhibition, actin disruption, ATP depletion and actin stabilization.** COS-7 cells under cholesterol depletion with MβCD, dynamin inhibition with Dynasore, actin disruption with Latrunculin A, ATP depletion with 2-deoxy-glucose and sodium azide and actin stabilization with Jasplakinolide were labeled with FL-CTxB and imaged live at 37°C. Bar equals 10 μm.

released from the plasma membrane, which may mean that ATP depletion is a more efficient inhibition of scission, or that ATP depletion is impairing the physical act of moving (or both).

Under ATP depletion, we identified HRas as a novel marker of plasma membrane invaginations. Furthermore, H-Ras labeled invaginations under ATP depletion in the absence of CTxB (Figure 17). To determine if the invaginations present under actin disruption or stabilization may represent the same class structures as those studied under ATP depletion, we tested for H-Ras localization. Consistent with our result under ATP depletion, membrane invaginations produced under both actin disruption and stabilization contained both GFP-HRas and A555-CTxB (Figure 31). Furthermore, these tubules persisted in the absence of CTxB (Figure 31), suggesting that the same class of structures may be tubulating under all three perturbations.

In our PLoS One paper (chapter III) we reported that under Lat A treatment GL-GPI, GT46, and $DiIC_{16}$ appear in plasma membrane invaginations, while no invaginations were observed with these three markers under ATP depletion. This observation was made concurrent with the collection of FRAP data. However, I have recently revisited ATP depletion and $DiIC_{16}$ and did see plasma membrane tubules. I now speculate that tubules formed under both treatments are probably equivalent, and that my lack of seeing them may be the result of three scenarios. First, the invaginations can be very difficult to identify, especially when labeled with markers that are enriched in internal compartments as well as at the plasma membrane. Both GT46 and GL-GPI are enriched in the Golgi complex and recycling endosomes as well as the plasma membrane, and therefore invaginations may have been difficult to discern in the presence of the bright fluorescence of internal pools of these proteins. My ability to identify the invaginations also improved over time. Third, the treatments themselves may have some effect on the sorting of plasma membrane components into or out of invaginations.

To determine if the formation of invaginations under actin disruption and actin stabilization is microtubule dependent, cells were pretreated with the nocodazole prior to incubation with Lat A or Jasplakinolide. Treating cells with nocodazole to disrupt microtubule prior to actin disruption prevented the formation of CTxB positive membrane tubules (Figure 32). Interestingly, when both treatments were combined, there was an extremely elevated formation of large vesicles. These vesicles morphologically appear to be pinosomes, although I
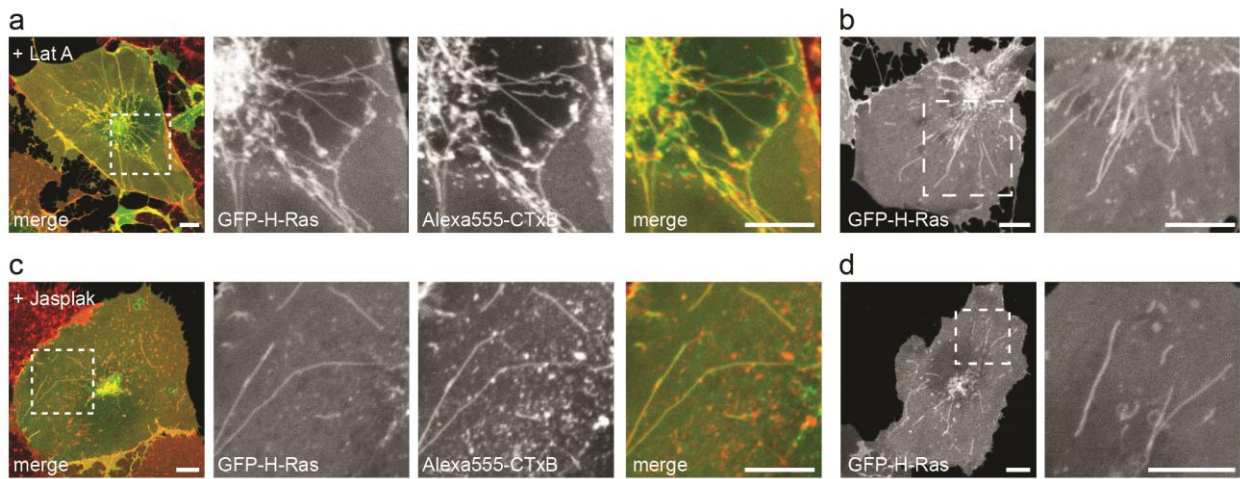
Figure 31. Tubules formed under actin disruption and actin stabilization contain H-Ras and are not dependent on CTxB binding. (A) GFP-HRas colocalized with A555-CTxB in plasma membrane invaginations in actin disrupted cells. (B) GFP-H-Ras labels membrane tubules in actin stabilized COS-7 cells. (A) GFP-H-Ras colocalized with A555-CTxB in plasma membrane invaginations in actin stabilized cells. (B) GFP-H-Ras labels membrane tubules in COS-7 under actin stabilization, in the absence of CTxB. Bar equals 10 μm.
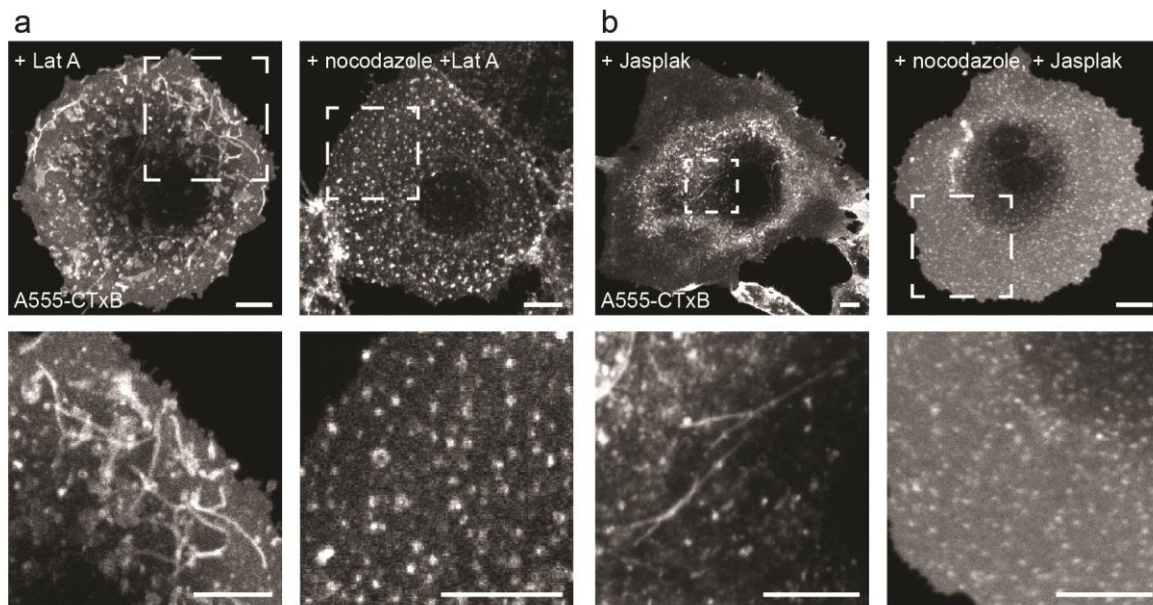
Figure 32. An intact microtubule network is necessary for the formation of membrane tubules under actin disruption and actin stabilization. (A) A555-CTxB labels tubular membrane structures in Lat A treated COS-7 cells. (B) However, pretreatment of the cells with nocodazole to disrupt microtubules blocked tubule formation. (C) Long A555-CTxB positive tubules are generated in Jasplakinolide treated COS-7 cells. (D) In Jasplakinolide treated cells with had been preincubated in nocodazole, no CTxB positive tubules were observed. Bar equals 10 μm.

have not confirmed that they are pinosomes with fluorescent dextran. Microtubule disruption also blocked formation of tubules following treatment with Jasplakinolide (Figure 32). Small pinosome-like structures were seen under these conditions as well. Taken together it is clear that microtubule dependent processes are responsible for membrane tubulation under conditions previously described to depolymerize or stabilize actin.

Role of actin in dynein-driven membrane deformation

The role of actin in regulating dynein mediated tubulation of the plasma membrane is not yet fully clear. As described earlier, actin depolymerization (by Lat A), actin stabilization (by Jasplakinolide), and actin remodeling (by ATP depletion) all lead to the formation of surface attached membrane tubules. The tubules generated under these treatments appear to be the same class of structures. However, assuming that that each treatment is producing tubules from the same class of nascent endocytic vesicles (and by the dynein pulling), we are left with a very interesting problem: how could three perturbations which produce opposing effects on actin be involved in generating the same structures from the plasma membrane?

One potential hypothesis is that all three treatments open actin corrals in the plasma membrane. In the case of Latrunculin A treatment it appears obvious that breaking up actin filament results will remove actin defined barriers in the plasma membrane. In response to ATP depletion, we have shown that long F-actin structures are formed (Figure 10). This remodeling could itself result in larger corrals (as explained earlier). Alternatively, one paper looking at the effect of ATP depletion on actin reported that long filaments form almost immediately after ATP depletion. This polymerization is followed by breaks occurring intermittently along the filaments over time [245]. This too could be opening corrals. Jasplak is commonly used to stabilize actin; however, one paper reported that Jasplak preferentially stabilizes F-actin in stress fibers while depolymerizing actin at the cell surface [246]. Assuming that all three perturbations are opening holes in cortical actin, we predict that they would result in reduced tension on the plasma membrane. If stress on the membrane induced by the pulling force of dynein is involved in the scission process, then reducing membrane tension may lead to impaired scission. An alternative hypothesis could be that actin applies forces laterally to the tubule membrane. This pressure to the sides of

invaginations may be mediation membrane breakage.   Therefore, anything that impairs the natural polymerization/depolymerization cycle of actin could reduce the pressure applied to the invagination.

Non-endocytosis related explanations for dynein-mediated plasma membrane invaginations

In unperturbed cells, STxB and CTxB can be seen moving in mobile tubes (in addition to puncta consistent with caveolae and clathrin mediated endocytic vesicles). The initial paper on toxin induced endocytosis proposed that it was these tubes which were being trapped by the various perturbations [20], and therefore that through characterizing the trapped invaginations we could understand the tubules which are normally involved in toxin uptake.   This is an assumption that has been further perpetuated in follow up papers and review articles [120, 128, 165]. However, there is no data in the literature to confirm the idea that these are in fact related to endocytic tubes that carry toxins into cells, or even have any relationship to endocytosis in unperturbed cells for that matter.

While it is certainly possible that the trapped invaginations correspond to trapped endocytic vesicles (an idea explored in great depth in the following section, "Relationship of invaginations to endocytosis"), there are other reasonable possibilities. For example, these invaginations may be induced by all the treatments because they are allowing dynein to make contact with the plasma membrane. At steady state, a bed of F-actin filaments lies just beneath the inner leaflet of the plasma membrane. It may be that this actin bed restricts microtubules and microtubule motors from normally making contact with the plasma membrane.   However, when actin is reorganized openings may form that allow dynein access to the plasma membrane, which normally it does not have.

A second possibility is that the invaginations are a mechanism for regulating plasma membrane tension. Normally the plasma membrane is under tension from the cortical actin bed and hydrostatic pressure from the cytoplasm. This tension is highly regulated by the cell [247]. In fact, a decrease in membrane tension is countered by the cell through increased endocytosis to remove lipid and return the membrane to a specific tension. Conversely, too much tension is met with an upregulation of exocytosis to add membrane to the plasma

membrane [247].   Under ATP depletion, Lat A, and Jasplak treatment the formation of invaginations often appeared to coincide in time with retraction of the cell body.

It may very well be that the retraction of the cell body under these perturbations results in a release of membrane tension. As the tension drops, the cell must find a way to account for the slack in the plasma membrane, and they do so by using microtubule motors to tug at the plasma membrane. This hypothesis would imply that if the perturbing agent were removed, the tubules would be reabsorbed by the plasma membrane to release tension caused by the cell returning to its previous shape.

Relationship between invaginations and endocytosis

The toxin-induced endocytosis model, as previously defined [20], proposes that the invaginations observed under ATP depletion, actin disruption and actin stabilization are nascent intermediates of an endocytic pathway. More specific it has been proposed that these invaginations correlate with the tubular vesicles sometimes observed to move toxin through the cell [20]. Thus far we have demonstrated that under these various cell perturbations, cytoplasmic dynein provides the force to tubulate the plasma membrane. However, whether this occurs at steady state remains unclear.

To determine if cytoplasmic dynein is necessary for the formation of endocytic vesicles at steady state, we quantified the uptake of cholera toxin B subunit in COS-7 cell expressing either EGFP or GFP-p50 to disrupt dynactin. Following labeling on ice with Alexa555-CTxB, cells were shifted to 37°C for 10 minutes to allow for endocytic uptake. Cells were then acid stripped to remove surface accessible fluorophores. Acid stripping also quenched GFP fluorescence in the cytoplasm so the cells were labeled with an anti-GFP antibody. Using confocal microscopy, the mean fluorescence of endocytosed Alexa555-CTxB per cell was determined. As a control, the uptake of rhodamine-transferrin by clathrin mediated endocytosis was also examined. As expected, p50 overexpression had no impact on the uptake of transferrin. Similarly, there was no statistical difference between the uptake of CTxB in GFP and GFP-p50 expressing cells, suggesting that dynein may not be necessary for endocytic

vesicle formation at steady state (Figure 33). However, CTxB is endocytosed by a wide variety of mechanisms. Therefore, we cannot rule out from the acid stripping experiment the possibility that only a very percentage of all the vesicles endocytosing CTxB are dynein mediated.

While toxin-positive tubules can be observed in unperturbed COS-7, they are very rare with the vast majority of toxin being trafficking in diffraction-limited puncta. Based on the assumption that it is these tubular structures that represent dynein mediated endocytosis, we choose to move into BSC-1 cells. These cells commonly display tubular plasma membrane invaginations (Figure 34), consistent with a previous report [93]. Furthermore, previous work by the Kirchhausen lab at Harvard has shown tubular endocytic vesicles are generating from these plasma membrane invaginations and that this endocytosis relies on intact microtubules [93]. To confirm that the tubular structures observed in BSC-1 cells at steady are equivalent to those trapped by ATP depletion we first tested for H-Ras localization to tubular structures in BSC-1 cells. Just as in COS-7 cells under ATP depletion, tubules in BSC-1 cells at steady state contain GFP-H-Ras and CTxB (Figure 34). Although I have not thoroughly evaluated H-Ras alone my preliminary data indicates the presence of H-Ras positive invaginations in these cells in the absence of CTxB. It appears from the work by Dr. Kirchhausen and our preliminary data that dynein is likely playing a major role for CTxB endocytosis in this cell type and hopefully future experiments will be directed at addressing this.

Together this preliminary data suggests that the dynein mediated pulling we uncovered under ATP depletion, may represent a processes used by cells to deform the plasma membrane and facilitate endocytosis at steady state. While more work needs to be done to cement the role of dynein in non-perturbed cells, between the data we have collected thus far and the literature I think there are good reasons to believe that dynein is involved in endocytosis.
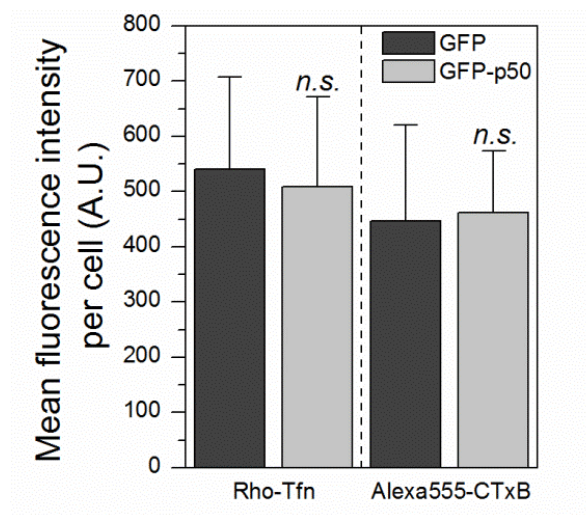
Figure 33. Dynactin disruption has no significant effect on the uptake of CTxB or transferrin in COS-7 cells. COS-7 cells expressing EGFP or GFP-p50 were labeled on ice with A555-CTxB. Serum starved COS-7 cells expressing EGFP or GFP-p50 were labeled on ice with A555-CTxB. Cells were then shifted to 37°C for 10 minutes before being acid stripped, fixed and labeled with anti-GFP antibodies. Cy5-anti GFP fluorescence was used to identify individual cells and mean A555 and rhodamine fluorescence measured. (Bars are averages and standard deviations of 23-70 cells; *n.s.* > 0.05; Student *t*-test).
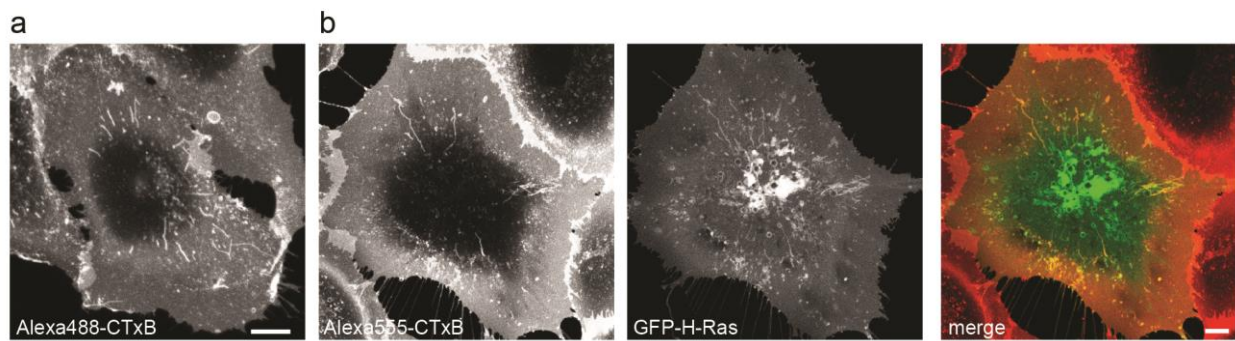
Figure 34. Control BSC-1 cells have CTxB positive tubules which incorporate GFP-H-Ras. (A) A488-CTxB accumulates in tubular structure in control BSC-1 cells at 37°C. (B) CTxB positive tubules BSC-1 cells are positive for GFP-H-Ras.

Caveolae are trafficking vesicles that require the caveolin proteins, specific adaptors proteins, and cholesterol [71, 73, 74, 76-79, 82]. While these vesicles are most commonly spherical in nature and probably rely primarily on actin for early trafficking events there are two reports that suggest at times dynein may also be involved. The first comes from the work of Debbie Brown at Stony Brook University, in a paper in which her group characterized CTxB-positive tubules that form under actin disruption. They report that these invaginations are caveolar in origin. Additionally, they found that the formation of these tubules could be inhibited by pretreatment with nocodazole [130] consistent with my research. Second, STxB has been reported in caveolar invaginations under ATP depletion [76]. Also, an interesting observation pertaining to caveolae was reported by Wayne Lencer and Thomas Kirchhausen's labs at Harvard. Using BSC-1 cells, the same line I used to study tubular endocytosis at steady state, they found that the short mobile tubules contained caveolin at the leading tip of the vesicles [93]. However, none of these publications directly tested for the direct involvement of cytoplasmic dynein. Therefore, if the assumption held in the endocytosis field that the tubules observed under ATP depletion represent stalled endocytic intermediates, then it seem reasonable to anticipate that the plasma membrane invaginations contain caveolin.

Unlike several other endocytic pathways, no coat protein has yet been identified on Arf6 vesicles. This apparent lack of coat may simply mean that there is a coat, but that the scientific community has yet to identify it. Alternatively, it may be that this pathway exists in the absence of a classical coat protein. This possibility is fascinating as it is possible that our current model for dynein mediated endocytosis implies that this form of endocytosis could exist without the use of a coat protein.

Importantly there are additional reasons to think that dynein may mediate vesicle formation in the Arf6 endocytic pathway. For one thing CTxB can enter cells by this pathway [93]. Furthermore, I identified H-Ras as the first membrane protein (beside exogenously added toxins) to associate with dynein-mediated membrane invaginations. I find this extremely telling as vesicular endocytosis of HRas is known to occur almost exclusively through the Arf6 pathway [116, 248]. Finally, the Arf6 pathway has previously been associated with endocytic tubules and membrane invaginations. While dynein has not been specifically examined, it has been shown that the invaginations and the trafficking tubules are sensitive to microtubule disruption [93, 117].

Possible scission mechanisms

Much of my work on dynein-mediated membrane tubulation has been done using drastic perturbations thought to inhibit the scission of nascent vesicles from the plasma membrane. More specifically, these include dynamin inhibition, actin disruption, actin stabilization, and ATP depletion. In the case of dynamin inhibition it is clear that dynamin is the scission-mediating protein that is being inhibited. However, the scission mechanism being blocked by the other three treatments is unclear, and should be examined in depth in future studies. It seems unlikely that actin disruption, actin stabilization, and ATP depletion are impairing dynamin as there are striking differences between the tubules observed under these treatments and those observed under dynamin inhibition.

Constitutive versus stimulated endocytosis of CTxB

My work suggests that the tubular uptake of the toxin is occurring through an endogenous mechanism. However, I did not test if the toxin was up regulating this process. Two mechanisms for the stimulated uptake of CTxB can easily be conceived.

The first model is very similar to the toxin-induced endocytosis model in that the toxin binding induces curvature of the membrane. While my data indicate that the long tubular invaginations are formed by microtubule motors pulling on the plasma membrane, it is possible that the toxin produces subresolution deformations, which are recognized by the cell and nucleate sites of microtubule attachment and membrane pulling.

Alternatively, the toxin may lead to raft remodeling similar to what has the reported in GUVs and GPMVs [13, 30]. This remodeling could conceivably redistribute signaling proteins in the plane of the plasma membrane, leading to altered activity of these proteins. This signaling may in turn stimulate dynein mediated endocytosis. Similar models have been proposed to explain cell signaling induced by the physical binding of STxB to the plasma membrane [249].

Universal role of microtubule motors in membrane tubulation

This study focused on cytoplasmic dynein as it is the only microtubule motor that moves cargo towards the MTOC. However, two unpublished observations strongly indicate that kinesins may tubulate membranes in a manner similar to dynein. First, in my experiments with mCherry-LAMP-1, under ATP depletion, a large number of lysosomes undergo long, directed motions away from the MTOC, suggesting kinesin activity. Second, I observed I could also generate intracellular tubules if I preloaded cells with CTxB prior to ATP depletion. In this experiment, a large quantity of the toxin had reached the perinuclear region prior to the drop in ATP levels necessary to inhibit scission. Once scission was inhibited we observed that this perinuclear pool of CTxB accumulated in tubules emanating away from the MTOC. Based on the directionality of this event, it appears that tubulation was driven by kinesin family members and not cytoplasmic dynein.

This finding is not entirely novel as microtubule motors have previously been shown to tubulate endosomal and Golgi membrane [250-252] (although the finding that microtubule motors continue to function under ATP depletion is itself interesting). Tubulation of these membranes has been proposed to function in sorting of cargo based on the affinity of the cargo for different degrees of membrane curvature [222].

Physiological significance of dynein-mediated endocytosis

Cholera toxin, along with other AB5 toxins, relies on retrograde trafficking in order to intoxicate the host cell. However, the mechanisms by which these toxins arrive at the Golgi complex and are sorted away from endocytic cargo going to other destinations remains unclear. Interestingly, approximately 50% of microtubule tracks originate at the Golgi membrane, rather than the MTOC [253]. While my research does not directly reveal whether the organization of CTxB at the cell surface or dynein-mediated endocytosis contribute to retrograde trafficking it does lay the ground work for an interesting hypothesis: that dynein-mediated endocytosis may be a rapid and direct route to get from the plasma membrane to the Golgi complex.

Evidence for a quick PM to Golgi endocytic mechanisms is based on my own observation that CTxB arrives in the perinuclear region approximately 4 fold faster in BSC-1 cells as compared to COS-7 and MEF cells (data not shown). Interestingly, BSC-1 cells have considerable more tubular endocytic structures containing CTxB than do these other cell lines. Based on this observation, it seems reasonable to propose that dynein-mediated endocytosis offers a quick route from the plasma membrane to the Golgi complex. Furthermore, this route may not require early endosomal sorting but may represent a direct route from the plasma membrane to the Golgi. The existence of a trafficking route that bypasses early endosomes is consistent with the fact that CTxB can access the Golgi even when trafficking out of early endosomes is blocked [254].

Prioritizing future research

Above I have outlined a very large number of unanswered questions. The obvious question then becomes how to proceed. I think three avenues of research present the most possible reward for the efforts. First, there is the question of if the invaginations are in fact stalled endocytic structures. This is extremely important as it cements the idea that what the endocytosis field has been studying isn't an artifact. This could be a very easy question to address as it appears that the invaginations probably represent stalled endocytic tubules which readily uptake CTxB in BSC-1 cells. Performing acid stripping experiments to assess CTxB uptake in BSC-1 cells under dynein/dynactin perturbations could quickly reveal if dynein is necessary for generating endocytic tubules in this cell system.

The second set of experiments I would engage in involve identifying if the invaginations correspond to any of the previously described endocytic mechanisms. As discussed elsewhere in this dissertation there is contradictory evidence in the literature that the invaginations are derived from clathrin coated pits, caveolae or neither [20, 76, 129, 130]. Furthermore, there is no data in the literature evaluating Arf6, GRAF-1 or flotillin in the tubules under ATP depletion. I have for a while wanted to address the question of whether these pathways are the source of the tubules and have amassed a large tool kit to do so. Among those tools are plasmids containing fluorescently tagged markers of a wide variety of endocytic pathways as well as antibodies against protein

components of these pathways. They also include a large number of markers for and siRNA's against CME, caveolae, flotillin, GRAF1 and Arf6 vesicles. Furthermore, we have obtained plasmids encoding fluorescent versions of and siRNA's against Pacsin2 and GRAF3. Both proteins label tubular structures and may be coat proteins [255] (Steve Hanks, unpublished), although more characterization needs to be done on these two proteins.

Finally, I would attempt to identify where CTxB that is endocytosed through dynein derived vesicles is trafficked. As laid out above, I think the possibility that this form of endocytosis is a quick and direct route from the plasma membrane to the Golgi is an exciting one. Such an endocytic route to my knowledge has never been identified, although some evidence indicates that one does exist [254]. As convention teaches that all cargo is taken to endosomes for sorting a pathway in which endosomes are not involved would be exciting and would certainly be worth of a very high impact journal. While this question is probably the most exciting of the three I have just laid out, it is also the most difficult to address. Currently there is no known chemical distinction between microtubule originating at the MTOC or the Golgi. Furthermore, very little is known about the similarity and difference in the nucleation of MTOC and Golgi derived microtubules. However, it is known that GCC185 and CLASP proteins are necessary for the formation of Golgi derived microtubules [138]. Therefore, I would start by knocking down these proteins and seeing if it affects invaginations in ATP depleted cells and CTxB trafficking in BSC-1 cells. While this experiment is certainly required in addressing if Golgi derived microtubules are involved in CTxB uptake, it alone does not prove that CTxB is traveling directly from the plasma membrane to Golgi. Therefore, I think addressing the question of where cargo is going will probably also require a great deal of image advanced biophysics to actually track CTxB positive tubules. This could be done with image processing (such as particle tracking) and at the microscope (for example, by photoactivating a fluorophore on CTxB while it is in the tubule and determining where those fluorescent toxin molecules accumulate). I believe that tracking CTxB as it leaves the plasma membrane will be highly laborious (even though the payoff could be big), which is why I put it third in the order of how to proceed with this project.

REFERENCES

1. Beddoe, T., A.W. Paton, J. Le Nours, J. Rossjohn, and J.C. Paton, *Structure, biological functions and applications of the AB5 toxins.* Trends Biochem Sci, 2010. **35**(7): p. 411-8.
2. World Health Organization. *Cholera*. 2012.
3. Bryce, J., C. Boschi-Pinto, K. Shibuya, and R.E. Black, *WHO estimates of the causes of death in children.* Lancet, 2005. **365**(9465): p. 1147-52.
4. Harris, J.B., R.C. LaRocque, F. Qadri, E.T. Ryan, and S.B. Calderwood, *Cholera.* Lancet, 2012. **379**(9835): p. 2466-76.
5. Chinnapen, D.J., H. Chinnapen, D. Saslowsky, and W.I. Lencer, *Rafting with cholera toxin: endocytosis and trafficking from plasma membrane to ER.* FEMS Microbiol Lett, 2007. **266**(2): p. 129-37.
6. Simons, K. and E. Ikonen, *Functional rafts in cell membranes.* Nature, 1997. **387**(6633): p. 569-72.
7. Pelkmans, L., T. Burli, M. Zerial, and A. Helenius, *Caveolin-stabilized membrane domains as multifunctional transport and sorting devices in endocytic membrane traffic.* Cell, 2004. **118**(6): p. 767-80.
8. Chinnapen, D.J., W.T. Hsieh, Y.M. te Welscher, D.E. Saslowsky, L. Kaoutzani, E. Brandsma, L. D'Auria, H. Park, J.S. Wagner, K.R. Drake, M. Kang, T. Benjamin, M.D. Ullman, C.E. Costello, A.K. Kenworthy, T. Baumgart, R.H. Massol, and W.I. Lencer, *Lipid sorting by ceramide structure from plasma membrane to ER for the cholera toxin receptor ganglioside GM1.* Dev Cell, 2012. **23**(3): p. 573-86.
9. Wolf, A.A., M.G. Jobling, S. Wimer-Mackin, M. Ferguson-Maltzman, J.L. Madara, R.K. Holmes, and W.I. Lencer, *Ganglioside structure dictates signal transduction by cholera toxin and association with caveolae-like membrane domains in polarized epithelia.* J Cell Biol, 1998. **141**(4): p. 917-27.
10. Saslowsky, D.E., J.A. Cho, H. Chinnapen, R.H. Massol, D.J. Chinnapen, J.S. Wagner, H.E. De Luca, W. Kam, B.H. Paw, and W.I. Lencer, *Intoxication of zebrafish and mammalian cells by cholera toxin depends on the flotillin/reggie proteins but not Derlin-1 or -2.* J Clin Invest, 2010. **120**(12): p. 4399-4409.
11. Chinnapen, D., W. Hsieh, Y.t. Welscher, D. Saslowsky, L. Kaoutzani, E. Brandsma, L. D'Auria, H. Park, J. Wagner, K. Drake, M. Kang, T. Benjamin, M. Ullman, C. Costello, A. Kenworthy, B, T, R. Massol, and W.I. Lencer, *Lipid-sorting by ceramide structure from plasma membrane to ER for the cholera toxin receptor ganglioside GM1.* Dev. Cell, 2012. **23**: p. 573-86.
12. Badizadegan, K., B.L. Dickinson, H.E. Wheeler, R.S. Blumberg, R.K. Holmes, and W.I. Lencer, *Heterogeneity of detergent-insoluble membranes from human intestine containing caveolin-1 and ganglioside G(M1).* Am J Physiol Gastrointest Liver Physiol, 2000. **278**(6): p. G895-904.
13. Hammond, A.T., F.A. Heberle, T. Baumgart, D. Holowka, B. Baird, and G.W. Feigenson, *Crosslinking a lipid raft component triggers liquid ordered-liquid disordered phase separation in model plasma membranes.* Proc Natl Acad Sci U S A, 2005. **102**(18): p. 6320-5.
14. London, E. and D.A. Brown, *Insolubility of lipids in triton X-100: physical origin and relationship to sphingolipid/cholesterol membrane domains (rafts).* Biochim Biophys Acta, 2000. **1508**(1-2): p. 182-95.
15. Kirkham, M. and R.G. Parton, *Clathrin-independent endocytosis: new insights into caveolae and non-caveolar lipid raft carriers.* Biochim Biophys Acta, 2005. **1745**(3): p. 273-86.
16. Montesano, R., J. Roth, A. Robert, and L. Orci, *Non-coated membrane invaginations are involved in binding and internalization of cholera and tetanus toxins.* Nature, 1982. **296**(5858): p. 651-3.
17. Tran, D., J.L. Carpentier, F. Sawano, P. Gorden, and L. Orci, *Ligands internalized through coated or noncoated invaginations follow a common intracellular pathway.* Proc Natl Acad Sci U S A, 1987. **84**(22): p. 7957-61.
18. Wolf, A.A., Y. Fujinaga, and W.I. Lencer, *Uncoupling of the cholera toxin-G(M1) ganglioside receptor complex from endocytosis, retrograde Golgi trafficking, and downstream signal transduction by depletion of membrane cholesterol.* J Biol Chem, 2002. **277**(18): p. 16249-56.
19. Sens, P., L. Johannes, and P. Bassereau, *Biophysical approaches to protein-induced membrane deformations in trafficking.* Curr Opin Cell Biol, 2008. **20**(4): p. 476-82.

20.	Romer, W., L. Berland, V. Chambon, K. Gaus, B. Windschiegl, D. Tenza, M.R. Aly, V. Fraisier, J.C. Florent, D. Perrais, C. Lamaze, G. Raposo, C. Steinem, P. Sens, P. Bassereau, and L. Johannes, *Shiga toxin induces tubular membrane invaginations for its uptake into cells.* Nature, 2007. **450**(7170): p. 670-5.

21.	Yang, Z., R.K. Vadlamudi, and R. Kumar, *Dynein light chain 1 phosphorylation controls macropinocytosis.* J Biol Chem, 2005. **280**(1): p. 654-9.

22.	Merritt, E.A., S. Sarfaty, F. van den Akker, C. L'Hoir, J.A. Martial, and W.G. Hol, *Crystal structure of cholera toxin B-pentamer bound to receptor GM1 pentasaccharide.* Protein Sci, 1994. **3**(2): p. 166-75.

23.	Merritt, E.A., T.K. Sixma, K.H. Kalk, B.A. van Zanten, and W.G. Hol, *Galactose-binding site in Escherichia coli heat-labile enterotoxin (LT) and cholera toxin (CT).* Mol Microbiol, 1994. **13**(4): p. 745-53.

24.	Kuziemko, G.M., M. Stroh, and R.C. Stevens, *Cholera toxin binding affinity and specificity for gangliosides determined by surface plasmon resonance.* Biochemistry, 1996. **35**(20): p. 6375-84.

25.	MacKenzie, C.R., T. Hirama, K.K. Lee, E. Altman, and N.M. Young, *Quantitative analysis of bacterial toxin affinity and specificity for glycolipid receptors by surface plasmon resonance.* J Biol Chem, 1997. **272**(9): p. 5533-8.

26.	Lauer, S., B. Goldstein, R.L. Nolan, and J.P. Nolan, *Analysis of cholera toxin-ganglioside interactions by flow cytometry.* Biochemistry, 2002. **41**(6): p. 1742-51.

27.	Spangler, B.D., *Structure and function of cholera toxin and the related Escherichia coli heat-labile enterotoxin.* Microbiol Rev, 1992. **56**(4): p. 622-47.

28.	Wolf, A.A., M.G. Jobling, D.E. Saslowsky, E. Kern, K.R. Drake, A.K. Kenworthy, R.K. Holmes, and W.I. Lencer, *Attenuated endocytosis and toxicity of a mutant cholera toxin with decreased ability to cluster ganglioside GM1 molecules.* Infect Immun, 2008. **76**(4): p. 1476-84.

29.	Shogomori, H. and A.H. Futerman, *Cholera toxin is found in detergent-insoluble rafts/domains at the cell surface of hippocampal neurons but is internalized via a raft-independent mechanism.* J Biol Chem, 2001. **276**(12): p. 9182-8.

30.	Lingwood, D., J. Ries, P. Schwille, and K. Simons, *Plasma membranes are poised for activation of raft phase coalescence at physiological temperature.* Proc Natl Acad Sci U S A, 2008. **105**(29): p. 10005-10.

31.	Baumgart, T., A.T. Hammond, P. Sengupta, S.T. Hess, D.A. Holowka, B.A. Baird, and W.W. Webb, *Large-scale fluid/fluid phase separation of proteins and lipids in giant plasma membrane vesicles.* Proc Natl Acad Sci U S A, 2007. **104**(9): p. 3165-70.

32.	Day, C.A. and A.K. Kenworthy, *Mechanisms underlying the confined diffusion of cholera toxin B-subunit in intact cell membranes.* PLoS ONE, 2012. **7**(4): p. e34923.

33.	Kenworthy, A.K., B.J. Nichols, C.L. Remmert, G.M. Hendrix, M. Kumar, J. Zimmerberg, and J. Lippincott-Schwartz, *Dynamics of putative raft-associated proteins at the cell surface.* J Cell Biol, 2004. **165**(5): p. 735-46.

34.	Bacia, K., D. Scherfeld, N. Kahya, and P. Schwille, *Fluorescence correlation spectroscopy relates rafts in model and native membranes.* Biophys J, 2004. **87**(2): p. 1034-43.

35.	Thomsen, P., K. Roepstorff, M. Stahlhut, and B. van Deurs, *Caveolae are highly immobile plasma membrane microdomains, which are not involved in constitutive endocytic trafficking.* Mol Biol Cell, 2002. **13**(1): p. 238-50.

36.	Lajoie, P., E.A. Partridge, G. Guay, J.G. Goetz, J. Pawling, A. Lagana, B. Joshi, J.W. Dennis, and I.R. Nabi, *Plasma membrane domain organization regulates EGFR signaling in tumor cells.* J Cell Biol, 2007. **179**(2): p. 341-56.

37.	Gonzalez-Munoz, E., C. Lopez-Iglesias, M. Calvo, M. Palacin, A. Zorzano, and M. Camps, *Caveolin-1 loss of function accelerates glucose transporter 4 and insulin receptor degradation in 3T3-L1 adipocytes.* Endocrinology, 2009. **150**(8): p. 3493-502.

38.	Miller, C.E., J. Majewski, E.B. Watkins, and T.L. Kuhl, *Part I: an x-ray scattering study of cholera toxin penetration and induced phase transformations in lipid membranes.* Biophys J, 2008. **95**(2): p. 629-40.

39.	Watkins, E.B., C.E. Miller, J. Majewski, and T.L. Kuhl, *Membrane texture induced by specific protein binding and receptor clustering: active roles for lipids in cellular function.* Proc Natl Acad Sci U S A, 2011. **108**(17): p. 6975-80.

40.	Ewers, H., W. Romer, A.E. Smith, K. Bacia, S. Dmitrieff, W. Chai, R. Mancini, J. Kartenbeck, V. Chambon, L. Berland, A. Oppenheim, G. Schwarzmann, T. Feizi, P. Schwille, P. Sens, A. Helenius, and L. Johannes, *GM1*

structure determines SV40-induced membrane invagination and infection. Nat Cell Biol, 2010. **12**(1): p. 11-8; sup pp 1-12.

41. Sako, Y. and A. Kusumi, *Compartmentalized structure of the plasma membrane for receptor movements as revealed by a nanometer-level motion analysis.* J Cell Biol, 1994. **125**(6): p. 1251-64.

42. Sako, Y. and A. Kusumi, *Barriers for lateral diffusion of transferrin receptor in the plasma membrane as characterized by receptor dragging by laser tweezers: fence versus tether.* J Cell Biol, 1995. **129**(6): p. 1559-74.

43. Ritchie, K. and J. Spector, *Single molecule studies of molecular diffusion in cellular membranes: determining membrane structure.* Biopolymers, 2007. **87**(2-3): p. 95-101.

44. Kusumi, A., Y. Sako, and M. Yamamoto, *Confined lateral diffusion of membrane receptors as studied by single particle tracking (nanovid microscopy). Effects of calcium-induced differentiation in cultured epithelial cells.* Biophys J, 1993. **65**(5): p. 2021-40.

45. Fujiwara, T., K. Ritchie, H. Murakoshi, K. Jacobson, and A. Kusumi, *Phospholipids undergo hop diffusion in compartmentalized cell membrane.* J Cell Biol, 2002. **157**(6): p. 1071-81.

46. Simons, K. and G. van Meer, *Lipid sorting in epithelial cells.* Biochemistry, 1988. **27**(17): p. 6197-202.

47. Simons, K. and A. Wandinger-Ness, *Polarized sorting in epithelia.* Cell, 1990. **62**(2): p. 207-10.

48. Brown, D.A. and J.K. Rose, *Sorting of GPI-anchored proteins to glycolipid-enriched membrane subdomains during transport to the apical cell surface.* Cell, 1992. **68**(3): p. 533-44.

49. Brown, D.A. and E. London, *Functions of lipid rafts in biological membranes.* Annu Rev Cell Dev Biol, 1998. **14**: p. 111-36.

50. Ahmed, S.N., D.A. Brown, and E. London, *On the origin of sphingolipid/cholesterol-rich detergent-insoluble cell membranes: physiological concentrations of cholesterol and sphingolipid induce formation of a detergent-insoluble, liquid-ordered lipid phase in model membranes.* Biochemistry, 1997. **36**(36): p. 10944-53.

51. Hao, M., S. Mukherjee, and F.R. Maxfield, *Cholesterol depletion induces large scale domain segregation in living cell membranes.* Proc Natl Acad Sci U S A, 2001. **98**(23): p. 13072-7.

52. Sengupta, P., B. Baird, and D. Holowka, *Lipid rafts, fluid/fluid phase separation, and their relevance to plasma membrane structure and function.* Semin Cell Dev Biol, 2007. **18**(5): p. 583-90.

53. Sharma, P., R. Varma, R.C. Sarasij, Ira, K. Gousset, G. Krishnamoorthy, M. Rao, and S. Mayor, *Nanoscale organization of multiple GPI-anchored proteins in living cell membranes.* Cell, 2004. **116**(4): p. 577-89.

54. Glebov, O.O. and B.J. Nichols, *Lipid raft proteins have a random distribution during localized activation of the T-cell receptor.* Nat Cell Biol, 2004. **6**(3): p. 238-43.

55. Kenworthy, A.K., N. Petranova, and M. Edidin, *High-resolution FRET microscopy of cholera toxin B-subunit and GPI-anchored proteins in cell plasma membranes.* Mol Biol Cell, 2000. **11**(5): p. 1645-55.

56. Saffman, P.G. and M. Delbruck, *Brownian motion in biological membranes.* Proc Natl Acad Sci U S A, 1975. **72**(8): p. 3111-3.

57. Lenne, P.F., L. Wawrezinieck, F. Conchonaud, O. Wurtz, A. Boned, X.J. Guo, H. Rigneault, H.T. He, and D. Marguet, *Dynamic molecular confinement in the plasma membrane by microdomains and the cytoskeleton meshwork.* EMBO J, 2006. **25**(14): p. 3245-56.

58. Meder, D., M.J. Moreno, P. Verkade, W.L. Vaz, and K. Simons, *Phase coexistence and connectivity in the apical membrane of polarized epithelial cells.* Proc Natl Acad Sci U S A, 2006. **103**(2): p. 329-34.

59. Mayor, S. and M. Rao, *Rafts: scale-dependent, active lipid organization at the cell surface.* Traffic, 2004. **5**(4): p. 231-40.

60. Jacobson, K., O.G. Mouritsen, and R.G. Anderson, *Lipid rafts: at a crossroad between cell biology and physics.* Nat Cell Biol, 2007. **9**(1): p. 7-14.

61. Hancock, J.F., *Lipid rafts: contentious only from simplistic standpoints.* Nat Rev Mol Cell Biol, 2006. **7**(6): p. 456-62.

62. Kusumi, A. and K. Suzuki, *Toward understanding the dynamics of membrane-raft-based molecular interactions.* Biochim Biophys Acta, 2005. **1746**(3): p. 234-51.

63. Maxfield, F.R., *Plasma membrane microdomains.* Curr Opin Cell Biol, 2002. **14**(4): p. 483-7.

64. Plowman, S.J., C. Muncke, R.G. Parton, and J.F. Hancock, *H-ras, K-ras, and inner plasma membrane raft proteins operate in nanoclusters with differential dependence on the actin cytoskeleton.* Proc Natl Acad Sci U S A, 2005. **102**(43): p. 15500-5.

65. Varma, R. and S. Mayor, *GPI-anchored proteins are organized in submicron domains at the cell surface.* Nature, 1998. **394**(6695): p. 798-801.

66. Goswami, D., K. Gowrishankar, S. Bilgrami, S. Ghosh, R. Raghupathy, R. Chadda, R. Vishwakarma, M. Rao, and S. Mayor, *Nanoclusters of GPI-anchored proteins are formed by cortical actin-driven activity.* Cell, 2008. **135**(6): p. 1085-97.

67. Gowrishankar, K., S. Ghosh, S. Saha, R. C, S. Mayor, and M. Rao, *Active remodeling of cortical actin regulates spatiotemporal organization of cell surface molecules.* Cell, 2012. **149**(6): p. 1353-67.

68. Jaqaman, K., H. Kuwata, N. Touret, R. Collins, W.S. Trimble, G. Danuser, and S. Grinstein, *Cytoskeletal control of CD36 diffusion promotes its receptor and signaling function.* Cell, 2011. **146**(4): p. 593-606.

69. Suzuki, K., K. Ritchie, E. Kajikawa, T. Fujiwara, and A. Kusumi, *Rapid hop diffusion of a G-protein-coupled receptor in the plasma membrane as revealed by single-molecule techniques.* Biophys J, 2005. **88**(5): p. 3659-80.

70. Morone, N., T. Fujiwara, K. Murase, R.S. Kasai, H. Ike, S. Yuasa, J. Usukura, and A. Kusumi, *Three-dimensional reconstruction of the membrane skeleton at the plasma membrane interface by electron tomography.* J Cell Biol, 2006. **174**(6): p. 851-62.

71. Hill, M.M., M. Bastiani, R. Luetterforst, M. Kirkham, A. Kirkham, S.J. Nixon, P. Walser, D. Abankwa, V.M. Oorschot, S. Martin, J.F. Hancock, and R.G. Parton, *PTRF-Cavin, a conserved cytoplasmic protein required for caveola formation and function.* Cell, 2008. **132**(1): p. 113-24.

72. Fra, A.M., E. Williamson, K. Simons, and R.G. Parton, *De novo formation of caveolae in lymphocytes by expression of VIP21-caveolin.* Proc Natl Acad Sci U S A, 1995. **92**(19): p. 8655-9.

73. Drab, M., P. Verkade, M. Elger, M. Kasper, M. Lohn, B. Lauterbach, J. Menne, C. Lindschau, F. Mende, F.C. Luft, A. Schedl, H. Haller, and T.V. Kurzchalia, *Loss of caveolae, vascular dysfunction, and pulmonary defects in caveolin-1 gene-disrupted mice.* Science, 2001. **293**(5539): p. 2449-52.

74. Liu, L., D. Brown, M. McKee, N.K. Lebrasseur, D. Yang, K.H. Albrecht, K. Ravid, and P.F. Pilch, *Deletion of Cavin/PTRF causes global loss of caveolae, dyslipidemia, and glucose intolerance.* Cell Metab, 2008. **8**(4): p. 310-7.

75. Moren, B., C. Shah, M.T. Howes, N.L. Schieber, H.T. McMahon, R.G. Parton, O. Daumke, and R. Lundmark, *EHD2 regulates caveolar dynamics via ATP-driven targeting and oligomerization.* Mol Biol Cell, 2012. **23**(7): p. 1316-29.

76. Hansen, C.G., N.A. Bright, G. Howard, and B.J. Nichols, *SDPR induces membrane curvature and functions in the formation of caveolae.* Nat Cell Biol, 2009. **11**(7): p. 807-14.

77. Bastiani, M., L. Liu, M.M. Hill, M.P. Jedrychowski, S.J. Nixon, H.P. Lo, D. Abankwa, R. Luetterforst, M. Fernandez-Rojo, M.R. Breen, S.P. Gygi, J. Vinten, P.J. Walser, K.N. North, J.F. Hancock, P.F. Pilch, and R.G. Parton, *MURC/Cavin-4 and cavin family members form tissue-specific caveolar complexes.* J Cell Biol, 2009. **185**(7): p. 1259-73.

78. McMahon, K.A., H. Zajicek, W.P. Li, M.J. Peyton, J.D. Minna, V.J. Hernandez, K. Luby-Phelps, and R.G. Anderson, *SRBC/cavin-3 is a caveolin adapter protein that regulates caveolae function.* EMBO J, 2009. **28**(8): p. 1001-15.

79. Fujimoto, T., M. Hayashi, M. Iwamoto, and Y. Ohno-Iwashita, *Crosslinked plasmalemmal cholesterol is sequestered to caveolae: analysis with a new cytochemical probe.* J Histochem Cytochem, 1997. **45**(9): p. 1197-205.

80. Ortegren, U., M. Karlsson, N. Blazic, M. Blomqvist, F.H. Nystrom, J. Gustavsson, P. Fredman, and P. Stralfors, *Lipids and glycosphingolipids in caveolae and surrounding plasma membrane of primary rat adipocytes.* Eur J Biochem, 2004. **271**(10): p. 2028-36.

81. Singh, R.D., D.L. Marks, E.L. Holicky, C.L. Wheatley, T. Kaptzan, S.B. Sato, T. Kobayashi, K. Ling, and R.E. Pagano, *Gangliosides and beta1-integrin are required for caveolae and membrane domains.* Traffic, 2009. **11**(3): p. 348-60.

82. Murata, M., J. Peranen, R. Schreiner, F. Wieland, T.V. Kurzchalia, and K. Simons, *VIP21/caveolin is a cholesterol-binding protein.* Proc Natl Acad Sci U S A, 1995. **92**(22): p. 10339-43.

83. Sargiacomo, M., M. Sudol, Z. Tang, and M.P. Lisanti, *Signal transducing molecules and glycosyl-phosphatidylinositol-linked proteins form a caveolin-rich insoluble complex in MDCK cells.* J Cell Biol, 1993. **122**(4): p. 789-807.

84. Tagawa, A., A. Mezzacasa, A. Hayer, A. Longatti, L. Pelkmans, and A. Helenius, *Assembly and trafficking of caveolar domains in the cell: caveolae as stable, cargo-triggered, vesicular transporters.* J Cell Biol, 2005. **170**(5): p. 769-79.

85. Lajoie, P., J.G. Goetz, J.W. Dennis, and I.R. Nabi, *Lattices, rafts, and scaffolds: domain regulation of receptor signaling at the plasma membrane.* J Cell Biol, 2009. **185**(3): p. 381-5.

86. Mayor, S. and R.E. Pagano, *Pathways of clathrin-independent endocytosis.* Nat Rev Mol Cell Biol, 2007. **8**(8): p. 603-12.

87. McMahon, H.T. and E. Boucrot, *Molecular mechanism and physiological functions of clathrin-mediated endocytosis.* Nat Rev Mol Cell Biol, 2011. **12**(8): p. 517-33.

88. Torgersen, M.L., G. Skretting, B. van Deurs, and K. Sandvig, *Internalization of cholera toxin by different endocytic mechanisms.* J Cell Sci, 2001. **114**(Pt 20): p. 3737-47.

89. Parton, R.G., *Ultrastructural localization of gangliosides; GM1 is concentrated in caveolae.* J Histochem Cytochem, 1994. **42**(2): p. 155-66.

90. Howes, M.T., M. Kirkham, J. Riches, K. Cortese, P.J. Walser, F. Simpson, M.M. Hill, A. Jones, R. Lundmark, M.R. Lindsay, D.J. Hernandez-Deviez, G. Hadzic, A. McCluskey, R. Bashir, L. Liu, P. Pilch, H. McMahon, P.J. Robinson, J.F. Hancock, S. Mayor, and R.G. Parton, *Clathrin-independent carriers form a high capacity endocytic sorting system at the leading edge of migrating cells.* J Cell Biol, 2010. **190**(4): p. 675-91.

91. Glebov, O.O., N.A. Bright, and B.J. Nichols, *Flotillin-1 defines a clathrin-independent endocytic pathway in mammalian cells.* Nat Cell Biol, 2006. **8**(1): p. 46-54.

92. Lundmark, R., G.J. Doherty, M.T. Howes, K. Cortese, Y. Vallis, R.G. Parton, and H.T. McMahon, *The GTPase-activating protein GRAF1 regulates the CLIC/GEEC endocytic pathway.* Curr Biol, 2008. **18**(22): p. 1802-8.

93. Massol, R.H., J.E. Larsen, Y. Fujinaga, W.I. Lencer, and T. Kirchhausen, *Cholera toxin toxicity does not require functional Arf6- and dynamin-dependent endocytic pathways.* Mol Biol Cell, 2004. **15**(8): p. 3631-41.

94. Hopkins, C.R., K. Miller, and J.M. Beardmore, *Receptor-mediated endocytosis of transferrin and epidermal growth factor receptors: a comparison of constitutive and ligand-induced uptake.* J Cell Sci Suppl, 1985. **3**: p. 173-86.

95. Ford, M.G., I.G. Mills, B.J. Peter, Y. Vallis, G.J. Praefcke, P.R. Evans, and H.T. McMahon, *Curvature of clathrin-coated pits driven by epsin.* Nature, 2002. **419**(6905): p. 361-6.

96. Henne, W.M., E. Boucrot, M. Meinecke, E. Evergren, Y. Vallis, R. Mittal, and H.T. McMahon, *FCHo proteins are nucleators of clathrin-mediated endocytosis.* Science, 2010. **328**(5983): p. 1281-4.

97. Ford, M.G., B.M. Pearse, M.K. Higgins, Y. Vallis, D.J. Owen, A. Gibson, C.R. Hopkins, P.R. Evans, and H.T. McMahon, *Simultaneous binding of PtdIns(4,5)P2 and clathrin by AP180 in the nucleation of clathrin lattices on membranes.* Science, 2001. **291**(5506): p. 1051-5.

98. Liu, J., Y. Sun, G.F. Oster, and D.G. Drubin, *Mechanochemical crosstalk during endocytic vesicle formation.* Curr Opin Cell Biol, 2010. **22**(1): p. 36-43.

99. Damke, H., T. Baba, D.E. Warnock, and S.L. Schmid, *Induction of mutant dynamin specifically blocks endocytic coated vesicle formation.* J Cell Biol, 1994. **127**(4): p. 915-34.

100. Urrutia, R., J.R. Henley, T. Cook, and M.A. McNiven, *The dynamins: redundant or distinct functions for an expanding family of related GTPases?* Proc Natl Acad Sci U S A, 1997. **94**(2): p. 377-84.

101. Sweitzer, S.M. and J.E. Hinshaw, *Dynamin undergoes a GTP-dependent conformational change causing vesiculation.* Cell, 1998. **93**(6): p. 1021-9.

102. Taylor, M.J., D. Perrais, and C.J. Merrifield, *A high precision survey of the molecular dynamics of mammalian clathrin-mediated endocytosis.* PLoS Biol, 2011. **9**(3): p. e1000604.

103. Ungewickell, E.J. and L. Hinrichsen, *Endocytosis: clathrin-mediated membrane budding.* Curr Opin Cell Biol, 2007. **19**(4): p. 417-25.

104. Fujimoto, L.M., R. Roth, J.E. Heuser, and S.L. Schmid, *Actin assembly plays a variable, but not obligatory role in receptor-mediated endocytosis in mammalian cells.* Traffic, 2000. **1**(2): p. 161-71.

105. Boucrot, E., S. Saffarian, R. Massol, T. Kirchhausen, and M. Ehrlich, *Role of lipids and actin in the formation of clathrin-coated pits.* Exp Cell Res, 2006. **312**(20): p. 4036-48.

106. Rothberg, K.G., J.E. Heuser, W.C. Donzell, Y.S. Ying, J.R. Glenney, and R.G. Anderson, *Caveolin, a protein component of caveolae membrane coats.* Cell, 1992. **68**(4): p. 673-82.

107. Liu, L. and P.F. Pilch, *A critical role of cavin (polymerase I and transcript release factor) in caveolae formation and organization.* J Biol Chem, 2008. **283**(7): p. 4314-22.

108. Kirkham, M., A. Fujita, R. Chadda, S.J. Nixon, T.V. Kurzchalia, D.K. Sharma, R.E. Pagano, J.F. Hancock, S. Mayor, and R.G. Parton, *Ultrastructural identification of uncoated caveolin-independent early endocytic vehicles.* J Cell Biol, 2005. **168**(3): p. 465-76.

109. Razani, B., X.B. Wang, J.A. Engelman, M. Battista, G. Lagaud, X.L. Zhang, B. Kneitz, H. Hou, Jr., G.J. Christ, W. Edelmann, and M.P. Lisanti, *Caveolin-2-deficient mice show evidence of severe pulmonary dysfunction without disruption of caveolae.* Mol Cell Biol, 2002. **22**(7): p. 2329-44.

110. Montesano, R., *Inhomogeneous distribution of filipin-sterol complexes in smooth muscle cell plasma membrane.* Nature, 1979. **280**(5720): p. 328-9.

111. Westermann, M., F. Steiniger, and W. Richter, *Belt-like localisation of caveolin in deep caveolae and its re-distribution after cholesterol depletion.* Histochem Cell Biol, 2005. **123**(6): p. 613-20.

112. Hayer, A., M. Stoeber, D. Ritz, S. Engel, H.H. Meyer, and A. Helenius, *Caveolin-1 is ubiquitinated and targeted to intralumenal vesicles in endolysosomes for degradation.* J Cell Biol, 2010. **191**(3): p. 615-29.

113. Pelkmans, L. and M. Zerial, *Kinase-regulated quantal assemblies and kiss-and-run recycling of caveolae.* Nature, 2005. **436**(7047): p. 128-33.

114. Henley, J.R., E.W. Krueger, B.J. Oswald, and M.A. McNiven, *Dynamin-mediated internalization of caveolae.* J Cell Biol, 1998. **141**(1): p. 85-99.

115. Radhakrishna, H. and J.G. Donaldson, *ADP-ribosylation factor 6 regulates a novel plasma membrane recycling pathway.* J Cell Biol, 1997. **139**(1): p. 49-61.

116. McKay, J., X. Wang, J. Ding, J.E. Buss, and L. Ambrosio, *H-ras resides on clathrin-independent ARF6 vesicles that harbor little RAF-1, but not on clathrin-dependent endosomes.* Biochim Biophys Acta, 2011. **1813**(2): p. 298-307.

117. Massol, R.H., J.E. Larsen, and T. Kirchhausen, *Possible role of deep tubular invaginations of the plasma membrane in MHC-I trafficking.* Exp Cell Res, 2005. **306**(1): p. 142-9.

118. Donaldson, J.G., N. Porat-Shliom, and L.A. Cohen, *Clathrin-independent endocytosis: a unique platform for cell signaling and PM remodeling.* Cell Signal, 2009. **21**(1): p. 1-6.

119. Eyster, C.A., J.D. Higginson, R. Huebner, N. Porat-Shliom, R. Weigert, W.W. Wu, R.F. Shen, and J.G. Donaldson, *Discovery of new cargo proteins that enter cells through clathrin-independent endocytosis.* Traffic, 2009. **10**(5): p. 590-9.

120. Kumari, S., S. Mg, and S. Mayor, *Endocytosis unplugged: multiple ways to enter the cell.* Cell Res, 2010. **20**(3): p. 256-75.

121. Sabharanjak, S., P. Sharma, R.G. Parton, and S. Mayor, *GPI-anchored proteins are delivered to recycling endosomes via a distinct cdc42-regulated, clathrin-independent pinocytic pathway.* Dev Cell, 2002. **2**(4): p. 411-23.

122. Kalia, M., S. Kumari, R. Chadda, M.M. Hill, R.G. Parton, and S. Mayor, *Arf6-independent GPI-anchored protein-enriched early endosomal compartments fuse with sorting endosomes via a Rab5/phosphatidylinositol-3'-kinase-dependent machinery.* Mol Biol Cell, 2006. **17**(8): p. 3689-704.

123. Bickel, P.E., P.E. Scherer, J.E. Schnitzer, P. Oh, M.P. Lisanti, and H.F. Lodish, *Flotillin and epidermal surface antigen define a new family of caveolae-associated integral membrane proteins.* J Biol Chem, 1997. **272**(21): p. 13793-802.

124. Chadda, R., M.T. Howes, S.J. Plowman, J.F. Hancock, R.G. Parton, and S. Mayor, *Cholesterol-sensitive Cdc42 activation regulates actin polymerization for endocytosis via the GEEC pathway.* Traffic, 2007. **8**(6): p. 702-17.

125. Cheng, Z.J., R.D. Singh, D.K. Sharma, E.L. Holicky, K. Hanada, D.L. Marks, and R.E. Pagano, *Distinct mechanisms of clathrin-independent endocytosis have unique sphingolipid requirements.* Mol Biol Cell, 2006. **17**(7): p. 3197-210.

126. Kumari, S. and S. Mayor, *ARF1 is directly involved in dynamin-independent endocytosis.* Nat Cell Biol, 2008. **10**(1): p. 30-41.

127. Safouane, M., L. Berland, A. Callan-Jones, B. Sorre, W. Romer, L. Johannes, G.E. Toombes, and P. Bassereau, *Lipid Cosorting Mediated by Shiga Toxin Induced Tubulation.* Traffic, 2010.

128. Simons, K. and M.J. Gerl, *Revitalizing membrane rafts: new tools and insights.* Nat Rev Mol Cell Biol, 2010. **11**(10): p. 688-99.

129. van Deurs, B., F. von Bulow, F. Vilhardt, P.K. Holm, and K. Sandvig, *Destabilization of plasma membrane structure by prevention of actin polymerization. Microtubule-dependent tubulation of the plasma membrane.* J Cell Sci, 1996. **109 (Pt 7)**: p. 1655-65.

130. Verma, P., A.G. Ostermeyer-Fay, and D.A. Brown, *Caveolin-1 induces formation of membrane tubules that sense actomyosin tension and are inhibited by polymerase I and transcript release factor/cavin-1.* Mol Biol Cell, 2010. **21**(13): p. 2226-40.

131. Huckaba, T.M., A.C. Gay, L.F. Pantalena, H.C. Yang, and L.A. Pon, *Live cell imaging of the assembly, disassembly, and actin cable-dependent movement of endosomes and actin patches in the budding yeast, Saccharomyces cerevisiae.* J Cell Biol, 2004. **167**(3): p. 519-30.

132. Toshima, J.Y., J. Toshima, M. Kaksonen, A.C. Martin, D.S. King, and D.G. Drubin, *Spatial dynamics of receptor-mediated endocytic trafficking in budding yeast revealed by using fluorescent alpha-factor derivatives.* Proc Natl Acad Sci U S A, 2006. **103**(15): p. 5793-8.

133. Aschenbrenner, L., T. Lee, and T. Hasson, *Myo6 facilitates the translocation of endocytic vesicles from cell peripheries.* Mol Biol Cell, 2003. **14**(7): p. 2728-43.

134. Tilney, L.G. and D.A. Portnoy, *Actin filaments and the growth, movement, and spread of the intracellular bacterial parasite, Listeria monocytogenes.* J Cell Biol, 1989. **109**(4 Pt 1): p. 1597-608.

135. Mostowy, S. and P. Cossart, *Cytoskeleton rearrangements during Listeria infection: clathrin and septins as new players in the game.* Cell Motil Cytoskeleton, 2009. **66**(10): p. 816-23.

136. Merrifield, C.J., M.E. Feldman, L. Wan, and W. Almers, *Imaging actin and dynamin recruitment during invagination of single clathrin-coated pits.* Nat Cell Biol, 2002. **4**(9): p. 691-8.

137. Pelkmans, L., D. Puntener, and A. Helenius, *Local actin polymerization and dynamin recruitment in SV40-induced internalization of caveolae.* Science, 2002. **296**(5567): p. 535-9.

138. Efimov, A., A. Kharitonov, N. Efimova, J. Loncarek, P.M. Miller, N. Andreyeva, P. Gleeson, N. Galjart, A.R. Maia, I.X. McLeod, J.R. Yates, 3rd, H. Maiato, A. Khodjakov, A. Akhmanova, and I. Kaverina, *Asymmetric CLASP-dependent nucleation of noncentrosomal microtubules at the trans-Golgi network.* Dev Cell, 2007. **12**(6): p. 917-30.

139. Pereira, G. and E. Schiebel, *Centrosome-microtubule nucleation.* J Cell Sci, 1997. **110 (Pt 3)**: p. 295-300.

140. Raynaud-Messina, B. and A. Merdes, *Gamma-tubulin complexes and microtubule organization.* Curr Opin Cell Biol, 2007. **19**(1): p. 24-30.

141. Chabin-Brion, K., J. Marceiller, F. Perez, C. Settegrana, A. Drechou, G. Durand, and C. Pous, *The Golgi complex is a microtubule-organizing organelle.* Mol Biol Cell, 2001. **12**(7): p. 2047-60.

142. Hirokawa, N., Y. Noda, Y. Tanaka, and S. Niwa, *Kinesin superfamily motor proteins and intracellular transport.* Nat Rev Mol Cell Biol, 2009. **10**(10): p. 682-96.

143. Krylyshkina, O., I. Kaverina, W. Kranewitter, W. Steffen, M.C. Alonso, R.A. Cross, and J.V. Small, *Modulation of substrate adhesion dynamics via microtubule targeting requires kinesin-1.* J Cell Biol, 2002. **156**(2): p. 349-59.

144. Anitei, M. and B. Hoflack, *Bridging membrane and cytoskeleton dynamics in the secretory and endocytic pathways.* Nat Cell Biol, 2012. **14**(1): p. 11-9.

145. Pralle, A., P. Keller, E.L. Florin, K. Simons, and J.K. Horber, *Sphingolipid-cholesterol rafts diffuse as small entities in the plasma membrane of mammalian cells.* J. Cell Biol., 2000. **148**(5): p. 997-1008.

146. Keller, P., D. Toomre, E. Diaz, J. White, and K. Simons, *Multicolour imaging of post-Golgi sorting and trafficking in live cells.* Nat. Cell Biol., 2001. **3**: p. 140-149.

147. Kenworthy, A.K., B.J. Nichols, C.L. Remmert, G.M. Hendrix, M. Kumar, J. Zimmerberg, and J. Lippincott-Schwartz, *Dynamics of putative raft-associated proteins at the cell surface.* J. Cell Biol., 2004. **165**(5): p. 735-46.

148. Tetaud, C., T. Falguieres, K. Carlier, Y. Lecluse, J. Garibal, D. Coulaud, P. Busson, R. Steffensen, H. Clausen, L. Johannes, and J. Wiels, *Two distinct Gb3/CD77 signaling pathways leading to apoptosis are triggered by anti-Gb3/CD77 mAb and verotoxin-1.* J Biol Chem, 2003. **278**(46): p. 45200-8.

149. Steffensen, R., K. Carlier, J. Wiels, S.B. Levery, M. Stroud, B. Cedergren, B. Nilsson Sojka, E.P. Bennett, C. Jersild, and H. Clausen, *Cloning and expression of the histo-blood group Pk UDP-galactose: Ga1beta-4G1cbeta1-cer alpha1, 4-galactosyltransferase. Molecular genetic basis of the p phenotype.* J Biol Chem, 2000. **275**(22): p. 16723-9.

150. Choy, E., V.K. Chiu, J. Silletti, M. Feoktistov, T. Morimoto, D. Michaelson, I.E. Ivanov, and M.R. Philips, *Endomembrane trafficking of ras: the CAAX motif targets proteins to the ER and Golgi.* Cell, 1999. **98**(1): p. 69-80.

151. Burkel, B.M., G. von Dassow, and W.M. Bement, *Versatile fluorescent probes for actin filaments based on the actin-binding domain of utrophin.* Cell Motil Cytoskeleton, 2007. **64**(11): p. 822-32.

152. Yi, J., X.S. Wu, T. Crites, and J.A. Hammer, 3rd, *Actin retrograde flow and actomyosin II arc contraction drive receptor cluster dynamics at the immunological synapse in Jurkat T cells.* Mol Biol Cell, 2012. **23**(5): p. 834-52.

153. Stepanova, T., J. Slemmer, C.C. Hoogenraad, G. Lansbergen, B. Dortland, C.I. De Zeeuw, F. Grosveld, G. van Cappellen, A. Akhmanova, and N. Galjart, *Visualization of microtubule growth in cultured neurons via the use of EB3-GFP (end-binding protein 3-green fluorescent protein).* J Neurosci, 2003. **23**(7): p. 2655-64.

154. Quintyne, N.J., S.R. Gill, D.M. Eckley, C.L. Crego, D.A. Compton, and T.A. Schroer, *Dynactin is required for microtubule anchoring at centrosomes.* J Cell Biol, 1999. **147**(2): p. 321-34.

155. Burkhardt, J.K., C.J. Echeverri, T. Nilsson, and R.B. Vallee, *Overexpression of the dynamitin (p50) subunit of the dynactin complex disrupts dynein-dependent maintenance of membrane organelle distribution.* J Cell Biol, 1997. **139**(2): p. 469-84.

156. Roland, J.T., A.K. Kenworthy, J. Peranen, S. Caplan, and J.R. Goldenring, *Myosin Vb interacts with Rab8a on a tubular network containing EHD1 and EHD3.* Mol Biol Cell, 2007. **18**(8): p. 2828-37.

157. Nehls, S., E.L. Snapp, N.B. Cole, K.J. Zaal, A.K. Kenworthy, T.H. Roberts, J. Ellenberg, J.F. Presley, E. Siggia, and J. Lippincott-Schwartz, *Dynamics and retention of misfolded proteins in native ER membranes.* Nat Cell Biol, 2000. **2**(5): p. 288-295.

158. Macia, E., M. Ehrlich, R. Massol, E. Boucrot, C. Brunner, and T. Kirchhausen, *Dynasore, a cell-permeable inhibitor of dynamin.* Dev Cell, 2006. **10**(6): p. 839-50.

159. Umemura, K. and H. Kimura, *Hydrogen sulfide enhances reducing activity in neurons: neurotrophic role of H2S in the brain?* Antioxid Redox Signal, 2007. **9**(11): p. 2035-41.

160. Kang, M., C.A. Day, K. Drake, A.K. Kenworthy, and E. DiBenedetto, *A generalization of theory for two-dimensional fluorescence recovery after photobleaching applicable to confocal laser scanning microscopes.* Biophys J, 2009. **97**(5): p. 1501-11.

161. Drake, K.R., M. Kang, and A.K. Kenworthy, *Nucleocytoplasmic distribution and dynamics of the autophagosome marker EGFP-LC3.* PLoS ONE, 2010. **5**(3): p. e9806.

162. Kenworthy, A.K., *Fluorescence recovery after photobleaching studies of lipid rafts*, in *Lipid Rafts*, T. McIntosh, Editor. 2007, Humana Press: Towata, NJ.

163. Jaqaman, K., D. Loerke, M. Mettlen, H. Kuwata, S. Grinstein, S.L. Schmid, and G. Danuser, *Robust single-particle tracking in live-cell time-lapse sequences.* Nat Methods, 2008. **5**(8): p. 695-702.

164. Simons, K. and E. Ikonen, *Functional rafts in cell membranes.* Nature, 1997. **387**: p. 569-572.

165. Johannes, L. and S. Mayor, *Induced domain formation in endocytic invagination, lipid sorting, and scission.* Cell, 2010. **142**(4): p. 507-10.

166. Pina, D.G. and L. Johannes, *Cholera and Shiga toxin B-subunits: thermodynamic and structural considerations for function and biomedical applications.* Toxicon, 2005. **45**(4): p. 389-93.

167. Kaiser, H.J., D. Lingwood, I. Levental, J.L. Sampaio, L. Kalvodova, L. Rajendran, and K. Simons, *Order of lipid phases in model and plasma membranes.* Proc Natl Acad Sci U S A, 2009. **106**(39): p. 16645-50.

168. Levental, I., D. Lingwood, M. Grzybek, U. Coskun, and K. Simons, *Palmitoylation regulates raft affinity for the majority of integral raft proteins.* Proc Natl Acad Sci U S A, 2010. **107**(51): p. 22050-4.

169. Romer, W., L.L. Pontani, B. Sorre, C. Rentero, L. Berland, V. Chambon, C. Lamaze, P. Bassereau, C. Sykes, K. Gaus, and L. Johannes, *Actin dynamics drive membrane reorganization and scission in clathrin-independent endocytosis.* Cell, 2010. **140**(4): p. 540-53.

170. Bacia, K., P. Schwille, and T. Kurzchalia, *Sterol structure determines the separation of phases and the curvature of the liquid-ordered phase in model membranes.* Proc Natl Acad Sci U S A, 2005. **102**(9): p. 3272-7.

171. Lencer, W.I. and D. Saslowsky, *Raft trafficking of AB5 subunit bacterial toxins.* Biochim Biophys Acta, 2005. **1746**(3): p. 314-21.

172. Wolf, A.A., M.G. Jobling, D.E. Saslowsky, E. Kern, K.R. Drake, A.K. Kenworthy, R.K. Holmes, and W.I. Lencer, *Attenuated endocytosis and toxicity of a mutant cholera toxin with decreased ability to cluster GM1.* Infect Immun, 2008. **76**(4): p. 1476-84.

173. Lingwood, D., B. Binnington, T. Rog, I. Vattulainen, M. Grzybek, U. Coskun, C.A. Lingwood, and K. Simons, *Cholesterol modulates glycolipid conformation and receptor activity.* Nat Chem Biol, 2011. **7**(5): p. 260-2.

174. Mahfoud, R., A. Manis, B. Binnington, C. Ackerley, and C.A. Lingwood, *A major fraction of glycosphingolipids in model and cellular cholesterol containing membranes are undetectable by their binding proteins.* J Biol Chem, 2010. **285**: p. 36049-59.

175. Hebbar, S., E. Lee, M. Manna, S. Steinert, G.S. Kumar, M. Wenk, T. Wohland, and R. Kraut, *A fluorescent sphingolipid binding domain peptide probe interacts with sphingolipids and cholesterol-dependent raft domains.* J Lipid Res, 2008. **49**(5): p. 1077-89.

176. Guo, L., D. Zhou, K.M. Pryse, A.L. Okunade, and X. Su, *Fatty acid 2-hydroxylase mediates diffusional mobility of raft-associated lipids, GLUT4 level and lipogenesis in 3T3-L1 adipocytes.* J Biol Chem, 2010. **285**: p. 25438-47.

177. Day, C.A. and A.K. Kenworthy, *Tracking microdomain dynamics in cell membranes.* Biochim Biophys Acta, 2009. **1788**(1): p. 245-53.

178. Sahl, S.J., M. Leutenegger, M. Hilbert, S.W. Hell, and C. Eggeling, *Fast molecular tracking maps nanoscale dynamics of plasma membrane lipids.* Proc Natl Acad Sci U S A, 2010. **107**(15): p. 6829-34.

179. Mueller, V., C. Ringemann, A. Honigmann, G. Schwarzmann, R. Medda, M. Leutenegger, S. Polyakova, V.N. Belov, S.W. Hell, and C. Eggeling, *STED nanoscopy reveals molecular details of cholesterol- and cytoskeleton-modulated lipid interactions in living cells.* Biophys J, 2011. **101**(7): p. 1651-60.

180. Eggeling, C., C. Ringemann, R. Medda, G. Schwarzmann, K. Sandhoff, S. Polyakova, V.N. Belov, B. Hein, C. von Middendorff, A. Schonle, and S.W. Hell, *Direct observation of the nanoscale dynamics of membrane lipids in a living cell.* Nature, 2009. **457**(7233): p. 1159-62.

181. Goodwin, J.S., K.R. Drake, C.L. Remmert, and A.K. Kenworthy, *Ras diffusion is sensitive to plasma membrane viscosity.* Biophys J, 2005. **89**(2): p. 1398-410.

182. Pang, H., P.U. Le, and I.R. Nabi, *Ganglioside GM1 levels are a determinant of the extent of caveolae/raft-dependent endocytosis of cholera toxin to the Golgi apparatus.* J Cell Sci, 2004. **117**(Pt 8): p. 1421-30.

183. Parton, R.G., *Ultrastructural localization of gangliosides; GM1 is concentrated in caveolae.* J. Histochem. Cytochem., 1994. **42**(2): p. 155-166.

184. Schnitzer, J.E., P. Oh, and D.P. McIntosh, *Role of GTP hydrolysis in fission of caveolae directly from plasma membranes [published erratum appears in Science 1996 Nov 15;274(5290):1069].* Science, 1996. **274**(5285): p. 239-42.

185. Thomsen, P., K. Roepstorff, M. Stahlhut, and B. van Deurs, *Caveolae are highly immobile plasma membrane microdomains, which are not involved in constitutive endocytic trafficking.* Mol. Biol. Cell, 2002. **13**: p. 238-250.

186. Shvartsman, D.E., M. Kotler, R.D. Tall, M.G. Roth, and Y.I. Henis, *Differently anchored influenza hemagglutinin mutants display distinct interaction dynamics with mutual rafts.* J. Cell Biol., 2003. **163**(4): p. 879-88.

187. Sharma, P., R. Varma, R.C. Sarasij, Ira, K. Gousset, G. Krishnamoorthy, M. Rao, and S. Mayor, *Nanoscale organization of multiple GPI-anchored proteins in living cell membranes.* Cell, 2004. **116**(4): p. 577-589.

188. Kusumi, A., C. Nakada, K. Ritchie, K. Murase, K. Suzuki, H. Murakoshi, R.S. Kasai, J. Kondo, and T. Fujiwara, *Paradigm shift of the plasma membrane concept from the two-dimensional continuum fluid to the partitioned fluid: high-speed single-molecule tracking of membrane molecules.* Annu Rev Biophys Biomol Struct, 2005. **34**: p. 351-78.

189. Kusumi, A. and Y. Sako, *Cell surface organization by the membrane skeleton.* Curr. Opin. Cell Biol., 1996. **8**(4): p. 566-574.

190. Marguet, D., P.F. Lenne, H. Rigneault, and H.T. He, *Dynamics in the plasma membrane: how to combine fluidity and order.* EMBO J, 2006. **25**(15): p. 3446-57.

191. Andrews, N.L., K.A. Lidke, J.R. Pfeiffer, A.R. Burns, B.S. Wilson, J.M. Oliver, and D.S. Lidke, *Actin restricts FcepsilonRI diffusion and facilitates antigen-induced receptor immobilization.* Nat Cell Biol, 2008. **10**(8): p. 955-63.

192.   Badizadegan, K., H.E. Wheeler, Y. Fujinaga, and W.I. Lencer, *Trafficking of cholera toxin-ganglioside GM1 complex into Golgi and induction of toxicity depend on actin cytoskeleton.* Am J Physiol Cell Physiol, 2004. **287**(5): p. C1453-62.

193.   Ewers, H., W. Römer, A.E. Smith, K. Bacia, S. Dmitrieff, W. Chai, R. Mancini, J. Kartenbeck, V. Chambon, L. Berland, A. Oppenheim, G. Schwarzmann, T. Feizi, P. Schwille, P. Sens, A. Helenius, and L. Johannes, *GM1 structure determines SV40-induced membrane invagination and infection.* Nat Cell Biol, 2010. **12**(1): p. 11-8; sup pp 1-12.

194.   Hinshaw, D.B., J.M. Burger, M.T. Miller, J.A. Adams, T.F. Beals, and G.M. Omann, *ATP depletion induces an increase in the assembly of a labile pool of polymerized actin in endothelial cells.* Am J Physiol, 1993. **264**(5 Pt 1): p. C1171-9.

195.   Herget-Rosenthal, S., M. Hosford, A. Kribben, S.J. Atkinson, R.M. Sandoval, and B.A. Molitoris, *Characteristics of EYFP-actin and visualization of actin dynamics during ATP depletion and repletion.* Am J Physiol Cell Physiol, 2001. **281**(6): p. C1858-70.

196.   Atkinson, S.J., M.A. Hosford, and B.A. Molitoris, *Mechanism of actin polymerization in cellular ATP depletion.* J Biol Chem, 2004. **279**(7): p. 5194-9.

197.   Frick, M., K. Schmidt, and B.J. Nichols, *Modulation of lateral diffusion in the plasma membrane by protein density.* Curr Biol, 2007. **17**(5): p. 462-7.

198.   Ling, H., A. Boodhoo, B. Hazes, M.D. Cummings, G.D. Armstrong, J.L. Brunton, and R.J. Read, *Structure of the shiga-like toxin I B-pentamer complexed with an analogue of its receptor Gb3.* Biochemistry, 1998. **37**(7): p. 1777-88.

199.   Umemura, Y.M., M. Vrljic, S.Y. Nishimura, T.K. Fujiwara, K.G. Suzuki, and A. Kusumi, *Both MHC class II and its GPI-anchored form undergo hop diffusion as observed by single-molecule tracking.* Biophys J, 2008. **95**(1): p. 435-50.

200.   Suzuki, K.G., T.K. Fujiwara, M. Edidin, and A. Kusumi, *Dynamic recruitment of phospholipase C gamma at transiently immobilized GPI-anchored receptor clusters induces IP3-Ca2+ signaling: single-molecule tracking study 2.* J Cell Biol, 2007. **177**(4): p. 731-42.

201.   Suzuki, K.G., T.K. Fujiwara, F. Sanematsu, R. Iino, M. Edidin, and A. Kusumi, *GPI-anchored receptor clusters transiently recruit Lyn and G alpha for temporary cluster immobilization and Lyn activation: single-molecule tracking study 1.* J Cell Biol, 2007. **177**(4): p. 717-30.

202.   Chen, Y., W.R. Thelin, B. Yang, S.L. Milgram, and K. Jacobson, *Transient anchorage of cross-linked glycosyl-phosphatidylinositol-anchored proteins depends on cholesterol, Src family kinases, caveolin, and phosphoinositides.* J Cell Biol, 2006. **175**(1): p. 169-78.

203.   Chen, Y., L. Veracini, C. Benistant, and K. Jacobson, *The transmembrane protein CBP plays a role in transiently anchoring small clusters of Thy-1, a GPI-anchored protein, to the cytoskeleton.* J Cell Sci, 2009. **122**(Pt 21): p. 3966-72.

204.   Fujita, A., J. Cheng, and T. Fujimoto, *Segregation of GM1 and GM3 clusters in the cell membrane depends on the intact actin cytoskeleton.* Biochim Biophys Acta, 2009. **1791**: p. 388-96.

205.   Gomez, G.A. and J.L. Daniotti, *Electrical properties of plasma membrane modulate subcellular distribution of K-Ras.* Febs J, 2007. **274**(9): p. 2210-28.

206.   Zhang, D., M. Manna, T. Wohland, and R. Kraut, *Alternate raft pathways cooperate to mediate slow diffusion and efficient uptake of a sphingolipid tracer to degradative and recycling compartments.* J Cell Sci, 2009. **122**(Pt 20): p. 3715-28.

207.   van Zanten, T.S., J. Gomez, C. Manzo, A. Cambi, J. Buceta, R. Reigada, and M.F. Garcia-Parajo, *Direct mapping of nanoscale compositional connectivity on intact cell membranes.* Proc Natl Acad Sci U S A, 2010. **107**(35): p. 15437-42.

208.   Pinaud, F., X. Michalet, G. Iyer, E. Margeat, H.P. Moore, and S. Weiss, *Dynamic partitioning of a glycosyl-phosphatidylinositol-anchored protein in glycosphingolipid-rich microdomains imaged by single-quantum dot tracking.* Traffic, 2009. **10**(6): p. 691-712.

209.   Blank, N., M. Schiller, S. Krienke, G. Wabnitz, A.D. Ho, and H.M. Lorenz, *Cholera toxin binds to lipid rafts but has a limited specificity for ganglioside GM1.* Immunol Cell Biol, 2007. **85**(5): p. 378-82.

210.   Yanagisawa, M., T. Ariga, and R.K. Yu, *Cholera toxin B subunit binding does not correlate with GM1 expression: a study using mouse embryonic neural precursor cells.* Glycobiology, 2006. **16**(9): p. 19G-22G.

211. Capraro, B.R., Y. Yoon, W. Cho, and T. Baumgart, *Curvature sensing by the epsin N-terminal homology domain measured on cylindrical lipid membrane tethers.* J Am Chem Soc. **132**(4): p. 1200-1.

212. Madsen, K.L., V.K. Bhatia, U. Gether, and D. Stamou, *BAR domains, amphipathic helices and membrane-anchored proteins use the same mechanism to sense membrane curvature.* FEBS Lett, 2010. **584**(9): p. 1848-55.

213. Roux, A., G. Koster, M. Lenz, B. Sorre, J.B. Manneville, P. Nassoy, and P. Bassereau, *Membrane curvature controls dynamin polymerization.* Proc Natl Acad Sci U S A, 2010. **107**(9): p. 4141-6.

214. Adler, J., A.I. Shevchuk, P. Novak, Y.E. Korchev, and I. Parmryd, *Plasma membrane topography and interpretation of single-particle tracks.* Nat Methods. **7**(3): p. 170-1.

215. Mahfoud, R., A. Manis, B. Binnington, C. Ackerley, and C.A. Lingwood, *A major fraction of glycosphingolipids in model and cellular cholesterol-containing membranes is undetectable by their binding proteins.* J Biol Chem, 2010. **285**(46): p. 36049-59.

216. del Valle, M., Y. Robledo, and I.V. Sandoval, *Membrane flow through the Golgi apparatus: specific disassembly of the cis-Golgi network by ATP depletion.* J Cell Sci, 1999. **112 (Pt 22)**: p. 4017-29.

217. Vaughan, K.T., *Surfing, regulating and capturing: are all microtubule-tip-tracking proteins created equal?* Trends Cell Biol, 2004. **14**(9): p. 491-6.

218. Mimori-Kiyosue, Y. and S. Tsukita, *"Search-and-capture" of microtubules through plus-end-binding proteins (+TIPs).* J Biochem, 2003. **134**(3): p. 321-6.

219. Vaughan, P.S., P. Miura, M. Henderson, B. Byrne, and K.T. Vaughan, *A role for regulated binding of p150(Glued) to microtubule plus ends in organelle transport.* J Cell Biol, 2002. **158**(2): p. 305-19.

220. Lomakin, A.J., I. Semenova, I. Zaliapin, P. Kraikivski, E. Nadezhdina, B.M. Slepchenko, A. Akhmanova, and V. Rodionov, *CLIP-170-dependent capture of membrane organelles by microtubules initiates minus-end directed transport.* Dev Cell, 2009. **17**(3): p. 323-33.

221. Yvon, A.M., P. Wadsworth, and M.A. Jordan, *Taxol suppresses dynamics of individual microtubules in living human tumor cells.* Mol Biol Cell, 1999. **10**(4): p. 947-59.

222. Stephens, D.J., *Functional coupling of microtubules to membranes - implications for membrane structure and dynamics.* J Cell Sci, 2012. **125**(Pt 12): p. 2795-804.

223. Waterman-Storer, C.M. and E.D. Salmon, *Endoplasmic reticulum membrane tubules are distributed by microtubules in living cells using three distinct mechanisms.* Curr Biol, 1998. **8**(14): p. 798-806.

224. Allan, V.J., *Cytoplasmic dynein.* Biochem Soc Trans, 2011. **39**(5): p. 1169-78.

225. Flores-Rodriguez, N., S.S. Rogers, D.A. Kenwright, T.A. Waigh, P.G. Woodman, and V.J. Allan, *Roles of dynein and dynactin in early endosome dynamics revealed using automated tracking and global analysis.* PLoS ONE, 2011. **6**(9): p. e24479.

226. Shubeita, G.T., S.L. Tran, J. Xu, M. Vershinin, S. Cermelli, S.L. Cotton, M.A. Welte, and S.P. Gross, *Consequences of motor copy number on the intracellular transport of kinesin-1-driven lipid droplets.* Cell, 2008. **135**(6): p. 1098-107.

227. Caviston, J.P., A.L. Zajac, M. Tokito, and E.L. Holzbaur, *Huntingtin coordinates the dynein-mediated dynamic positioning of endosomes and lysosomes.* Mol Biol Cell, 2010.

228. Firestone, A.J., J.S. Weinger, M. Maldonado, K. Barlan, L.D. Langston, M. O'Donnell, V.I. Gelfand, T.M. Kapoor, and J.K. Chen, *Small-molecule inhibitors of the AAA+ ATPase motor cytoplasmic dynein.* Nature, 2012. **484**: p. 125-9.

229. Schroer, T.A., *Dynactin.* Annu Rev Cell Dev Biol, 2004. **20**: p. 759-79.

230. Leduc, C., O. Campas, J.F. Joanny, J. Prost, and P. Bassereau, *Mechanism of membrane nanotube formation by molecular motors.* Biochim Biophys Acta, 2010. **1798**(7): p. 1418-26.

231. Coudrier, E. and C.G. Almeida, *Myosin 1 controls membrane shape by coupling F-Actin to membrane.* Bioarchitecture, 2011. **1**(5): p. 230-235.

232. Hunt, S.D. and D.J. Stephens, *The role of motor proteins in endosomal sorting.* Biochem Soc Trans, 2011. **39**(5): p. 1179-84.

233. Wassmer, T., N. Attar, M. Harterink, J.R. van Weering, C.J. Traer, J. Oakley, B. Goud, D.J. Stephens, P. Verkade, H.C. Korswagen, and P.J. Cullen, *The retromer coat complex coordinates endosomal sorting and dynein-mediated transport, with carrier recognition by the trans-Golgi network.* Dev Cell, 2009. **17**(1): p. 110-22.

234. Traer, C.J., A.C. Rutherford, K.J. Palmer, T. Wassmer, J. Oakley, N. Attar, J.G. Carlton, J. Kremerskothen, D.J. Stephens, and P.J. Cullen, *SNX4 coordinates endosomal sorting of TfnR with dynein-mediated transport into the endocytic recycling compartment.* Nat Cell Biol, 2007. **9**(12): p. 1370-80.

235. Hong, Z., Y. Yang, C. Zhang, Y. Niu, K. Li, X. Zhao, and J.J. Liu, *The retromer component SNX6 interacts with dynactin p150(Glued) and mediates endosome-to-TGN transport.* Cell Res, 2009. **19**(12): p. 1334-49.

236. Cullen, P.J. and H.C. Korswagen, *Sorting nexins provide diversity for retromer-dependent trafficking events.* Nat Cell Biol, 2012. **14**(1): p. 29-37.

237. Galic, M., S. Jeong, F.C. Tsai, L.M. Joubert, Y.I. Wu, K.M. Hahn, Y. Cui, and T. Meyer, *External push and internal pull forces recruit curvature-sensing N-BAR domain proteins to the plasma membrane.* Nat Cell Biol, 2012. **14**(8): p. 874-81.

238. Hsieh, W.T., C.J. Hsu, B.R. Capraro, T. Wu, C.M. Chen, S. Yang, and T. Baumgart, *Curvature sorting of peripheral proteins on solid-supported wavy membranes.* Langmuir, 2012. **28**(35): p. 12838-43.

239. McNally, F.J., *Mechanisms of spindle positioning.* J Cell Biol, 2013. **200**(2): p. 131-40.

240. Redemann, S., J. Pecreaux, N.W. Goehring, K. Khairy, E.H. Stelzer, A.A. Hyman, and J. Howard, *Membrane invaginations reveal cortical sites that pull on mitotic spindles in one-cell C. elegans embryos.* PLoS ONE, 2010. **5**(8): p. e12301.

241. Verma, P., A.G. Ostermeyer-Fay, and D.A. Brown, *Caveolin-1 Induces Formation of Membrane Tubules That Sense Actomyosin Tension and Are Inhibited by PTRF/Cavin-1.* Mol Biol Cell, 2010.

242. Hansen, G.H., S.M. Dalskov, C.R. Rasmussen, L. Immerdal, L.L. Niels-Christiansen, and E.M. Danielsen, *Cholera toxin entry into pig enterocytes occurs via a lipid raft- and clathrin-dependent mechanism.* Biochemistry, 2005. **44**(3): p. 873-82.

243. Anderson, R.G. and K. Jacobson, *A role for lipid shells in targeting proteins to caveolae, rafts, and other lipid domains.* Science, 2002. **296**(5574): p. 1821-5.

244. Boyd, B., G. Magnusson, Z. Zhiuyan, and C.A. Lingwood, *Lipid modulation of glycolipid receptor function. Availability of Gal(alpha 1-4)Gal disaccharide for verotoxin binding in natural and synthetic glycolipids.* Eur J Biochem, 1994. **223**(3): p. 873-8.

245. White, P., L. Gu, and J. Chen, *Decreased actin solubility observed during ATP-depletion is mimicked by severing agents but not depolymerizing agents in isolated and cultured proximal tubular cells.* Clin Physiol Funct Imaging, 2002. **22**(5): p. 312-9.

246. Bubb, M.R., I. Spector, B.B. Beyer, and K.M. Fosen, *Effects of jasplakinolide on the kinetics of actin polymerization. An explanation for certain in vivo observations.* J Biol Chem, 2000. **275**(7): p. 5163-70.

247. Gauthier, N.C., T.A. Masters, and M.P. Sheetz, *Mechanical feedback between membrane tension and dynamics.* Trends Cell Biol, 2010. **22**(10): p. 527-35.

248. Porat-Shliom, N., Y. Kloog, and J.G. Donaldson, *A unique platform for H-Ras signaling involving clathrin-independent endocytosis.* Mol Biol Cell, 2008. **19**(3): p. 765-75.

249. Lauvrak, S.U., S. Walchli, T.G. Iversen, H.H. Slagsvold, M.L. Torgersen, B. Spilsberg, and K. Sandvig, *Shiga toxin regulates its entry in a Syk-dependent manner.* Mol Biol Cell, 2006. **17**(3): p. 1096-109.

250. Soppina, V., A.K. Rai, A.J. Ramaiya, P. Barak, and R. Mallik, *Tug-of-war between dissimilar teams of microtubule motors regulates transport and fission of endosomes.* Proc Natl Acad Sci U S A, 2009. **106**(46): p. 19381-6.

251. Robertson, A.M. and V.J. Allan, *Brefeldin A-dependent membrane tubule formation reconstituted in vitro is driven by a cell cycle-regulated microtubule motor.* Mol Biol Cell, 2000. **11**(3): p. 941-55.

252. Skjeldal, F.M., S. Strunze, T. Bergeland, E. Walseng, T.F. Gregers, and O. Bakke, *The fusion of early endosomes induces molecular-motor-driven tubule formation and fission.* J Cell Sci. **125**(Pt 8): p. 1910-9.

253. Zhu, X. and I. Kaverina, *Quantification of asymmetric microtubule nucleation at subcellular structures.* Methods Mol Biol, 2011. **777**: p. 235-44.

254. Nichols, B.J., A.K. Kenworthy, R.S. Polishchuk, R. Lodge, T.H. Roberts, K. Hirschberg, R.D. Phair, and J. Lippincott-Schwartz, *Rapid cycling of lipid raft markers between the cell surface and Golgi complex.* J Cell Biol, 2001. **153**(3): p. 529-41.

255. Ritter, B., J. Modregger, M. Paulsson, and M. Plomann, *PACSIN 2, a novel member of the PACSIN family of cytoplasmic adapter proteins.* FEBS Lett, 1999. **454**(3): p. 356-62.